Sustainable Energy & Fuels

ROYAL SOCIETY OF CHEMISTRY

REVIEW

View Article Online
View Journal | View Issue

Cite this: *Sustainable Energy Fuels*, 2022, **6**, 29

Valorisation of xylose to renewable fuels and chemicals, an essential step in augmenting the commercial viability of lignocellulosic biorefineries

Vivek Narisetty,[a] Rylan Cox,[ab] Rajesh Bommareddy,[c] Deepti Agrawal,[d] Ejaz Ahmad,[e] Kamal Kumar Pant,[f] Anuj Kumar Chandel,[g] Shashi Kant Bhatia,[h] Dinesh Kumar,[i] Parmeswaran Binod,[j] Vijai Kumar Gupta[k] and Vinod Kumar *[af]

Biologists and engineers are making tremendous efforts in contributing to a sustainable and green society. To that end, there is growing interest in waste management and valorisation. Lignocellulosic biomass (LCB) is the most abundant material on the earth and an inevitable waste predominantly originating from agricultural residues, forest biomass and municipal solid waste streams. LCB serves as the renewable feedstock for clean and sustainable processes and products with low carbon emission. Cellulose and hemicellulose constitute the polymeric structure of LCB, which on depolymerisation liberates oligomeric or monomeric glucose and xylose, respectively. The preferential utilization of glucose and/or absence of the xylose metabolic pathway in microbial systems cause xylose valorization to be alienated and abandoned, a major bottleneck in the commercial viability of LCB-based biorefineries. Xylose is the second most abundant sugar in LCB, but a non-conventional industrial substrate unlike glucose. The current review seeks to summarize the recent developments in the biological conversion of xylose into a myriad of sustainable products and associated challenges. The review discusses the microbiology, genetics, and biochemistry of xylose metabolism with hurdles requiring debottlenecking for efficient xylose assimilation. It further describes the product formation by microbial cell factories which can assimilate xylose naturally and rewiring of metabolic networks to ameliorate xylose-based bioproduction in native as well as non-native strains. The review also includes a case study that provides an argument on a suitable pathway for optimal cell growth and succinic acid (SA) production from xylose through elementary flux mode analysis. Finally, a product portfolio from xylose bioconversion has been evaluated along with significant developments made through enzyme, metabolic and process engineering approaches, to maximize the product titers and yield, eventually empowering LCB-based biorefineries. Towards the end, the review is wrapped up with current challenges, concluding remarks, and prospects with an argument for intense future research into xylose-based biorefineries.

Received 21st June 2021
Accepted 25th October 2021

DOI: 10.1039/d1se00927c

rsc.li/sustainable-energy

1. Introduction

Biomass is a potential alternative to non-renewable and non-sustainable fossil fuels causing massive harm to the atmosphere through colossal carbon emission and generation of pollutants.[1] Analogous to a petroleum refinery, a biorefinery processes biomass into multiple products with a green and sustainable approach leading to low carbon biomanufacturing technologies.[1,2] First generation biorefineries making use of edible feedstocks such as sugar, starch, and vegetable oils for

[a]*School of Water, Energy and Environment, Cranfield University, Cranfield MK43 0AL, UK. E-mail: Vinod.Kumar@cranfield.ac.uk; Tel: +44 (0)1234754786*

[b]*School of Aerospace, Transport and Manufacturing, Cranfield University, Cranfield MK43 0AL, UK*

[c]*Department of Applied Sciences, Northumbria University, Newcastle upon Tyne NE1 8ST, UK*

[d]*Biochemistry and Biotechnology Area, Material Resource Efficiency Division, CSIR-Indian Institute of Petroleum, Mohkampur, Dehradun 248005, India*

[e]*Department of Chemical Engineering, Indian Institute of Technology (ISM), Dhanbad 826004, India*

[f]*Department of Chemical Engineering, Indian Institute of Technology Delhi, New Delhi 110016, India*

[g]*Department of Biotechnology, Engineering School of Lorena (EEL), University of São Paulo, Lorena 12.602.810, Brazil*

[h]*Department of Biological Engineering, College of Engineering, Konkuk University, Seoul 05029, Republic of Korea*

[i]*School of Bioengineering & Food Technology, Shoolini University of Biotechnology and Management Sciences, Solan 173229, Himachal Pradesh, India*

[j]*Microbial Processes and Technology Division, CSIR-National Institute for Interdisciplinary Science and Technology (CSIR-NIIST), Thiruvananthapuram 695 019, Kerala, India*

[k]*Scotland's Rural College, Barony Campus, Dumfries DG1 3NE, UK*

generating biofuels are well established, but pose a significant concern and are a regular subject of the food *vs.* fuel debate.[3] On the other hand, second generation biorefineries based on non-edible feedstocks such as lignocellulosic biomass (LCB) do not interfere in any food chain and offer a clear value proposition for the production of bulk and speciality chemicals. LCB is the most abundant feedstock on the planet (~200 billion tonnes) with a significant contribution stemming from post-harvest agricultural residues. It is composed of lignin (15–20%), the outermost protective layer, cellulose (40–50%), the inner amorphous and crystalline component of the secondary wall, and hemicellulose (25–30%) microfibrils that connect the outermost and inner cellulose layers (Fig. 1A).[4] Cellulose is a linear homo-polymer of D-glucose units connected by β-1,4-glycosidic bonds, and hemicellulose is a complex hetero-polymer containing D-xylose, L-arabinose, D-glucose, L-galactose, D-mannose, D-glucuronic acid and D-galacturonic acid (Fig. 1B). Hemicelluloses constitute 26% dry weight in hard woods, 22% in soft woods, and up to 25% in agro-residues with various polymeric forms such as xylan, arabinoxylan, xyloglucan, and glucuronoxylan.[5,6] To utilize this three-dimensional polymeric structure as the feedstock for fermentative production of value-added chemicals, the polymer is converted into simple fermentable sugars. However, the major limitation is that most of the microorganisms are incapable of metabolizing all the fermentable sugars present in LCB, especially pentoses. The pentose sugars are present in the hemicellulosic fraction with xylan as the major polysaccharide which is composed of β-1,4-linked xylose residues. The depolymerization of the hemicellulosic fraction generates a mixture of sugars containing ~90% xylose. In fact, xylose is the second most abundant sugar available after glucose in LCB (Fig. 1A).[7] Despite this, the application of xylose as a potential feedstock is overlooked for biorefineries and it is discarded as waste or incinerated for energy purposes. This is due to a lack of efficient fermentation systems, as many of the microorganisms do not have a native pathway for metabolizing xylose. In addition, uptake of xylose is suppressed in the presence of glucose due to carbon catabolite repression.[8] That is why the number of literature reports using glucose as a substrate for bioproduction is much larger in comparison to that using xylose. However, while exploiting biochemical platforms, the techno-commercial success of an

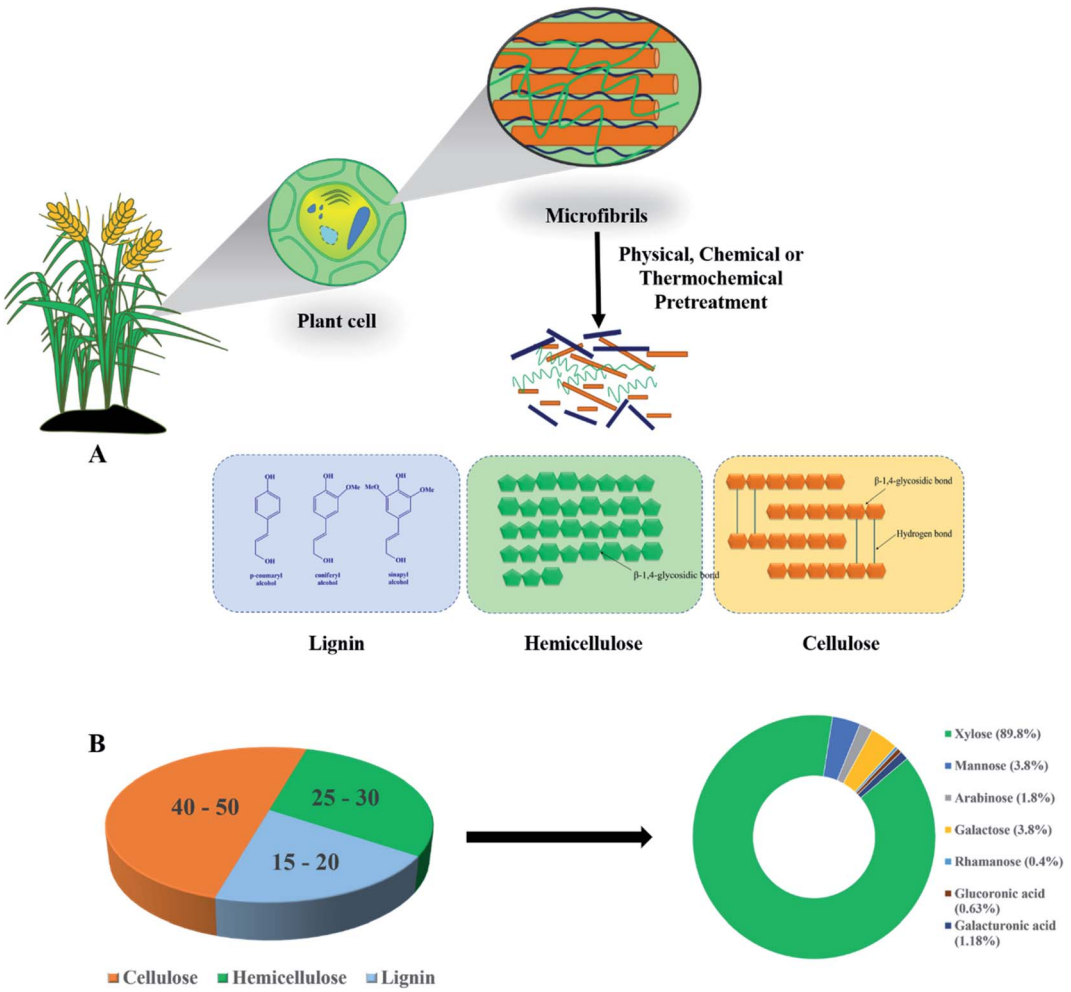

Fig. 1 (A) Structural components of lignocellulosic biomass (LCB). (B)Illustration of the composition of individual subunits of LCB and compositions of sugar and sugar acids in the hemicellulosic fraction.

LCB-based biorefinery largely thrives on the revival of the carbohydrate economy, which in turn is dependent on efficient depolymerization of both the structural polysaccharides to simple sugars and their subsequent valorisation to various commercially important products either through chemical or biotechnological routes.[9,10] Therefore, efficient conversion of xylose is necessary and it is imperative to find robust microbial systems for metabolizing xylose for simultaneous assimilation of glucose and xylose for the pragmatic development of profitable LCB-based biorefineries.

Considering the challenges associated with xylose utilization, the current review (i) covers the efficient pretreatment processes assisting in xylan extraction from different LCB residues, (ii) discusses the bottlenecks impeding xylose assimilation and strategies to overcome them, (iii) describes the major native and engineered microbial cell factories available for efficient bioconversion of xylose to chemical building blocks, (iv) includes implementation of elementary flux mode analysis to understand the optimal pathway for xylose utilization to produce biomass and end metabolites with a case study of succinic acid, and (v) briefly covers alternative chemical catalysis of xylose for manufacturing value-added products. Finally, the limitations and future perspectives for constructing microbial cell factories to effectively utilize xylose and produce a wide array of products are included.

1.1 Pretreatment strategies for the extraction of fermentable sugars from LCB

Recalcitrance is a natural and intrinsic feature of any LCB, originating from its three principal constituents, cellulose, hemicellulose, and lignin, that chemically interact to form a complex network popularly known as a lignin–carbohydrate complex (LCC).[11,12] During biorefining *via* a biochemical route, pretreatment is an imperative module that disrupts the lignocellulosic matrix by breaking LCC linkages leading to delignification and partial or complete hydrolysis of xylan, thereby improving the surface characteristics of biomass and enhancing the accessibility of cellulose for enzymatic hydrolysis. Invariably, most of the traditional pretreatment strategies primarily result in lignin removal, releasing fermentable sugars from the thermolabile hemicellulosic/xylan fraction, or are focused on selective delignification enriching the biomass in glucan and xylan fractions.[13]

1.1.1 Pretreatment method targeting xylan hydrolysis. Conventional techniques like steam explosion (SE), liquid hot water (LHW), dilute acid (DA), and hydrothermal (HT) pretreatments result in the solubilization of the hemicellulose fraction and partial lignin removal.[14] However, the extent of xylan hydrolysis and release of inhibitors during pretreatment significantly depends on the process severity. Process variables such as solid loading during pretreatment, temperature, pressure, residence time and concentration of acid in case of DA pretreatment, biomass composition and pretreatment reactor configuration directly or indirectly govern the successful xylan extraction as monomers, oligomers or its degradation products like furfural, the release of lignin-derived inhibitory derivatives and loss of cellulose as glucose or its dehydrated product namely 5-hydroxymethylfurfural (HMF) in the hydrolysed fraction.[15–17] Generally, SE, LHW and HT pretreatments favour deacetylation of thermolabile acetyl groups attached to the

Table 1 State of the art showcasing pretreatment strategies leading to selective xylan hydrolysis[a]

Type of LCB	Type of pretreatment	Pretreatment conditions	Biomass composition (%)		Removal (%)		References
			Before pretreatment	After pretreatment	Xylan	Lignin	
Poplar	DA	Temp: 170 °C; time: 8.5 min; H_2SO_4: 0.5% (w/w)	Gln-57.9; HC-17.5; KL-24.6	Gln-74.2; HC-<2.0; KL-25	99	—	198
MS	HT pretreatment at low acid	Temp: 180 °C; 10 min; H_2SO_4: 0.3% (w/w)	Gln-41.9; #XMG-22.1; KL-22.0	Gln-64.4; #XMG-5.0; KL-29.3	86.4	20.2	199
CS	DA in steam gun	Temp: 160 °C; time: 5 min; H_2SO_4: 2% (w/w)	Gln-34.0; Xln-22.0; KL-12.3	Gln-57.4; Xln-3.2; KL-24.8	∼92.8	∼<1.5	200
SCB	DA	Temp: 140 °C; time: 8 min; H_3PO_4: 0.2% (w/v)	Gln- 40.1; HC-27.5; TL-18.5	Gln-58.5; HC-1.8; TL-29.05	96.5	14.8	201
SG	DA	Temp: 160 °C; time: 30 min; H_2SO_4: 1% (w/w)	Gln-33.5; Xln-22.7; KL-16.3	Gln-53.2; Xln-0.8; KL-33.3	98.6	18.3	202
WS	DA	Temp: 140 °C; time: 90 min; H_2SO_4: 0.5% (w/w)	Gln-43.2; Xln-24.4; KL-20.8	Gln-59.1; Xln-2.4; KL-30.7	91.5	—	203
CS	HT	Temp: 180 °C	Gln-36.1; Xln-21.4; TL-13.6	Gln-33.0; Xln: 5.4; TL-13.5	74.9	—	200
CC	HT	Temp: 207 °C	Gln-28.8; Xln-29.6; KL-18.6	Gln-54.5; Xln-10.2; KL-21.8	80.4	33.1	204
SS	LHW	Temp: 220 °C; time: 5 min	Gln-33.13; HC-26.2; KL-18.2	Gln-56.7; Xln-2.0; KL-37.0	96.5	6.6	205
SCB	H_3PO_4 catalysed SE	Temp: 195 °C; time: 7.5 min; H_3PO_4: 0.95% (w/w)	Gln-31.8; Xln-12.2; KL-24.3	Gln-49.7; Xln-2.3; KL-31.9	90.6	14.4	206
	H_2SO_4 catalysed SE	Temp: 195 °C; time: 7.5 min; H_2SO_4: 0.2% (w/w)		Gln-49.4; Xln-3.3; KL-31.5	86.6	12.1	

[a] MW: maple wood; SCB: sugarcane bagasse; SG: switchgrass; WS: wheat straw; CC: corn cob; SS: sugarcane straw; DA: dilute acid; SE: steam explosion; LHW: liquid hot water; HT: hydrothermal; Gln: glucan; Xln: xylan; HC: hemicellulose; KL: Klason lignin: TL: acid soluble and insoluble lignin; #XMG: xylan, mannan and galactan.

Table 2 Acid catalysed SE and DA pretreatment carried out at semi-pilot and pilot scales with different types of lignocellulosic feedstock[a]

LCB type	Reactor type	Reaction conditions	Biomass composition (%)		Composition of pre-hydrolysate		References
			Untreated	Pretreated	Sugars	Non-sugar component	
CC	Screw steam explosive extruder	Pressure: 15.5 bar	Gln-42.23		Xylose: 27.5 wt%	Acetic acid: 1.1 wt%	207
		Time: 5.5 min	HC-39.01		XOS: 2.4 wt%	TP: 1.7 wt%	
		H_2SO_4: 2.4% (w/w) + steam explosion	KL-14.42		Glucose: 3.9 wt%	Furfural: 0.5 wt%	
					Arabinose: 3.7 wt%	5 HMF: 0.2 wt%	
SCB	350-L SS reactor with stirrer & thermal oil heating	Temp: 120 °C	Gln-45.1	Gln-54.6	C5: 17.4 g L^{-1}	Acetic acid: 2.3 g L^{-1}	208
		Time: 10 min	HC-26.9	HC-10		TA: 7.5 g L^{-1}	
		H_2SO_4: 1% (w/v)	KL-22.2	KL-32	C6: 1.6 g L^{-1}	Furfural: 0.8 g L^{-1}	
						5 HMF: 0.2 g L^{-1}	
WS	Continuous pretreatment reactor (250 kg day^{-1})	Temp: 160 °C Pressure: 5.2 bar	Gln-47.1	Gln-63.1	Xylose: 29.2 g L^{-1}	Acetic acid: 1.9 g L^{-1}	209
		Time: 10 min	HC-24.3	HC-1.0	Glucose: 8.4 g L^{-1}	Furfural: 0.9 g L^{-1}	
		H_2SO_4: 0.5% (v/v)	KL-28.5	KL-35.8	Arabinose: 2.6 g L^{-1}	5 HMF: 0.6 g L^{-1}	
EG	150 L horizontal Andritz reactor	Temp: 180 °C; time: 15 min; H_2SO_4: 2.4% (w/w) + steam explosion	Gln-38.5	Gln-55.5	92% xylan recoverable and 74% as xylose	Acetic acid: 2.9 wt%	210
			Xln-11.0	Xln: 0.8		Furfural: 0.9 wt%	
			KL-25.2	KL-37.1		5 HMF: 0.2 wt%	
RS	Continuous pretreatment reactor (250 kg day^{-1})	Temp: 162 °C; time: 10 min	Gln-37	Gln-51.8	100 g xylose in hydrolysate/kg initial dry substrate	Acetic acid: 2 g L^{-1}	211
		Final H_2SO_4: 0.35% (w/w)	Xln-20	Xln-3.6		Furfural: 1.2 g L^{-1}	
		Preasoaking in acid: 0.5 h acid	TL-13.4	TL-28.8		5 HMF: 1.1 g L^{-1}	
WS	Steam explosion in a 30L rig	Pressure: 12 bar; time: 12 min; final H_3PO_4: 1.2% (w/v); acid pre-soaked biomass introduced	Gln-41.6 Xln-30.3 TL-19.3		Xylose: 17.7 wt%	—	212
CS			Gln-38.5 Xln-24.3 TL-18.3		Xylose: 13.9 wt%	—	
MS			Gln-47.0 Xln-25.1 TL-26.15		Xylose: 14.7 wt%	—	

[a] CC: corn cobs; SCB: sugarcane bagasse; RS: rice straw; WS: wheat straw; EG: *Eucalyptus grandis*; CS: corn stover; MA: Miscanthus; Gln: glucan; Xln: xylan; HC: hemicellulose; KL: Klason lignin; TL: acid soluble and insoluble lignin; C5: pentose sugars; C6: hexose sugars; XOS: xylooligosaccharides; GOS: glucooligosaccharides; DA: dilute acid; TPL: total phenolics; TA: total aromatics; wt%: Wt in g/100 g biomass.

hemicellulose backbone and cause release of acetic acid in a temperature range of 180–250 °C.[16] Since acetic acid is weak compared to inorganic acids, partial xylan hydrolysis occurs, and the resulting pre-hydrolysates are predominant in xylooligosaccharides (XOS) with fewer xylose monomers.[18] Yao *et al.* have recently confirmed that the pH of the medium plays a decisive role in the breaking of LCC linkages.[15] Thus, HT pretreatment likely induces deacetylation and catalyses the cleavage of glycosidic linkages within the xylan backbone, but the addition of strong acid even at low concentration reduces pH that preferentially breaks the ester linkages between lignin and xylan.[15] Therefore, during DA pretreatment, lower temperatures are recommended (120–180 °C) as the addition of acid demands lower operating conditions favouring xylan hydrolysis. Further, combinatorial pretreatment involving a low concentration of inorganic acid and water facilitates the release of xylose monomers from the hemicellulose backbone. It enhances the efficiency of the process owing to milder operating conditions and less inhibitor generation, while preserving the cellulosic fraction in the biomass. Table 1 exclusively showcases a few examples of previously published literature where SE, LHW and DA pretreatments and their combinations selectively hydrolysed the xylan fraction (>85%) and gave <25% delignification. Since HT and DA pretreatments are among the most popular, efficient, and economically attractive pretreatment strategies that lead to selective xylan hydrolysis keeping the

glucan fraction in the biomass intact, these technologies have been scaled up to semi-pilot and pilot plant levels as well, as shown in Table 2. The following section describes conventional pretreatment methods, which lead to enrichment of xylan and glucan fractions in the biomass, targeting selective delignification.

1.1.2 Pretreatment strategies favouring glucan and xylan enrichment. The use of sodium hydroxide (NaOH) during pretreatment is one of the most popular and industrially scalable delignification strategies. It cleaves LCC linkages (phenolic α-aryl, phenolic α-alkyl, and phenolic and non-phenolic β-aryl ether linkages) between lignin and hemicellulosic fractions, and improves the surface properties and digestibility of cellulose.[19] Unfortunately, hemicellulose, being amorphous, acetylated and thermolabile, is easily extracted when a high NaOH concentration is used above 70 °C, resulting in significant losses (≥35%). Hence, there are isolated reports of alkali pretreatment wherein xylan enrichment in the solid fraction has been successfully demonstrated. For example, Zhang and associates reported <20% xylan removal from wheat straw and sugarcane bagasse when they pretreated the biomasses with 0.5 M NaOH at 80 °C for 6 h. The resulting pretreated wheat straw and sugarcane bagasse contained 89.9% and 92.9% carbohydrate fraction, respectively.[20] Earlier, while evaluating various pretreatment methods for anaerobic digestion of *Miscanthus floridulus*, alkaline peroxide (2% H_2O_2 at 35 °C for 24 h at pH 11.8) pretreatment removed >70% lignin, enriching pretreated biomass with 99.82 and 83.03% glucan and xylan fractions, respectively.[21] In yet another variation, Gong *et al.* (2020) achieved >70% delignification of corn stover by treating it with 5% alkaline methanol at 80 °C for an hour and retaining ∼89.5 and 88.5% glucan and xylan fractions in the solid biomass.[22]

1.1.3 Pretreatment strategies favouring biomass fractionation & holistic utilization of biomass components. The two-stage fractionation process has been another lucrative alternative for xylan removal in the first stage, followed by delignification in the later stage. Recently, beechwood was subjected to a two-step fractionation process in which pre-hydrolysis at 150 °C for 90 min was performed with 20 mM H_2SO_4. As a result, ∼85.8 wt% xylan was recovered in stage I. When in the second step, organosolv treatment was performed with a 1 : 1 ethanol–water mix and 80 mM H_2SO_4 at 150 °C for 70 min, ∼82.7 wt% lignin yield was obtained in the liquid fraction leading to the generation of a highly digestible cellulose-rich pulp.[23] Earlier, Smit and Huijen evaluated seven different feedstocks: wheat straw, corn stover, beechwood, poplar, birchwood, spruce, and pine for mild organosolv pretreatment with 50% acetone and <50 mM H_2SO_4 at 140 °C for 2 h. Irrespective of biomass type, 87–97% xylan hydrolysis was observed. Poor delignification yields were obtained only in spruce and pine, while glucan recoveries ranged between 68 and 94%. Later the group precipitated the dissolved lignin by diluting with water, leading to effective fractionation of all three components of different LCBs.[24]

Recently, Xu *et al.* devised a mild technique for hemicellulose extraction from poplar wood with a binary solvent system containing formic acid and water. Pretreatment at 90 °C for 4 h resulted in 73.1% xylose yield while the solvent was recovered by fractional distillation and recycled back for a second round of pretreatment.[25] The following section emphasizes the use of novel solvents for complete LCB fractionation. Chen *et al.* used 1% H_2SO_4 with 75% choline chloride to fractionate cellulose of switchgrass from lignin and xylan fractions. Treatment with this acidified deep eutectic solvent (DES) at 120 °C for 25 min removed 76% of the xylan fraction along with 51.1% delignification. Five cycles of recycling and reuse of this acidified liquor enriched the hydrolysed xylan and lignin fraction. Later, the group used xylose-rich liquor for furfural production at 160 °C for 15 min with 2% w/v $AlCl_3$ and recovered lignin.[26] Very recently, a biphasic acidic water/phenol system was used for the fractionation of *Populus* wood chips.[27] This unique biphasic system enriched the water-soluble phase with 77% xylose and negligible by-products when the chips were subjected to 120 °C for an hour. In contrast, the phenolic phase contained 90% dissolved lignin (90%), leaving solids retaining 96% of the original cellulosic fraction.[27] Likewise, a novel biphasic system comprising 2-phenoxyethanol and acidified water (70 : 30) was used to fractionate rice straw.[28] Pretreatment at 130 °C for 2 h led to cellulose-rich (86.48% retained) biomass, facilitated by 92.1 and 63.16% removal of hemicellulose and lignin fractions, respectively. Later, 92.6% pure lignin was recovered by simple precipitation and 81.83% of xylan/xylose enriched in the aqueous phase.[28] Yang *et al.* evaluated the effect of *p*-toluenesulfonic acid (*p*-TsOH) on the fractionation of three feedstocks: corncobs, wheat straw, and miscanthus. Pretreatment at 80 °C for 10 min resulted in significant removal of lignin and xylan, leaving a cellulose-rich pulp. Later, spent liquor was diluted to precipitate lignin, and the reusability of *p*-TsOH was shown to be ∼5 times higher.[29] A similar attempt was made by yet another green hydrotrope, maleic acid (MA), for the effective fractionation of birchwood.[30] At 100 °C and 50 wt% MA, 94.5% of the cellulosic fraction was obtained as a solid after 30 min. Lignin was precipitated by dilution, and the solubilised xylan was converted to furfural with ∼70% yield. Furthermore, MA displayed ∼3 times recyclability with comparable performance.[30] Earlier, the cosolvent enhanced lignocellulose fractionation (CELF) method was developed for pre-treating corn stover using 0.5% H_2SO_4 and tetrahydrofuran (THF) in the ratio of 1 : 1. The dilute acid hydrolysed xylan to xylose which later dehydrated to furfural, while THF led to lignin dissolution enriching the cellulosic biomass. Later, the group separated furfural from THF. The latter was recovered by vacuum distillation and recycled, leaving lignin as a powder.[31]

2. Chemo-catalytic transformation of xylose to high-value chemicals

Chemo-catalytic routes are the conventional processes for the conversion of petroleum derivatives into bulk, fine and speciality chemicals. Like biological routes, several chemical routes exist *via* which xylose can be converted to a wide range of products such as furfural, furfuryl alcohol, xylitol, levulinic acid, levulinic ester, and other value-added chemicals, as shown in

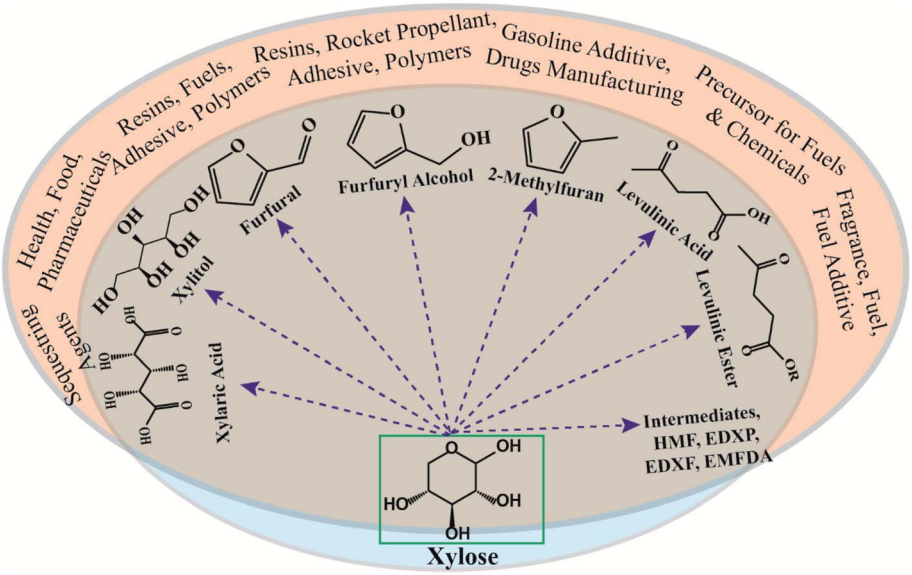

Fig. 2 Catalytic routes for xylose conversion to value-added chemicals.

Fig. 2.[32,33] In general, xylose conversion proceeds either *via* hydrogenation reaction in the presence of a metal catalyst to yield xylitol or isomerization reaction in the presence of a Lewis acid catalyst to produce xylulose. Xylulose further dehydrates to yield furfural in the presence of a Brønsted acid catalyst. Notably, furfural's estimated global market size was valued at $1.2 billion in 2019 and is expected to grow further to $2 billion by 2027 which makes it the most attractive and widely produced product from xylose (https://www.alliedmarketresearch.com/press-release/furfural-market.html, accessed on 29-03-2021). Xylose can be converted to furfural *via* an enol route, β-elimination, tautomerization and several other routes in the presence of a homogeneous or a heterogeneous catalyst, and the catalyst must have acidic properties.[34] Therefore, a wide range of homogeneous mineral acids such as sulfuric acid, hydrochloric acid, nitric acid, phosphoric acid, acetic acid, and formic acid have been used for xylose conversion to furfural.[35] It is noteworthy that 60–70% of the total furfural produced globally is used for manufacturing furfuryl alcohol.

Interestingly, xylose can also be directly converted to furfuryl alcohol *via* the hydrogenation route by using a metal catalyst. The development of such processes may minimize the conventional multistep and tedious method of converting xylose to furfural and then hydrogenating it to produce furfuryl alcohol. In this regard, the Zhu group reported 87.2% furfuryl alcohol yield in the presence of a $Cu/ZnO/Al_2O_3$ catalyst in a continuous fixed-bed reactor at a temperature of 150 °C.[36] Furthermore, the authors observed that increasing the reaction temperature to 190 °C alters the xylose conversion pathway to yield 86.8% 2-methyl furan.[36] Therefore, the final product from xylose conversion *via* hydrogenation can be altered by tuning the operating parameters and catalytic materials. For example, Li and co-workers have carried out the xylose conversion to levulinic acid and levulinic esters in a high-pressure hydrogenation reactor using a Pd/Al_2O_3 catalyst. The conversion yields of levulinic acid and levulinic esters achieved were 40 and 10%, respectively.[37]

It is also worth mentioning that hydrogenation of xylose at an industrial scale is being done since the 1970s to produce an essential chemical, xylitol.[38] In general, the xylitol production process takes place in the presence of a metal catalyst and hydrogen source at 353–413 K temperature and 1–8 MPa pressure for 15–360 minutes of reaction time.[39] The xylose to xylitol conversion is a surface controlled reaction; therefore, the interaction between adsorbed/unadsorbed xylose and chemisorbed hydrogen and the catalyst surface dictates the process's overall yield. In contrast, the product xylitol does not desorb easily from the catalyst surface, thereby causing the catalyst's saturation.[40] Interestingly, some of these metal catalysts can also be used to convert xylose into xylaric acid *via* oxidation reaction. For example, Saha and co-workers have observed 60% xylaric acid yield in the presence of a Pt/C catalyst *via* oxidation reaction. However, limited data are available for such reactions. The xylose-based conversion *via* chemical routes suffers from lower yields and furthermore, the use of acidic catalysts and reaction operation at higher temperatures and pressures make the process environmentally unfriendly. Although many chemical processes such as xylitol production are running at the commercial scale, the long-term sustainability is doubtful due to the high cost of production and environmental incompatibility.

3. Xylose metabolism: genetics and biochemistry of enzymes and their regulation

Xylose valorisation through biotechnological intervention has the potential to become the most popular route for producing various bio-based chemicals and fuels. A diverse group of

microbes such as bacteria, yeast, and fungi are known to assimilate xylose naturally through different metabolic pathways leading to formation of a range of products such as xylitol, 2,3-butanediol, ethanol-*n*-butanol, lactic acid, succinic acid, *etc.* A considerable knowledge on these pathways can provide guidance in constructing efficient xylose assimilatory strains.

3.1 Xylose assimilation

The process of D-xylose assimilation is quite different from that of D-glucose assimilation, which is metabolized through the Embden–Meyerhof–Parnas (EMP) pathway. D-Xylose undergoes isomerization or reduction and subsequent oxidation to form D-xylulose. D-Xylulose is the key intermediate for the pentose phosphate pathway, and upon phosphorylation is converted into xylulose-5-phosphate (X5P), which is funnelled to the central carbon metabolism to generate C3–C7 metabolites (Fig. 3). These metabolites can be either precursors or intermediates for the EMP pathway, and biosynthesis of amino acids and nucleotides.[41,42]

3.1.1 Xylose isomerase (XI) pathway. The XI pathway (Fig. 3) is commonly found in prokaryotes. In this pathway, the initial isomerization of xylose to xylulose is mediated by xylose isomerase (XI), followed by phosphorylation of xylulose to xylulose-5-phosphate (X5P) by xylulose kinase (XK). The X5P enters the pentose phosphate pathway (PPP) and later the central carbon metabolism through a C3 metabolite, glyceraldehyde-3-phosphate.[43]

Xylose isomerases (EC. 5.3.1.5) (D-xylose → D-xylulose) encoded by the *XylA* gene are metal dependent enzymes classified into two different classes, I and II. These two enzyme classes differ in length of the polypeptide chain, where class II enzymes have an additional 34 amino acid residues on the N-terminus compared to class I. The catalytic activity of XI is conserved at two sites of histidine residues H101 and H271 and induced in the presence of xylose. XI mediates the synthesis of xylulose *via* a hybrid shift mechanism for ring opening to form an open chair conformation.[44] The substrate binding at the active site was observed by fluorescence quenching at two conserved regions W29 and W188 with the tryptophan residue at W29 being essential for catalytic activity. The genome mining and sequencing in the thermophilic *Bacillus coagulans* strain identified that the *XylA* gene consisting of 1338 base pairs encodes for 50 KDa class II protein with 445 amino acids. The amino acid identity of *B. coagulans* XI gave a homology of 65, 64, 58, 48 and 25% with *Lactobacillus brevis*, *L. pentosus*, *L. lactis*, *Piromyces* sp. E2, and *Streptomyces albus*, respectively.[45] Thermostable XI with maximum enzyme activity at 85 °C and neutral pH was isolated from thermophilic strains like *Thermoanaerobacterium ethanolicus*.[46] Similarly, the *Streptomyces* sp. F-1 strain, a new isolate, has two copies of *XylA* genes, and the biochemical characterization presented a significant difference in their optimal temperature. The protein coded from *XylA*1 and *XylA*2 displayed maximum activity at 60 and 75 °C, respectively.[47] The structural characteristics and enzyme kinetics of XI are well investigated. An interesting feature of XI is that the enzyme operates with high activity within a broad temperature range of 30–85 °C. However, it is sensitive to pH change and the maximum specific activity was observed at a physiological pH range of 6.0–8.0 which declined rapidly under strong acidic or alkaline conditions.[46,48] It was also observed that the divalent metal ions are a pre-requisite for the activation and stabilization of the enzyme activity. The presence of Mg^{2+}, Co^{2+}, or Mn^{2+} has a profound positive effect compared to other divalent metal ions, while Ni^{2+} has been found to be inhibitory for the enzyme. These metallic cofactors also protect the enzyme from thermal denaturation.[45]

Xylulokinase (XK) (EC 2.7.1.17) is a substrate (D-xylulose) specific kinase enzyme catalysing the phosphorylation reaction D-xylulose + ATP → D-xylulose-5-phopsphate + ADP. XK in *B. coagulans* is a 56 kDa protein consisting of 1536 bp with 511 amino acids. The amino acid identity of XK from *B. coagulans* revealed a sequence homology of 56, 49, 38 and 25% with *L. pentosus*, *L. lactis*, *E. coli*, and *Scheffersomyces stipitis*, respectively. However, the homology between xylulokinase of *B. coagulans* and *L. brevis* was only 19%. During the activity measurement at different pHs, the maximum activity of XK was observed at an optimal pH and temperature of 7 and 85 °C, respectively, while the enzyme lost 20% and >50% of the activity when the pH was reduced to 6.0 or increased to 8.0, respectively. Similar to XI, the divalent ions Co^{2+}, Mn^{2+}, and Fe^{2+} enhanced the activity of XK.[45]

3.1.2 Xylose reductase (XR)–xylitol dehydrogenase (XDH) pathway. In yeast and fungi, xylose is assimilated through the xylose reductase (XR)–xylitol dehydrogenase (XDH) pathway. In the first step, xylose is reduced to xylitol mediated by NAD(P)H dependent xylose reductase (XR; EC 1.1.1.21) followed by oxidation of xylitol to xylulose catalysed by NAD^+ dependent xylitol dehydrogenase (XDH; EC 1.1.1.9) (Fig. 3). Identical to bacterial metabolism, xylulose is further phosphorylated to xylulose-5-phosphate and metabolised through the pentose phosphate pathway.[49–52] The xylose fermenting yeasts (*Candida shehatae*, *Scheffersomyces* (*Pichia*) *stipitis*, *Pichia fermentans*, *Spathaspora* sp., *etc*) employ the XR–XDH pathway for assimilation of xylose, and most of the yeasts utilize xylose under aerobic conditions.[53–55]

Xylose reductase (XR; EC 1.1.1.21) [D-xylose + NAD(P)H → xylitol + $NAD(P)^+$] is a 36 KDa protein containing 322 amino acids and is a member of aldoketoreductase family 2 (AKR2). AKRs are superfamilies of enzymes that catalyse the reversible reduction of aldehydes or ketones to their respective alcohols utilizing NADPH as a cofactor. XR is a highly important enzyme when the desired product is xylitol, a molecule with nutritional and pharmaceutical value. Son *et al.* (2018) reported the crystal structure of XR from *S. stipitis*. XR is a dimer with two polypeptide chains made of 15 α-helices and 10 β-strands each with conserved catalytic sites at Asp43, Tyr48, Lys77 and His110.[51] The literature describes the flexibility of XR in using NADPH as well as NADH as a cofactor. The K_m values of NADPH and NADH for XR in *S. stipitis* are 0.0277 and 0.136 mM, respectively, indicating more affinity and specificity for NADPH than NADH. Although the physiological function of XR is to reduce D-xylose, the K_m value of D-xylose for XR is very high (39.4 mM), indicating that a high level of xylose is needed to drive xylose metabolism

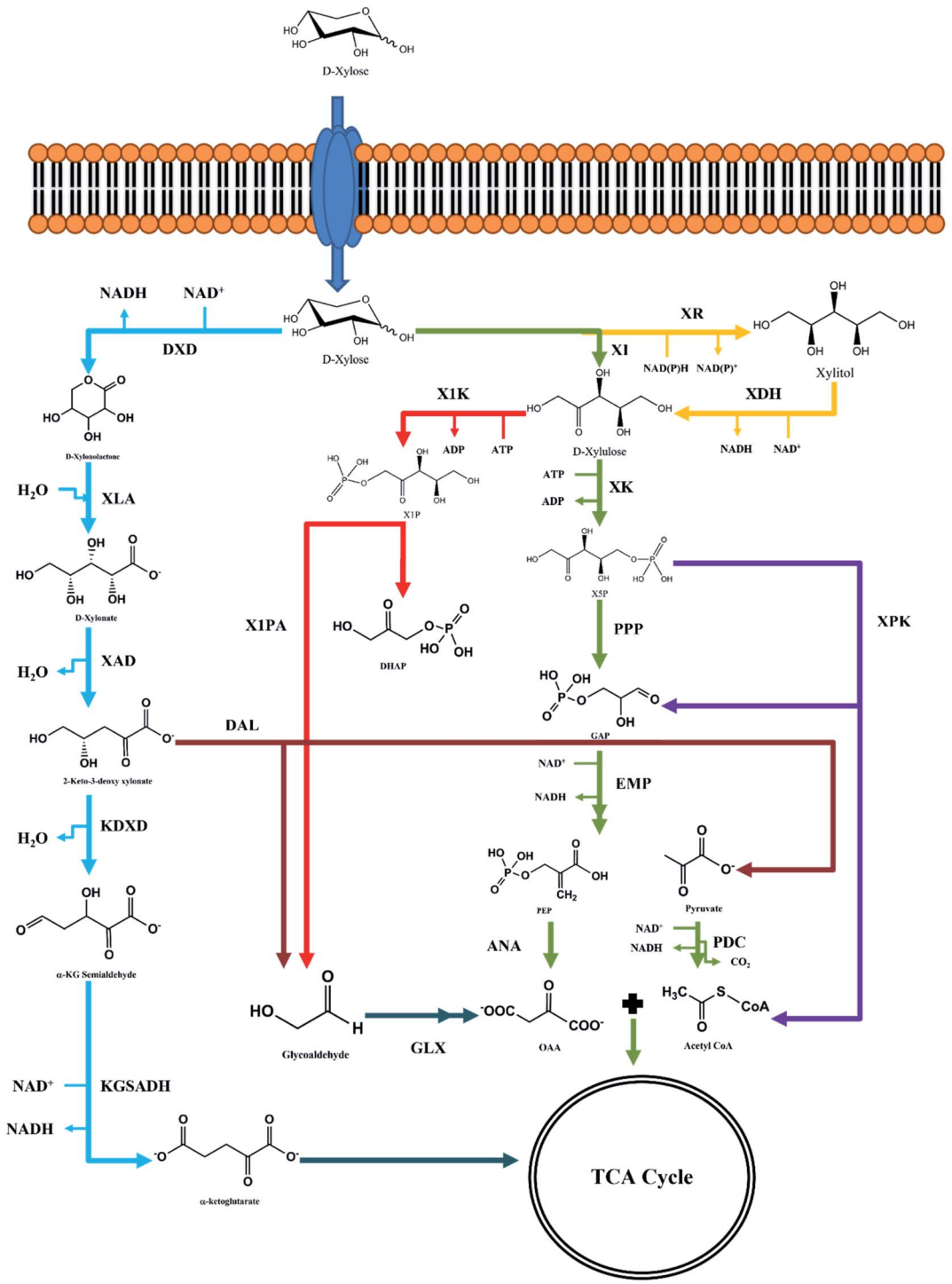

Fig. 3 Illustration of xylose transport inside the microbial cell and further dissimilatory pathways directing the carbon flux into central carbon metabolism. Abbreviations: DXD: xylose dehydrogenase; XLA: xylonate synthase; XAD: xylonate dehydratase; KDXD: 2-keto-3-deoxyxylonate dehydratase; KGSADH: ketoglutarate semialdehyde dehydrogenase; XI: xylose isomerase; XR: xylose reductase; XDH: xylitol dehydrogenase; X1K: xylulose-1-kinase; X1PA: xylulose-1-phosphate aldolase; DAL: 2-keo-3-deoxyxylonate aldolase; GLX: glyoxylate shunt; XLK: xylulose-5-kinase; XPK: phosphoketolase; PPP: pentose phosphate pathway; EMP: Embden–Meyerhof–Parnas pathway; Weimberg pathway (blue); isomerase pathway (green); Dahms pathway (brown); XR–XDH pathway (yellow); phosphoketolase pathway (violet); synthetic pathway (red).

efficiently. The structural conformation of the enzyme displays the presence of a hydrophobic binding pocket. It could be one of the reasons for the low affinity of XR towards xylose which has a high degree of hydrophilicity due to the presence of five hydroxyl groups. Similar to *S. stipitis*, a dimeric XR structure with K_m of 87 mM for D-xylose has been elucidated in *Candida*

tenuis.[56] Recently, new xylose utilizing yeasts of *Spathaspora* sp. were characterized to have high XR activity which were mostly NADPH dependent, except three species, *Sp. arborariae*, *Sp. gorwiae*, and *Sp. passalidarum*.[57,58] The genome mining resulted in two putative XR genes, where *SpXYL1.2* has relatively higher XR activity with NADH, and the strain could assimilate xylose effectively under anaerobic conditions. In *Sp. arborariae*, XR accepts NADH and NADPH as cofactors, with an affinity (K_m) of 12.8 (NADH) and 26.1 (NADPH) μM, respectively. In the presence of xylose as a substrate, the affinity was observed to strengthen with K_m of 29.5 (NADH) and 57.5 (NADPH) mM, respectively.[53,57]

Xylitol dehydrogenase (XDH; EC 1.1.1.9) or xylulose reductase (xylitol + NAD^+ → D-xylulose + NADH) mediates the conversion of xylitol to D-xylulose and is a well characterized enzyme encoded by a nucleotide sequence of 1089 bp, and the operon reading frame codes for a protein containing 363 amino acids, with an approximate mass of 38.5 KDa. The XDH mediates the oxidation of xylitol using NAD^+ as a cofactor.[59,60] The NAD^+-dependent XDH is a homotetramer which forms heteronuclear multi-metal protein with 1 mol of Zn^{2+} and 6 mol of Mg^{2+} ions per mol of 37.4 kDa protomer (structural subunit of an oligomeric protein) with K_m of 39 μM for xylitol. The XDH enzyme displayed a half-life of 300 h in 50 mM Tris buffer at pH 7.5. Metal ions like Co^{2+}, Mn^{2+}, and Zn^{2+} exert an inhibitory effect on the enzyme and the activity completely ceases at 5.0 mM concentration of these metal ions. But complete dissociation of Zn^{2+} from the enzyme was observed to inactivate XDH completely.[61]

3.1.3 Weimberg pathway. In 1946, Lockwood and Nelson identified a non-phosphorylative hexose and pentose sugar pathway in *Pseudomonas* and *Acetobacter* spp., wherein the oxidation of sugars resulted in accumulation of the respective sugar (gluconic and pentonic) acids.[62] Later in 1961, Ralph Weimberg elucidated the pathway in *Pseudomonas fragi*, and the pathway was termed after Ralph Weimberg as the Weimberg pathway. Analogous to the glyoxylate cycle, it is a carbon conserving route for xylose metabolism to α-ketoglutarate as there is no carbon loss like in the TCA cycle. The oxidative route consisted of five step enzymatic reactions converting pentose sugars to α-ketoglutarate without any loss of carbon (Fig. 3).[63] The pathway starts with oxidation of D-xylose to D-xylonolactone by D-xylose dehydrogenase (DXD encoded by *XylB*) which is further hydrolysed to D-xylonate by xylonolactone lactonase (XLA encoded by *XylC*) *via* a ring opening mechanism. The D-xylonate formed is dehydrated in subsequent reactions to form α-ketoglutarate semialdehyde with 2-keto-3-deoxy xylonate as an intermediate. Both the dehydration reactions were predicted to be catalysed by xylonate dehydratase (XAD encoded by *XylD*) and 2-keto-3-deoxy-xylonate dehydratase (KDXD encoded by *XylX*). Finally, the α-ketoglutarate semialdehyde is oxidized to form α-ketoglutarate, by an α-ketoglutarate semialdehyde dehydrogenase enzyme (KGSADH encoded by *XylA*).[64]

The BLAST analysis of the *P. fragi* genomic database revealed that *Caulobacter crescentus*, *Burkholderia xenovorans*, and *Chromohalobacter salexigens* have possible genes mediating the Weimberg pathway. In 2007, Craig Stephens and associates observed the expression of *XylXABCD* genes, when a freshwater bacterium, *C. crescentus*, was grown on D-xylose as the sole carbon and energy source. Recently, it has been found that *Pseudomonas taiwanensis* VLB120 can assimilate D-xylose through the Weimberg pathway, but the initial oxidation and hydrolysis reactions are mediated by glucose dehydrogenase (EC 1.1.5.2) and gluconolactonase (EC 3.1.1.17) instead of DXD and XLA. Similar behaviour was also observed in *P. putida* strains wherein DXD and XLA are involved in gluconic acid production.[65] Further, determination of kinetic parameters K_m and V_{max} revealed two rate limiting reactions in the Weimberg pathway mediated by Mn^{2+} dependent XDH and NAD^+ dependent KGSADH.[66] Therefore, D-xylose assimilation by the Weimberg pathway requires external supplementation of metal ions (Mn^{2+}) and availability of NAD^+ for complete conversion of D-xylose into α-ketoglutarate.

3.1.4 Dahms pathway. Until 1974, it was understood that xylose is metabolized *via* XI and XR–XDH pathways and rarely through the Weimberg pathway. But, a novel aldolase (EC 4.1.2.18) was discovered by Stephen Dahms in *Pseudomonas* sp. to cleave 2-keto-3-deoxy xylonate, the intermediate of the Weimberg pathway, to pyruvate and glycolaldehyde and the pathway was termed as the Dahms pathway (Fig. 3). The aldolase is specific to 2-keto-3-deoxy-D-xylonate, but not to L-isomers. Similarly, the pathway was also elucidated for L-arabinose assimilation where the enzyme mediating the conversion is an L-isomer specific aldolase.[67–69]

3.1.5 Non-natural or synthetic pathway. With the advancements in the genetic engineering approaches and availability of numerous genomic databases, it would be simpler to find alternative routes to the natural pathways so that the end product can be achieved in a few simple steps without imposing the metabolic burden and disturbing the microbial cell integrity. To this end, a non-natural synthetic pathway was constructed for xylose metabolism, where D-xylulose is converted to D-xylulose-1-phosphate (X1P) instead of X5P. This phosphorylation reaction leading to X1P is mediated by xylulose-1-kinase and the pathway is termed as the X1P pathway. In further aldolytic cleavage, X1P is converted to glycolaldehyde and dihydroxyacetone phosphate (DHAP), an intermediate of the EMP pathway (Fig. 3). Through this non-natural or synthetic pathway, D-xylose is converted to DHAP in two sequential steps, whereas in PPP or through EMP pathways multiple steps are involved.[70]

3.2 Xylose operon

The genes responsible for the xylose transport and assimilation are clustered into an open reading frame called a xylose (*xyl*) operon. In bacteria, xylose metabolism is mediated through the XI pathway.[71] The genes responsible for the metabolism of xylose were observed to be organized into two major transcriptional units *XylAB* and *XylFGHR* with promoters P_A and P_E, respectively. It was observed that the transcriptional activation is induced by xylose and repressed by glucose, *i.e.* as long as glucose is available, the xylose assimilation will be suppressed.[72] The transcriptional units *XylAB* and *XylFGHR* were observed to

be located at 80 min on the chromosome map.[73] *XylAB* consists of genes encoding for XI (*XylA*) and XK (*XylB*), respectively. *XylFGHR*, a high affinity ABC type transporter for transport of xylose, consists of four subunits where *XylH* acts as the transmembrane transporter, *XylF* binds to xylose and *XylG* is an ATP binding protein that mediates the phosphorylation of xylose. Subsequently, the transported xylose is acted upon by XI and XK, to form xylulose-5-phosphate. The *XylR* gene has been observed to be constitutively expressed under a weak promoter P_R regardless of xylose or glucose availability. The repressor tends to bind two DNA binding regions I_A and I_E, upstream to the transcriptional promoter's consensus sequences and adjacent to the RNA polymerase binding site. In the presence of xylose, *XylR* forms a dimer with the xylose substrate, and causes activation of two promoters P_A and P_E, resulting in simultaneous transcription of *XylFGH* and *XylAB* genes. Any mutation in the repressor protein *XylR* was observed to abolish the expression of P_A and P_E promoters.[74,75] In *E. coli* the xylose transport into the microbial cell is mediated by low affinity transporter *xylE*, and the expression was observed to be 10-fold higher when the external medium was supplemented with xylose.[76] Though the xylose dissimilation follows the XI pathway in Gram-positive bacteria, the regulation was observed to be different in few enteric bacteria like *B. subtilis* and *Lactobacillus* strains, where the *XylR* gene displays repressive behaviour rather than acting as a transcriptional activator. The *XylR* of *B. subtilis* and *Lactobacillus* strains is not homologous to its counterpart in *E. coli* and binds to a palindromic sequence upstream to the transcriptional start codon, repressing the transcription activation and the repression effect is relieved in the presence of xylose.[77] In *Staphylococcus xylosus*, three open reading frames containing 4520 nucleotide bases were annotated as *XylR*, *XylA* and *XylB* genes. The BLAST studies of the *XylA* gene presented 65% and 51% similarity with *B. subtilis* and *E. coli*, respectively.[78]

In the genera Clostridia, *C. acetobutylicum* is the representative strain for investigating different metabolic activities. The whole genome sequence is available along with the required genetic tools for strain engineering. Genome mining through a subsystem-based approach revealed the presence of a novel XI (CAC2610), and further characterization indicated that it is not homologous to known XI (*XylA*) genes. Along with XI, XK (*XylB*, CAC2612), a xylose proton symporter (*XylT*, CAC1345), and a transcriptional regulator (*XylR*, CAC3673) were also sequenced and characterized. The *C. acetobutylicum* strains are well known to utilize a broad range of monosaccharides, disaccharides, starches, and other polysaccharides like xylan and xyloglucan. Xylan and xyloglucan are the major components of the hemicellulosic fraction of plants. The depolymerization of xyloglucan and xylan results in α- and β-xylosides, respectively. These xylosides are transported into the cell and further degraded into xylose. The genetic make-up for utilizing these xylosides was mainly observed in firmicutes like *Bacillus*, *Lactobacillus* and *Clostridium* spp. In *B. subtilis* and *C. acetobutylicum*, xylose operon contains two clusters, *XylAB* and *XynTB*. The *XynT* gene encodes the ABC transporter that transports β and α-xylosides into the microbial cell and further the *XynB* gene converts xyloside into D-xylose.[73,79]

In yeast and fungi, xylose is sequentially metabolised through three cytosolic enzymes, XR, XDH and XK, to convert it to xylulose-5-phosphate. *S. stipites* the most efficient xylose fermenting yeast was characterized to reveal the genes encoding XR (*Xyl1*), XDH (*Xyl2*), and XK (*Xyl3*) enzymes. The genes are either co-localized or distributed in the genome; for example in *S. stipitis*, *Xyl1* was observed on chromosome (Chr) V, *Xyl2* on Chr I, and Xyl3 on Chr VIII. Although *S. cerevisiae* strains are not native xylose utilizing strains, a putative XDH (*Xyl2*) gene was identified on Chr XV, and XK on Chr VII.

3.3 Carbon catabolite repression or the glucose effect: the natural phenomenon arresting the simultaneous conversion of mixed sugars

Microorganisms cultured on mixed sugar substrates display a pattern of two successive exponential phases during growth, called diauxic growth. The occurrence of this growth pattern is due to utilization of the preferred substrate which suppresses the uptake of other carbon sources present in the medium and this phenomenon is known as carbon catabolite repression (CCR) or the glucose repression effect.[80,81] The diauxic growth significantly affects the utilization of mixed sugars and increases the length of fermentation (decreased productivity).

LCB or agricultural residues as the feedstock for the production of biofuels and bioproducts has received considerable interest.[6] It is not just surplus agro-residual biomass, utilizing LCB as feedstock addresses various environmental concerns and the food *vs.* feed debate with first generation starchy feedstocks. As LCBs are polymers of celluloses and hemicelluloses, hydrolysates derived after pretreatment and saccharification contain a mixture of hexoses (mostly glucose) and pentoses (mostly xylose).[41,80] The growth of microorganisms on hydrolysates containing mixed sugars results in suppression of pentose sugar utilisation. The mechanism and the strategies to overcome the limitation are discussed in this section. Aidelberg and co-workers observed a hierarchical fashion of utilization of hexoses and pentoses. When the microorganism is grown on mixed sugars (glucose, arabinose and xylose) as substrates, the most preferred carbon source has an inhibitory effect on other sugars; for example, glucose represses the uptake of arabinose and xylose, and upon glucose depletion, the next preferred substrate is arabinose, and the xylose utilization mechanism is still inhibited.[82] From the literature, it was explained that the mechanism occurs due to two reasons: (i) inhibition of expression of the genes involved in the non-glucose sugars by 3′,5′-cyclic adenosine monophosphate (cAMP). cAMP is a secondary messenger, derivative of ATP, synthesized by an adenylate cyclase enzyme. In bacteria, cAMP levels depend on the type of growth medium. Intracellular transportation of glucose inhibits the adenylate cyclase enzyme and decreases cAMP and cAMP receptor protein (CRP), which inhibits the transcription of the *xyl* operon;[83] (ii) inhibition of xylose transport mediated by dephosphorylated PTC component $EIIA^{glc}$ that binds to the cognate sugar transporter and

prevents the transport, and the mechanism is inducer exclusion (Fig. 4A).[84] However, in the phosphorylated form, the EIIA^{glc} component activates the adenylate cyclase, which improves intracellular cAMP levels. Improved cAMP levels bind with CRP to form a complex, and the active cAMP–CRP complex could bind to the ORF and express the permeases and other genes involved in the metabolism of non-glucose sugars (Fig. 4B).[85]

In *B. megaterium*, the glucose mediated xylose repression was 14-fold, and the *XylR* gene which regulates the transcription initiation by binding to promoters of *XylAB* and *XylFGH* was modified by incorporating a kanamycin resistance gene resulting in lowering the repression to 8-fold, and deletion of 184 bp at the 5′-end of the *XylR* gene further reduced repression by 2-fold.[85,86] An alternative CCR mechanism called feedback inhibition was observed in a few Gram-positive bacteria, in which catabolite control is exerted by catabolite control protein A (*ccpA*). The *ccpA* is a dimeric transcriptional regulator, expressed constitutively regardless of the carbon source. In the presence of glucose and other glycolytic intermediates like fructose 1,6-bisphosphate, the histone protein (HPr) component of the enzyme phosphorylation cascade (PTS enzyme I, HPr, and Enzyme II), the major facilitator of sugars, is phosphorylated at the serine residue (*HPr-Ser^{46}-P*) instead of the histidine residue. The phosphorylated *HPr* binds to catabolite control protein (*ccpA*), and the complex binds to catabolite repressive element (*CRE*) within the transcriptional or coding sequence upstream of the promoter region by blocking the transcription of pentose sugars.[87] In *C. acetobutylicum*, deletion

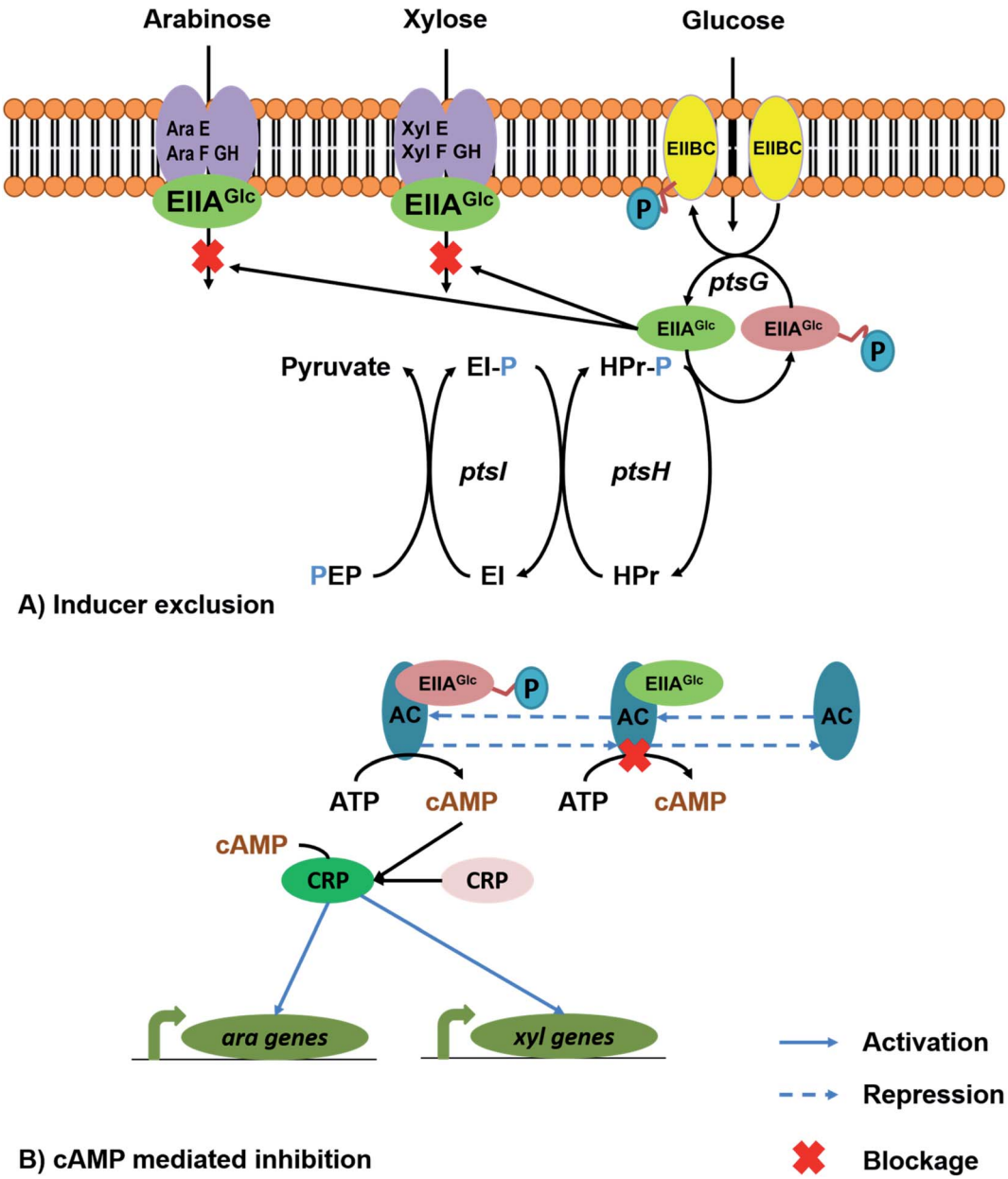

Fig. 4 Illustration of possible mechanisms for carbon catabolite repression: (A) inducer exclusion and (B) cAMP mediated inhibition.

of *ccpA* and the enzyme II complex was attempted but it resulted in an impaired growth rate and failure in metabolic flux.[87] But in *B. subtilis*, deletion of CRE protein could overcome the degree of repression from 13- to 2.5-fold.[88] The successful development of the CCR negative strain would be of high value with the capacity to assimilate glucose and non-glucose sugars simultaneously causing an increase in the yield and productivity.

4. Hurdles requiring debottlenecking for efficient xylose metabolism

4.1 Transport of xylose into the microbial cell

Xylose metabolism is well investigated and characterised in bacteria, fungi, yeast, and few archaea. In these prokaryotic and eukaryotic organisms, the xylose metabolism is either native or heterologously expressed to shape the cellular metabolism to rely on xylose as a sole carbon and energy source. Before the start of xylose metabolism, the sugar must be transported into the microbial cell (Fig. 5). The possible mechanisms for transport of sugars through the membrane are passive diffusion, facilitated diffusion and active transport.[89] Passive diffusion is the simplest process that occurs based on the concentration gradient of the substrate between the intracellular environment and the extracellular medium, while in facilitated diffusion a carrier protein mediates the transfer based on the concentration gradient. In active transport, the translocation of sugar through the transmembrane proteins happens with energy expenditure. Usually, transmembrane proteins that span across the outer membrane mediate the translocation from the extracellular space to the intracellular environment. These transmembrane proteins belong to the major facilitator superfamily (MFS), and are divided into three classes based on the functionality, (i) uniporters, which transport a single substrate across the membrane; (ii) symporters, which transport one substrate coupled with a charged molecule; and (iii) antiporters, by which two different substrates are translocated in the opposite directions.[90]

In bacteria there are three possible mechanisms known for the transport of xylose into the microbial cell, (i) the H^+/Na^+-symporter, which is identified in *E. coli*,[91] *Salmonella typhimurium*, *B. megaterium*, *L. brevis*, and *B. subtilis*, (ii) PEP:carbohydrate phosphotransferase system, which is identified in *E. coli* and uses PEP as the source of energy, and (iii) ATP driven ABC transportation periplasmic binding protein, identified in *E. coli* and few other *Bacillus* spp. Facilitated diffusion is not well known in bacterial populations, except the glycerol facilitator protein (*GlpF*) in *E. coli* and glucose transporter (*GlfZ*) in *Zymomonas mobilis*. In lactic acid bacteria, the phosphoenol pyruvate (PEP) D-mannose phosphotransferase system (PTS) with two integral membrane proteins EIICMan and EIIDMan, and cytoplasmic phosphorylation proteins EIIAMan and EIIBMan is observed to have a significant role in xylose transport.[89]

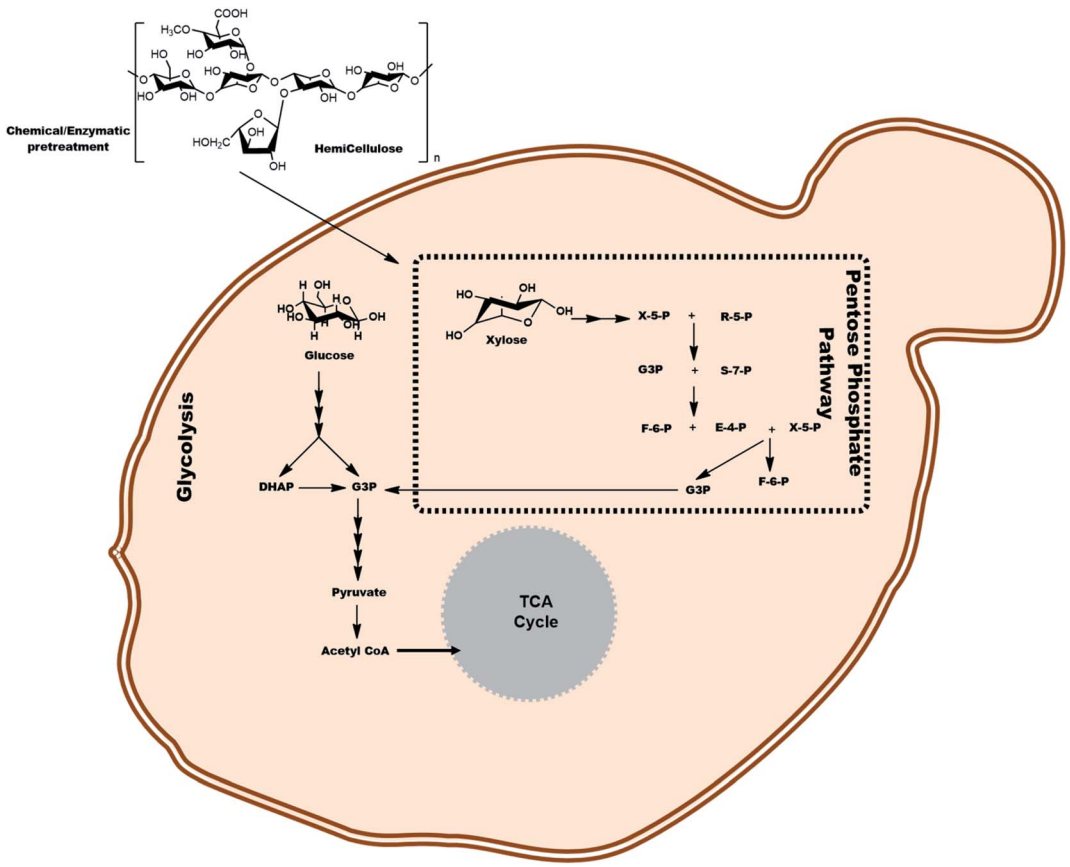

Fig. 5 Transport of xylose into the microbial cell and further flux into central carbon metabolism.

The endogenous transporters in the microbial cells have an affinity for glucose from low (K_m 50–100 mM) to high (K_m 1–2 mM), whereas for xylose the numbers can be up to 10 times higher.[92] For example, *Glf*, a promiscuous glucose-facilitated diffusion protein from *Z. mobilis* expressed in *E. coli*, has lower affinity towards xylose (K_m 40 mM) than glucose (K_m 4.1 mM), and V_{max} was observed to be two-fold higher for glucose, resulting in delayed xylose uptake and assimilation, when expressed in *E. coli* cells.[91]

There are two mechanisms identified in yeast for xylose transport, (i) membrane potential due to proton symport, or (ii) facilitative diffusion through low affinity transporters. *Scheffersomyces stipitis*, a well-known xylose metabolizing strain has low and high affinity carriers to mediate xylose transport, whereas in *C. shehatae*, facilitated diffusion and a low affinity symport mechanism was observed.[93,94] The sugar binding pockets in the transmembrane proteins have residues specific for sugar, and any alteration or changes in the glucose specific residues can alter the D-glucose uptake rate and increase the endogenous xylose transport. Farwick *et al.* (2014) implemented this method in altering the amino acid sequence which interacts with the C6-hydroxymethyl group of D-glucose, but the deletion of those specific amino acids led to deleterious effects on the transport of glucose as well as xylose.[92] Wang and associates have studied the effect of 28 different site directed mutations on the xylose uptake rate and metabolism in the Mgt05196p transporter of *Meyerozyma guilliermondii*. The substitution mutations at Phe432Ala and Asn360Ser on Mgt05196p improved the xylose uptake, but diminished the glucose uptake, whereas the N360F mutation specifically enhanced the xylose transport without any glucose inhibition.[95]

Evolution is the natural mechanism of adapting to new environmental or physiological conditions. To create an order of natural evolution, a new approach called adaptive laboratory evolution (ALE) was attempted to increase the efficiency of xylose transporters *XUT3* and *GXS1* from *S. stipitis* and *C. intermedia*, respectively.[96] The *XUT3* is one of the seven high affinity xylose (*XUT*) transporters annotated in *S. stipitis* with similar specificity towards both glucose and xylose. The *GXS1* in *C. intermedia* is a broad range sugar transporter with specificity to carbon sources like glucose, arabinose, ribose, and xylose.[96] In this directed evolutionary approach, the substitution mutations Phe40Val, Phe465Ser, and Phe500Ser in *GXS1*, and Leu122Val, Phe343Leu, Gln345Arg, Ala298Thr, Tyr304Phe, and Lys542Arg in *XUT3* influenced the xylose uptake. The heterologous expression of these mutated transporters in *S. cerevisiae* resulted in a 70% increase in the specific growth rate on xylose.[96] The mutant transporters also displayed a phenomenal alteration in the diauxic growth and the evolved strain could simultaneously utilize xylose and glucose. In the sugar transporters, motif G–G/F-XXX-G is a conserved sequence present on the transmembrane component. After site-directed mutagenesis or ALE, a modified motif GGFIMG with larger side chains restricting the pore size for glucose transport and allowing smaller xylose molecules was identified. The alteration in the motif sequence because of point mutations increased the pentose specificity to the binding site by decreasing the pore size and transporting xylose efficiently compared to glucose.[97] However, bioprospecting for a novel xylose specific transporter or modification of an existing transporter to overcome the CCR induced by glucose will be beneficial and could significantly improve simultaneous glucose and xylose consumption.

4.2 Availability of redox cofactors and homeostasis

Redox homeostasis is an important consideration in microbial cell factories as it affects a wide range of genes, cellular functions and metabolite profiles, and redox balancing plays a critical role in coupling catabolism and anabolism. The co-factors involved in maintaining homeostasis are NADH and NADPH, which usually act as electron carriers and are involved in respiratory chain reactions (catabolism) and cell synthesis (anabolism), respectively. NADH is the predominant redox product of catabolism while NADPH has a greater role in anabolism with a major fraction coming from the pentose phosphate pathway and a delicate balance in the intracellular level of these cofactors is required to ascertain an optimal metabolic output. The $NADH/NAD^+$ ratio which reflects the intracellular redox state of a living cell and is influenced by various factors such as the physiological state of the cell, oxidation state of the substrate, the nature and presence of electron acceptors, and enzymes requiring redox factors.[98–101] The cells often start side reactions leading to byproduct formation which contributes towards the redox homeostasis. For example, during ethanol fermentation by *S. cerevisiae*, the yeast starts parallel formation of acetate and glycerol, NADH consuming reactions.

In the case of change in the substrate from glucose to xylose, a myriad of changes were observed in the metabolism, and the responses observed were increased amino acid concentrations, increased TCA cycle intermediates, and reduction in sugar phosphates and reducing equivalents or redox cofactors.[102] One of the challenges with xylose metabolism is maintaining redox homeostasis. After the first 3–4 specific steps of xylose metabolism, it is connected to central carbon metabolism. The majority of this problem stems from the first two steps where xylose is isomerised to xylulose *via* XR and XDH. The higher preference of XR towards NADPH generates $NADP^+$ while the second step requires NAD^+. The diminished synthesis of reducing equivalents and uneven demand during the xylose assimilation results in cofactor imbalance, which in turn affects the ATP yield and metabolic fluxes. The different cofactor preference of these two enzymes results in NAD^+ deficiency resulting in accumulation of the intermediate xylitol. The condition mostly prevails under anaerobic or oxygen limited conditions, where NADH cannot be oxidized to NAD^+, due to the absence of oxygen, the final electron acceptor.[103] This problem could be overcome by a continuous supply of NADPH and NAD^+.

To prevent the xylitol accumulation and further direct the flux of xylose carbon to central carbon metabolism, NADH oxidase (NOX) can be used. NOX catalyses a water forming reaction using oxygen as the electron acceptor ($NADH + H^+ + 0.5O_2 \rightarrow NAD^+ + H_2O$), thereby regenerating the NAD^+ molecules. The xylose assimilation through the XR–XDH pathway

linked with NADH oxidase could enable redox homeostasis. Zhang *et al.* (2012) constructed a cycle of regeneration using NOX, for regeneration of NAD^+.[104] In a similar approach, NOX from *L. lactis* was heterologously overexpressed in *S. cerevisiae* harbouring XR–XDH from *S. stipites* which resulted in a 69.6% decrease in xylitol accumulation, and more carbon flux was directed towards ethanol leading to an improvement of 39.3% in molar yields.[105]

Scheffersomyces stipitis has the ability to ferment xylose under anaerobic conditions, and thus under unfavourable conditions such as redox imbalance, the accumulated NADH can be utilized by NADH-dependent XR and circumvents the pathway.[50] In yeasts such as *S. stipitis*, XR has affinity for NADH as well as NADPH, and hence using advanced genetic engineering techniques, the cofactor specificity of XR in the required host strain can be altered, so that the cofactor requirement for the first two steps can be compensated internally and the continuous availability of cofactors can lead to improved xylose uptake and fermentation efficiency. A mutant XR enzyme K270M from *S. stipitis* with lower specificity to NADPH was expressed in *S. cerevisiae* and the cultivation of the strain with mutated XR on xylose showed a 16-fold reduction in NADPH and 4.3-fold increase in NADH specificity.[93] After a site directed mutagenesis approach on the XR enzyme in *C. tenuis*, a 170-fold change in cofactor preference from NADPH to NADH was observed in a Lys274Arg and Asn276Asp double mutant. When the mutant XR along with XDH from *Galactocandida mastotermitis* was expressed in *S. cerevisiae*, a 42% increase in ethanol, and a 52 and 57% decrease in xylitol and glycerol yields was observed, respectively, with xylose as the sole carbon source.[106] Similarly, a double mutant of *S. stipitis* XR (Arg276His and Lys270Arg/Asn270Asp) showed a decrease in catalytic efficiency and increase in K_m values towards NADPH, resulting in enhanced XR dependence on NADH. The strain expressing NADH-dependent XR efficiently utilized xylose, resulting in a 20% increase in the ethanol level and 52% decrease in xylitol accumulation.[107] A wild type NADH specific XR was identified from *C. parapsilosis*, in which the conserved motifs have arginine residues instead of lysine. Later, the structural integrity of NADH specific XR of *S. stipitis* was altered (Lys270Arg), and the *S. cerevisiae* strain expressing this modified XR diverted the flux of carbon towards ethanol with reduced xylitol accumulation.[108]

Besides overexpression of NOX and change in cofactor preference, a number of other approaches have been employed to alleviate the problem of redox imbalance. Under anaerobic conditions, NADH molecules are oxidized through a transhydrogenase shunt with malic enzyme (*MAE1*) (malate + $NADP^+$ → pyruvate + NADPH), malate dehydrogenase (*MDH2*) (oxaloacetate + NADH → malate + NAD^+), and pyruvate carboxylase (*PYC2*) (pyruvate + ATP → oxaloacetate + ADP) that can regulate the redox balance in *S. cerevisiae*. In a combinatorial cassette along with xylose metabolizing (XR, XDH, and XK) genes, two different strains were constructed. Strain 1 expressing *MAE1* with *Xyl* genes was observed to improve the xylose uptake and caused an increment in the NADPH/$NADP^+$ ratio. The co-expression of *MAE1* and *MDH2* along with *Xyl* genes resulted in a 1.25-fold increase in ethanol titers due to regeneration of cofactors required for the 1st and 2nd steps of the XR–XDH pathway.[109] Alternative to multiple gene overexpression, a native NADH kinase (NADH + $NADP^+$ → NADPH + NAD^+) enzyme was overexpressed replenishing the NADPH and NAD^+ cofactors.[110] In another study, NADPH dependent glutamate dehydrogenase (*GDH1*) (α-ketoglutarate + NH_4^+ + NADPH → glutamate + $NADP^+$) was deleted in *S. cerevisiae* and NAD^+ dependent glutamate dehydrogenase (glutamate + NAD^+ + ATP + H_2O → α-ketoglutarate + NH_4^+ + NADH + ADP) was overexpressed resulting in increased ethanol production and reduced xylitol accumulation.[111] Recently, two NADH oxidation approaches were demonstrated in *L. lactis*, where external supplementation of hemin[112] and flavinium[113] catalyses the oxidation of NADH molecules in the presence of O_2. Although the mechanism was demonstrated in *L. lactis*, this *in situ* regeneration of reducing cofactors could be of wide significance from an industrial perspective.

Like NADH, NADPH is also a crucial electron donor in various metabolic pathways. Celton and associates reported that *S. cerevisiae* cells growing on pentose sugars respond to an increase in NADPH demand by directing the carbon flux through the pentose phosphate pathway (PPP) and acetate synthesis pathway, as well as transforming NADH to NADPH in the cytosol *via* the transhydrogenase cycle. The enzymes involved in the regeneration of NADPH and NAD^+ cofactors are glucose-6-phosphate dehydrogenase (Reaction 1), 6-phosphogluconate dehydrogenase (Reaction 2), and transhydrogenase (Reaction 3).

$$\text{Glucose-6-phosphate} + NADP^+ = \text{6-phosphoglucono-}\delta\text{-lactone} + \text{NADPH(PPP)} \quad (1)$$

$$\text{6-Phosphogluconate} + NADP^+ = \text{ribulose-5-phosphate} + \text{NADPH(PPP)} \quad (2)$$

$$\text{NADH} + NADP^+ = NAD^+ + \text{NADPH (transhydrogenase cycle)} \quad (3)$$

In the case of higher xylose concentrations and increased uptake, the demand for NAD(P)H will be further increased, a predicted glycerol–DHA cycle has been reported to exchange NADH and $NADP^+$ for NAD^+ and NADPH, at the expense of an ATP molecule. In the glycerol–DHA cycle, dihydroxyacetone phosphate (DHAP) is reduced to glycerol by NADH-dependent glycerol-3-phosphate dehydrogenase (Reaction 4), glycerol is then oxidised to dihydroxyacetone (DHA) by $NADP^+$ dependent glycerol dehydrogenase (Reaction 5) and finally DHA is phosphorylated to DHAP at the expense of one ATP molecule (Reaction 6).[114] Thus, the glycerol–DHA cycle generates both the redox factors (NADPH and NAD^+) required for the XR–XDH pathway.

$$\text{DHAP} + \text{NADH} = \text{glycerol} + NAD^+ \quad (4)$$

$$\text{Glycerol} + NADP^+ = \text{DHA} + \text{NADPH} \quad (5)$$

$$\text{DHA} + \text{ATP} = \text{DHAP} + \text{ADP} \quad (6)$$

$$\text{NADH} + NADP^+ + \text{ATP} = NAD^+ + \text{NADPH} + \text{ADP} \quad (7)$$

5. Xylose as an alternative carbon source for microbial growth and product development

The bioconversion of xylose into value-added chemicals has received a lot of attention in recent years. Many naturally occurring or engineered microbial strains have been discovered or designed to synthesize various industrially important chemicals and fuels using xylose as a sole carbon and energy source. Table 3 summarizes various chemicals that can be produced from xylose through the biological route and their commercial applications.

5.1 Xylitol

Xylitol ($C_5H_{12}O_5$), a platform chemical, is a five-carbon sugar alcohol with a wide spectrum of applications in personal care, food, confectionary, and pharmaceutical industries.[115] Xylitol is equivalent to common table sugar with a lower calorific value (2.4 *vs.* 4 calories per gram), lower glycaemic index (7 *vs.* 60–70%) and insulin independent metabolism. In 2016, the global xylitol market was worth US$ 725.9 million with a production capacity of 190.9 thousand metric tons. It has been forecasted that with the increased global market demand and compound annual growth rate (CAGR) of 5.7%, the production capacity should be increased to 265.5 thousand metric tons (US$ 1 billion) by 2022.[116] The commercial production of xylitol is performed *via* a chemical route by catalytic dehydrogenation of pure xylose, involving expensive Ni based catalyst, sulfuric acid, calcium oxide, phosphoric acid and activated charcoal treatments at high pressure (5000 kPa) and temperature (140 °C).[117] The process is uneconomical due to the requirement of pure xylose as the substrate, the process generates heavy metal pollutants, and there is a high risk associated with operating conditions and environmental pollution.[117] An alternative route for the production of xylitol is the biological process, wherein whole/immobilized cells expressing XR or cell-free extracts with XR activity act as biocatalysts (Fig. 3), producing xylitol from pure and crude renewable sources rich in xylose. The process offers the advantages of mild operation conditions and non-requirement of purified xylose.[118]

Xylose is a native substrate for xylitol which is accumulated due to lack of synchronisation between steps catalysed by XR and XDH. Various microorganisms having natural xylitol producing ability include bacteria, yeast, and fungi. Among them yeasts are predominant such as *Candida athensensis*, *C. boidinii*, *C. guilliermondii*, *Debaryomyces hansenii*, *C. tropicalis*, *C. magnolia*, and *S. stipitis* that can accumulate xylitol with significant yields and productivities (Table 4). Later with the introduction of heterologous pathway engineering, *S. cerevisiae*, *Kluyveromyces* and other *Candida* spp. have been engineered to accumulate xylitol. Usually bacterial systems present the XI pathway for xylose assimilation, but a few bacterial strains like *Bacillus coagulans*, *Cellulomonas cellulans*, *Corynebacterium glutamicum*, *Corynebacterium ammoniagenes*, *Enterobacter liquefaciens*, *Mycobacterium smegmatis*, and *Serratia marcescens* present the XR–XDH pathway for producing xylitol.[119] A new bacterial isolate, *Pseudomonas putida*, was screened for xylitol production and characterized to have XR activity of 48.7 IU mg^{-1}. The strain accumulated 35.2 g L^{-1} xylitol with a productivity of 0.98 g L^{-1} h^{-1} when cultured on xylose under optimized growth conditions.[118]

One of the most critical environmental parameters to be considered during processing of yeast for xylitol production is dissolved oxygen concentration. Since oxygen limited conditions usually favour xylitol formation, conversion of NADH to NAD^+ is hampered and the reduced availability of NAD^+ impedes xylitol to xylulose conversion, resulting in the accumulation of xylitol.[59] The XR catalysing reduction of xylose to xylitol is NAD(P)H dependent, and hence to improve NAD(P)H levels, overexpression of glucose-6-phosphate dehydrogenase (glucose-6-phosphate + $NADP^+$ → 6-phosphogluconolactone + NADPH) from the PP pathway in *S. cerevisiae* resulted in a xylitol titer and productivity of 196.3 g L^{-1} and 4.27 gL^{-1}h, respectively.[120] A new isolate, *P. fermentans*, subjected to chemical mutagenesis resulted in a strain with improved XR activity (34%) and reduced XDH (22.9%) activity. The fed-batch fermentation using a mutant strain of *P. fermentans* produced 98.9 g L^{-1} xylitol with conversion yield of 0.67 g g^{-1} using pure xylose as a substrate. Further, using non-detoxified xylose rich pre-hydrolysate from sugarcane bagasse, the strain amassed 79.0 g L^{-1} xylitol with an overall yield of 0.54 g g^{-1} respectively.[55] *S. stipitis* is well known for its high xylose utilization rate, but as xylose assimilation leads to high ethanol production, the host is not suitable for xylitol production. *Yarrowia lipolytica*, an oleaginous yeast is well known for production of lipids and TCA cycle intermediates. The yeast has a cryptic xylose metabolic pathway or inactive xylose assimilatory enzymes. As a result of it, *Y. lipolytica* is unable to grow on xylose as a sole carbon source but can biotransform xylose into xylitol when cultivated in xylose along with other carbon sources like glucose or glycerol. The *Y. lipolytica* Polt strain accumulated 53.2 g L^{-1} xylitol with a yield of 0.97 g g^{-1} using pure glycerol and xylose as carbon sources, where glycerol was used for biomass production. Similar results were obtained when pure glycerol was substituted with crude glycerol from the biodiesel industry (titer: 50.5 g L^{-1}; yield: 0.92 g g^{-1}).[121]

Other than the environmental characteristics, basic mechanisms like substrate and product mediated growth inhibition limits the final product titers in biological processes. Xylitol, a polyhydroxy compound, can interfere with the membrane fluidity of the host cell's membrane, disrupting growth and increasing xylitol accumulation. Nystatin, a membrane porin agent that can increase the permeability of the lipid membranes to ions, water and non-electrolytes, was used to increase the xylitol transport from the cell. The *C. tropicalis* ATCC 13803 strain cultured along with nystatin could accumulate 197 g L^{-1} xylitol with 0.75 g g^{-1} and 3.9 g L^{-1} h^{-1} yield and productivity, respectively.[122]

5.2 Lactic acid

Lactic acid (LA) or 2-hydroxyproponoic acid is an optically active compound and exists in L and D forms. Being a platform

Table 3 Commercial products from xylose

Chemical	Commercial applications
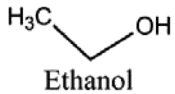 Ethanol	Solvent, automotive gasoline, alcohol beverages, distilled spirits, hand sanitizers and medical antiseptics
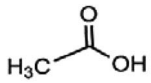 Acetic acid	Polymeric monomers, paints, adhesives, inks, coatings, and food additives
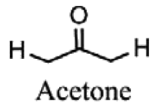 Acetone	Plastics, cosmetics, and solvents
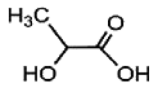 Lactic acid	Food, beverages, polyesters, textiles, and pharmaceuticals
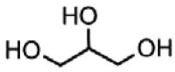 Glycerol	Pharmaceutical, food, polymer, humectant, solvent, lubricant, personal care, and household products
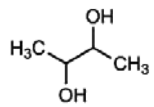 2,3-Butanediol	Polymers, solvents, fine chemicals, lactones, fuel additives
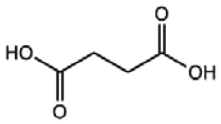 Succinic acid	Pharmaceutical products, surfactants, detergents, plastics and food grade ingredients
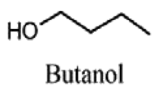 Butanol	Lubricants, brake fluids, synthetic rubber, polymers, and automotive fuels
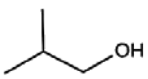 Isobutanol	Coatings, chemical derivatives, paints, fuel additive, and solvents
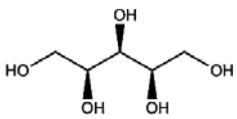 Xylitol	Confectionery, chewing gums, syrups, and odontological and pharmaceutical products
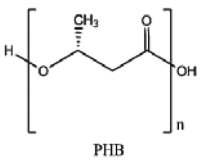 PHB	Biodegradable plastics

chemical, LA has diverse industrial applications in food, cosmetics, polymers and packaging. The most valued application of LA as a monomer is in the production of poly lactic acid (PLA), an alternative to commercial petrochemical polymers. The market price for food grade LA is approximately $1400–$1600 per metric ton. It has been estimated that the global market size of LA would reach ~$8.7 billion by 2025, with a CAGR of 18.7%.[123]

Various microorganisms like bacteria, fungi and yeast have been employed for the production of LA using xylose as the sole

Table 4 Summary of products obtained from conversion of pure and crude xylose by native microorganisms

Product	Pretreatment	Form of substrate	Additional steps prior to fermentation	Microorganism	Mode of fermentation	Titer (g L^{-1})	Yield (g g^{-1})	Productivity (g L^{-1} h^{-1})	References
Xylitol	Hydrothermally pretreated SCB	Xylose-rich hydrolysate	None	*Pichia fermentans*	Batch	79	0.67	0.47	55
	HNO_3 pretreated CC	Xylose-rich hydrolysate	Detoxification & decolorization	*Candida tropicalis* MTCC 6192	Batch	34.35	0.62	0.26	213
	Pure xylose	Pure xylose + pure glycerol	None	*Yarrowia lipolytica* Polt	Batch	53.2	0.97	0.36	121
	Pure xylose	Pure xylose + crude glycerol	None	*Y. lipolytica* Polt	Batch	50.5	0.92	0.35	121
	Steam exploded poplar	Xylose-rich hydrolysate	Detoxification	*C. guilliermondii*	Batch	28.78	0.59	0.81	214
	Steam exploded *Eucalyptus globulus* chips	Xylose-rich hydrolysate	Detoxification	*Kluyveromyces marxianus* NRRL Y-6373	Batch	28.05	0.68	0.16	215
	H_2SO_4 pretreated SS	Xylose-rich hydrolysate	None	*Corynebacterium glutamicum* Cg-ax3	Fed-batch	27.0		2.25	216
	Hydrothermally pretreated CC	Whole slurry of corn cobs	None	*Saccharomyces cerevisiae* PE-2 (GM)	Fed-batch	29.61	0.93	0.54	115
	CC	Corn cob hydrolysate	Detoxification	*S. cerevisiae* IS5-d	Fed-batch	143	0.93	1.83	217
				S. cerevisiae 2bpgi	Fed-batch	162		2.13	
Lactic acid	HCl pretreatedSCB	Xylose-rich hydrolysate	None	*Bacillus coagulans* DSM ID 14-300	Batch	55.99	0.87	1.70	218
	H_2SO_4 pretreated SCB	Xylose-rich hydrolysate	None	*Lactobacillus pentosus* ATCC 8041	Batch	42.4	0.71	1.02	125
					Batch SScF[a]	64.8	0.93	1.01	
	DryPB pretreated CS	Carbohydrate-rich biomass	None	*Pediococcus acidilactici* ZY1	Fed-batch SScF	97.3[$]	0.926[#]	1.01	219
	NaOH pretreated CS	Carbohydrate-rich & delignified biomass	Washed	*P. acidilactici* PA204	Fed-batch SScF	104	0.69	1.24	220
	NaOH pretreated CC	Carbohydrate-rich & delignified biomass	None	*K. marxianus* YKX071 (GM)	Fed-batch SScF	101.7	0.56	1.10	221
	Organosolv pretreated beechwood	Cellic CTec2 & HTec2 hydrolysed mixed sugars	None	*B. coagulans* DSM ID 14-298	Batch	88.09	0.674	2.93	222
Succinic acid	NaOH pretreated SCB	Delignified carbohydrate-rich biomass hydrolysed by cellulclast 1.5L	None	*Y. lipolytica* PSA02004	Batch	33.2	0.58	0.33	223
	Sulfuric acid pretreated CS	Mixed hydrolysate (81% xylose; 14% glucose)	None	*Escherichia coli* BA408	Batch	23.1	0.85	0.24	224
	Sulfuric acid pretreated EG	Mixed hydrolysate (69% xylose; 29.4% glucose)	None	*E. coli*M6PM	Dual phase (aerobic growth and anaerobic production phase)	30.03	0.64	0.41	225
	Acid sulphite pulping of *Eucalyptus globulus*	Xylose-rich spent sulphite liquor	Nanofiltration using a vibratory shear-enhanced processing filtration unit	*Actinobacillus succinogenes* DSM 22257	Continuous (dilution rate 0.2 h^{-1})	19	0.48	—	226
				Basfia succiniciproducens DSM 22022		22	0.55	—	
	CS hydrolysate	Glucose: xylose (70 : 30)		*C. glutamicum* CGS5 (GM)	Two stage (initial growth and production stage)	98.6	0.87	4.29	227

Table 4 (*Contd.*)

Product	Pretreatment	Form of substrate	Additional steps prior to fermentation	Microorganism	Mode of fermentation	Titer (g L^{-1})	Yield (g g^{-1})	Productivity (g L^{-1} h^{-1})	References
	Dilute acid pretreated CC	Xylose rich hydrolysate	Detoxification	*C. glutamicum* NC-2 (GM)	Two stage (initial growth and production stage)	40.8	0.69	0.85	228
	SCB	Hydrolysate (glucose: xylose; 2 : 1)	None	*E. coli* BA305	Fed-batch	39.3	0.97	0.327	229
2,3 Butanediol	Hydrothermally pretreated SCB	Xylose-rich hydrolysate	None Detoxification	Mutant of *E. ludwigii*	Fed-batch	32.3 63.5	0.36 0.33	0.84 0.43	148
	KOH pretreated corn cobs followed by hemicellulose precipitation	Enzymatically derived xylose-rich hydrolysate	None	*K. oxytoca* XF7	Batch	12.18	0.97	0.50	230
	H_2SO_4 pretreated soybean hulls	Xylose-rich hydrolysate	None None	*Pantoea agglomerans* BL1 *K.pneumoniae* BLh-1	Batch	20.5 21.9	0.50 0.40	0.55 0.30	231
	H_2SO_4 pretreated soybean hulls	Xylose-rich hydrolysate	None	*P. agglomerans* BL1	Batch	14.02	0.53	1.17	232
	H_2SO_4 pretreated wheat straw	Xylose-rich hydrolysate + exogenous glucose	None	*Paenibacillus polymyxa* DSM 365	Batch	23.4	0.27	0.28	233
	Sulphite pretreated oil palm empty fruit bunches	Hydrolysed slurry + xylose-rich spent liquor	None	*K. pneumoniae* PM2	SHF	75.03	0.43	0.78	234
	Corn cobs pretreated with mixed acids	Xylose-rich hydrolysate	None	*Enterobacter cloacae* M22	Batch	23.2	0.44		235
	Hot water extracted Birchwood	Xylose-rich hydrolysate	Detoxification by ultra-filtration	*B. vallismortis* B-14891	Batch	22.7	0.43	0.63	236
Ethanol	NaOH pretreated SCB	Xylose-rich hydrolysate	None	*Scheffersomyces stipitis Y-7124*	Sequential fed-batch with cell-recycle	18.52	0.32	0.36	158
	NaOH pretreated SCB	Xylose-rich hydrolysate	None	*Spathaspora passalidarum Y-27907*	Sequential fed-batch with cell-recycle	23.3	0.46	0.81	158
	Steam exploded WS	Whole biomass slurry	None	*S. cerevisiae F12* (GM)	Batch	23.7	0.43	0.7	237
	1.5% v/v H_2SO_4 pretreated SCB	Xylose-rich hydrolysate	Detoxification by $Ca(OH)_2$	*Spathaspora passalidarum Y-27907*	Batch	19.4	0.4	0.8	238
n-Butanol	Hydrothermally pretreated SCB	Xylose-rich hydrolysate fortified with xylose	None	*C. saccharoperbutylacetonicum* DSM 14923	Batch	5.8	0.22	0.08	239
	Hot water extracted debarked hybrid poplar	Xylose-rich hydrolysate	Detoxification	*C. acetobutylicum* ATCC 824	SScF	6.8	0.16	0.07	240
	Xylan	Pure xylan	None	*C. acetobutylicum* NJ4	Batch-CBP involving co-culturing with hemicellulase secreting *Thermoanaerobacterium thermosaccharolyticum* M5	13.28	0.19	0.08	241
	Hot water extraction and steam treatment with chips (60% aspen and 40% maple)	Xylose-rich hydrolysate	Laccase mediated detoxification	*C. acetobutylicum*	Batch	4.17	—	—	242

[a] SCB: sugarcane bagasse; CC: corn cobs; CS: corn stalk; EG: elephant grass; SHF: separate hydrolysis and fermentation; SScF: simultaneous saccharification and fermentation; GM: genetically modified.

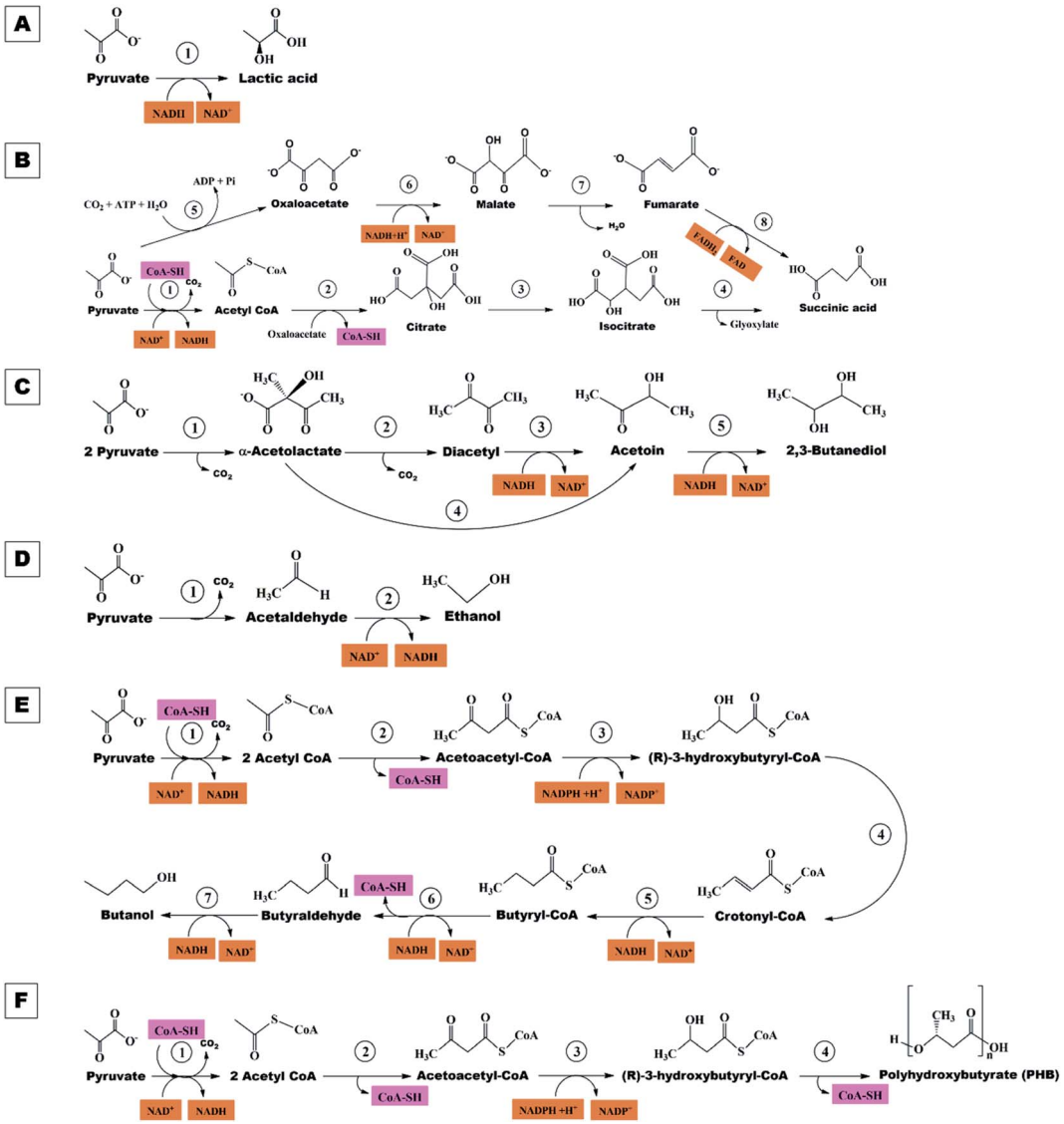

Fig. 6 Biochemical pathways: (A) lactic acid, enzymes and genes involved: (1) lactate dehydrogenase (*ldh*). (B) Succinic acid, enzymes and genes involved: 1, acetyl-CoA synthetase (*acs*); 2, citrate synthase (gltA); 3, aconitase (acnAB); 4, isocitrate lyase (aceA); 5, pyruvate carboxylase (*pyc*); 6, malate dehydrogenase (*mdh*); 7, fumarase (*fh*); 8, fumarate reductase (*frd*) or succinate dehydrogenase (*sdh*). (C) 2,3-Butanediol, enzymes and genes involved: 1, α-acetolactate synthase (*alsS*); 2, spontaneous reaction; 3, diacetyl reductase (*butA*); 4, α-acetolactate decarboxylase (*aldc*); 5, butanediol dehydrogenase (*bdh*). (D) Ethanol, enzymes, and genes involved: 1, pyruvate decarboxylase (*pdc*); 2, alcohol dehydrogenase (*Adh*). (E) Butanol, enzymes and genes involved: 1, acetyl-CoA synthease (*acs*); 2, thiolase (*thl*); 3, 3-hydroxybutyryl-CoA dehydrogenase (*Hbd*); 4, crotonase (*Crt*); 5, butyryl-CoA dehydrogenase (*EtfAB*); 6, butyraldehyde dehydrogenase (*AdhE2*). (F) Polyhydroxybutyrate (*PHB*), enzymes and genes involved: 1, acetyl-CoA synthase (*acs*); 2,3-ketothiolase (*PhaA*); 3, acetoacetyl-CoA reductase (*PhaB*); 4, PHB synthase (*PhaC*).

carbon and energy source (Table 4). Lactic acid bacteria (LAB) are considered predominant for industrial scale LA production. Based on the end products, LAB strains can be divided into two categories: homofermentative (*Lactobacillus delbrukii*, *L. acidophilus*, *L. plantarum*, and *L. helveticus*) and heterofermentative (*L. brevis*, *L. diolivorans*, *L. fermentum*, and *L. reuteri*) for lactic acid fermentation. In homofermentative bacteria, the carbon flux is directed only to lactic acid (LA) with no by-product formation, whereas in case of heterofermentative bacteria, a mixture of LA, acetic acid and ethanol are obtained with LA as the main product. One of the most common routes for LA production is the simple reduction reaction of pyruvate obtained from the EMP and/or PP pathway catalysed by the NADH-dependent lactate dehydrogenase enzyme (Fig. 6A). *Lactobacillus pentoses* and *L. brevis* can naturally ferment xylose through the pentose phosphate and phosphoketolase pathways, producing LA and a mixture of acetic and LA, respectively.[124] Wischral *et al.* (2019) investigated different *Lactobacillus* spp., for fermentation of xylose-rich hemicellulosic hydrolysates and identified the *L. pentoses* strain efficiently utilizing the xylose-rich SCB hydrolysate obtained from combined alkali and acid pretreatment and accumulated 65 g L^{-1} LA with yield and productivity of 0.93 g g^{-1} and 1.01 g L^{-1} h^{-1}, respectively.[125] Similarly an engineered *E. coli* JU15 strain was supplemented

with 32 g L^{-1} xylose and 42 g L^{-1} glucose, a simulated corn stover hydrolysate, resulting in 40 g L^{-1} LA with a conversion yield of 0.60 g_{LA} g_{sugar}^{-1}.[126] *Pediococcus acidilactici* is a facultative anaerobic lactic acid producing strain with specificity to a wide range of substrates including xylose, but the strain *P. acidilactici* TY112 was not able to utilise xylose. Qui and associates blocked the PK pathway by deleting the *pkt* gene, and overexpressed heterologous xylose assimilation pathway genes xylA and xylB along with transketolase (*tkt*) (X5P + E4P → F6P + G3P) and transaldolase (*tal*) (G3P + S7P → F6P + E4P) genes, directing the carbon flux from the phosphoketolase to the pentose phosphate pathway. The recombinant strain accumulated 130.8 g L^{-1} LA with 0.68 g g^{-1} yield in simultaneous saccharification and fermentation mode using dilute acid pretreated wheat straw as feedstock.[124] The group have employed a similar overexpression and deletion strategy in the D-LA producing *P. acidilactici* ZP26 strain, and the modified strain was adapted under laboratory conditions with xylose as the sole carbon source. The adapted strain *P. acidilactici* ZY15 accumulated 97.3 g L^{-1} D-LA with 0.92 g g^{-1} conversion yield through a simultaneous saccharification and co-fermentation strategy using dry dilute acid pretreated and detoxified corn stover feedstock.[127] However the CCR limits the performance of various strains on LCB hydrolysates as they consist of both hexose and pentose sugars, and the *E. coli* JH15 strain was engineered to overcome CCR by deletion of the *ptsG* gene which encodes for *IIBCglc* (a PTS enzyme for glucose transport). The engineered strain produced 83 g L^{-1} D-LA with 0.83 g g^{-1} yield and 0.86 g L^{-1} h^{-1} productivity from co-fermentation with a mixture containing glucose and xylose in a 1 : 1 ratio.[128]

The commercially viable yeast *S. cerevisiae* produces LA in very minute quantities, and hence requires either a homologous or heterologous expression to increase the titers. Ethanol is the natural and dominant product by *S. cerevisiae* and would be the major competitor for LA production. The competition is for the precursor/substrate, pyruvate, and cofactor NADH between pyruvate decarboxylase and alcohol dehydrogenase. In order to prevent this, a *pdc* deficient strain was constructed which exhibited poor growth and productivities.[129] In *S. cerevisiae*, heterologous overexpression of *Xyl1*, *Xyl2*, and *Xyl3* from *S. stipitis*, a cellodextrin transporter (cdt-1) and a β-glucosidase (gh1-1) from the cellulolytic fungus *Neurospora crassa*, and additional laboratory evolution on medium containing cellobiose, resulted in a strain that could produce 83 g L^{-1} LA, with 0.66 g g^{-1} yield when cultivated on LCB hydrolysate containing 10 g L^{-1} glucose, 40 g L^{-1} xylose and 80 g L^{-1} cellobiose.[130]

5.3 Succinic acid

Succinic acid (SA) is an aliphatic dicarboxylic acid containing four carbon atoms with potent application as a precursor in pharmaceutical, polymer, and chemical industries. Like LA, SA is a platform chemical and due to the presence of two carboxyl acid groups, SA can be converted into a variety of products such as succinic anhydride, succinic esters, 2-pyrrolidine, and polyesters for synthesizing biodegradable plastics.[131] According to global market research, the market size was expected to reach $237.8 million by 2022 with a CAGR of 9.2% (Succinic Acid Market Size & Share | Industry Analysis Report, 2022 (grandviewresearch.com)). SA production from pure sugars and LCB hydrolysates has been reported using natural producers *Anaerobiospirillum succiniciproducens*, *Actinobacillus succinogenes*, *Mannheimia succiniciproducens*, *Basfia succiniciproducens* and genetically engineered strains *E. coli* and *Y. lipolytica* (Table 4).[132,133] The three different biochemical pathways for SA production are the oxidative tricarboxylic acid (TCA) cycle, the reductive branch of the TCA cycle, and the non-frequent glyoxylate pathway (Fig. 6B).[134]

Actinobacillus succinogenes and *Basfia succiniciproducens* are the most evaluated and predominant native SA producing strains, with the ability to utilise either pure sugars or LCB hydrolysates.[135] *Actinobacillus succinogenes* 130Z, a natural SA producer, was immobilized and continuously fed with xylose-rich hydrolysate from corn stover and generated 39.6 g L^{-1} SA, with yield and productivity of 0.78 g g^{-1} and 1.77 g L^{-1} h^{-1}, respectively.[136] In another study, when the same strain was cultivated using dilute acid pretreated corn stover hydrolysate, an SA titer, yield and productivity of 42.8 g L^{-1}, 0.74 g g^{-1} and 1.27 g L^{-1} h^{-1} were obtained, respectively.[137] Pateraki *et al.* (2016) cultivated *A. succinogenes* and *B. succiniciproducens* on mixed sugar feedstock (synthetic solution) containing 72% xylose, 12.2% galactose, 10.9% glucose, 4.2% mannose, and 0.1% arabinose. The SA titer, yield and productivity achieved with *A. succinogenes* were 26 g L^{-1}, 0.76 g g^{-1} and 0.66 g L^{-1} h^{-1}, respectively. Similar results were obtained with *B. succiniciproducens*: 27.4 g L^{-1}, 0.69 g g^{-1} and 0.60 g L^{-1} h^{-1}.[138] In addition to single strains, microbial consortiums have been used for SA production. A microbial consortium containing *Thermoanaerobacterium thermosaccharolyticum* M5 and *A. succinogenes* 130Z was employed to utilize hemicellulosic derived sugars to produce SA. The *T. thermosaccharolyticum* M5 strain has the ability to saccharify the LCB components, by secretion of extracellular enzymes like xylanase where the xylose obtained was converted into SA by *A. succinogenes*. The consortium with the consolidated bioprocessing approach was able to generate 32.5 g L^{-1} SA with a yield of 0.39 g g^{-1}.[139]

The *E. coli* KJ122 strain was previously modified to reduce the by-products by deleting the respective genes, which increased the SA yield, titers and productivity when cultivated on glucose and sucrose in mineral medium under anaerobic conditions.[140] The strain was observed to be defective in growth and SA production during cultivation on xylose medium. It was speculated that the major reason behind this could be energy limitations as transport and phosphorylation of 1 mole of xylose requires 2 moles of ATP, but only 1.67 moles of ATP are generated when xylose is used for biosynthesis of SA.[141] Thus, xylose as the sole carbon source cannot provide efficient energy currency for the cell growth and development. Hence Khunnonkwao and associates deleted the *xylFGH* (ATP dependent ABC transporter), which is an energy expensive xylose transporting transmembrane protein and the resultant mutant strain was subjected to adaptive evolution on xylose media. When the recombinant *E. coli* KJ12201-14T strain was cultured on a glucose and xylose mixture, it utilized both the sugars and

accumulated 84.6 g L^{-1} SA with yield and productivity of 0.86 g g^{-1} and 1.01 gL^{-1}h, respectively.[142] An engineered *E. coli* strain, YL104H, with deleted pathways for LA, ethanol and other byproducts was evaluated for SA production using corn-based liquor containing glucose and xylose in a ratio of 2 : 1. Employing an alternative strategy to that followed where the ABC transporter was deleted, Zhang and associates attempted a process modification approach where the intracellular ATP concentration was maintained by co-substrate fermentation with supplementing glucose and xylose in a 2 : 1 ratio. The process resulted in accumulation of 61.66 g L^{-1} SA, with 0.95 g L^{-1} h^{-1} productivity.[143]

Bacterial strains are more sensitive to changes in the physiological pH and require continuous addition of neutralizing agents. The addition of neutralizing agents not only dilutes the concentration of SA in the fermented broth but also converts organic acids into the salt form which complicate the downstream processing and increase the production cost. On the other hand, yeast strains are more promising for SA production, as they have better tolerance and can withstand lower pH. In a study, Prabhu and associates (2020) engineered the *Y. lipolytica* PSA02004 strain to utilize xylose as the sole source of carbon and energy by overexpressing the pentose phosphate pathway comprising XR, XDH and XK under a strong constitutive promoter. The recombinant strain accumulated 22.3 g L^{-1} SA using xylose-rich hydrolysate from SCB hydrolysate.[144]

5.4 2,3-Butanediol

2,3-Butanediol (BDO) is a 4-carbon diol, with applications in food, cosmetics, fuel-additives, agrochemicals, and pharmaceuticals. One of the major applications of BDO is production of methyl ethyl ketone (MEK), an organic solvent used in production of resins and lacquers.[145,146] Microbial physiology adaptation for the BDO pathway is hypothesized to prevent intracellular acidification and balance the reducing equivalents. Two moles of pyruvate undergo sequential oxidoreductive reactions to form BDO with α-acetolactate and acetoin/diacetyl as intermediates as shown in Fig. 6C.

In biological BDO synthesis, the main factor influencing the economy of the process is the substrate cost which accounts for 50% of the total production cost.[147] Microorganisms of different genera, *Klebsiella*, *Lactobacillus*, *Enterobacter*, and *Bacillus* (Table 4), have been reported to accumulate large amounts of BDO (50–120 g L^{-1}) from a variety of renewable feedstocks like cane molasses, cane sugar, SCB, and fruit and vegetable waste. In our recent study, we evaluated the performance of a mutant *Enterobacter ludwigii* strain on pure xylose, non-detoxified and detoxified xylose-rich hydrolysates obtained from the thermochemical pretreatment of SCB. During the fed-batch cultivation, the strain produced 71.1 g L^{-1} BDO using pure xylose with a conversion yield and productivity of 0.40 g g^{-1} and 0.94 g L^{-1} h^{-1}, respectively. In case of non-detoxified and detoxified hydrolysates, BDO titers of 32.7 and 63.5 g L^{-1} with yield of 0.33 and 0.36 g g^{-1}, and productivity of 0.43 and 0.84 g L^{-1} h^{-1}, were achieved, respectively.[148] A study conducted by Wang and associates implemented a process engineering approach by optimizing the media components to improve the BDO titers and productivity using *Klebsiella pneumoniae*. The *K. pneumoniae* strain with optimal media components and physiological conditions could produce 42.7 g L^{-1} BDO with 95% theoretical maximum yields and 99% xylose sugar uptake efficiency.[147] Although *Klebsiella* is a known workhorse in production of value-added chemicals, its resistance to xylose is not satisfactory; xylose concentration >70 g L^{-1} was observed to inhibit the growth and metabolic performance of the strain. A global transcription regulating sigma (σ) factor encoded by the *rpoD* gene was observed to improve the substrate consumption rate and metabolic behaviour in *E. coli* strains. Hence, to overcome the xylose mediated inhibition, the *rpoD* gene was overexpressed in *K. pneumoniae* which caused an increment in substrate tolerance up to 125 g L^{-1} xylose, and product tolerance by 200%. Xylose transport, glycerol-3-phosphate acyl transferase, and phosphate kinase genes were observed to be upregulated by 5.7, 2.2 and 3-fold, respectively.[149]

To modulate the commercially viable *S. cerevisiae* for BDO production, the biochemical pathway for BDO should be overexpressed and biosynthetic pathways leading to byproduct (ethanol, acetic acid and glycerol) formation must be eliminated. Kim *et al.* (2015) constructed a BDO producing *S. cerevisiae* strain by introducing the BDO pathway and to this end, α-acetolactate synthase (*AlsS*) and α-acetolactate decarboxylase (*AlsD*) from *B. subtilis*, and endogenous BDO dehydrogenase (*BDH1*) and *NoxE* from *L. lactis* were overexpressed. Further, production of ethanol (*adh* 1–5) and glycerol (*gpd* 1 and *gpd* 2) was blocked by deleting the relevant genes. The resulting engineered strain produced 72.9 g L^{-1} BDO with 0.41 g g^{-1} and 1.43 g L^{-1}.h yield and productivity, respectively, using glucose as the carbon source.[150] Extending the work, later Kim and associates constructed a xylose assimilatory *S. cerevisiae* strain by overexpressing the *S. stipitis* transaldolase (S7P + G3P → E4P + F6P) and endogenous NADH preferring XR. The recombinant strain showed a 2.1-fold increase in xylose consumption rate and 1.8-fold increase in BDO productivity. Further NOX and PDC1 genes from *L. lactis* and *C. tropicalis* were heterologously overexpressed resulting in the BD5X-TXmNP strain. The fed-batch cultivation of the resultant strain on xylose produced 96.8 g L^{-1} BDO with 0.58 g L^{-1} h^{-1} productivity.[151]

5.5 Ethanol

Ethanol/ethyl-alcohol/bioethanol is the most widely used biofuel in the transportation sector and offers several advantages such as a higher octane number, high combustion efficiency and increased heat of vaporization. Bioethanol is less toxic, readily biodegradable and produces fewer air-borne pollutants in comparison to petroleum fuel and most promising alternatives to gasoline. However, due to its hygroscopic nature, complete replacement of gasoline with ethanol is not possible as water vapour can corrode the engine.[152,153] Currently, ethanol is blended with gasoline at different levels (5–20%) across the globe. It has been found that the blended fuel causes a substantial reduction in emission of hydrocarbons and greenhouse gases.[154] The commercial production of ethanol

from various renewable feedstocks has gained significant interest due to its increased application as a fuel component in gasoline. In 2019, the global ethanol production was 115 billion litres ($38.83 billion), and with a CAGR of 1.77% the demand has been expected to increase to $43.14 billion by 2025. (Global Ethanol Market – forecasts from 2020 to 2025 (researchandmarkets.com)). Ethanol fermentation by *S. cerevisiae* is one of the oldest practices in Biotechnology. *S. cerevisiae* is the most promising cell factory for ethanol production and is employed at the industrial level. Currently, yeast is used for generating ethanol from a variety of feedstocks.[155]

The ethanol production from xylose follows production of X5P through the pentose phosphate pathway and further proceeds through the EMP pathway. Pyruvate, the final product of the EMP pathway, is converted to ethanol through acetaldehyde as an intermediate as shown in Fig. 6D. However, *S. cerevisiae* lacks pentose assimilatory pathways and can generate ethanol from xylose only after introducing the enzymes connecting xylose to the central carbon metabolism.[156] Even though few strains like *S. stipitis*, *P. fermentans*, *P. kudriavzevii*, and *Spathaspora* (*S. passalidarum*) are well-known xylose assimilating yeast, the processes are limited due to substrate and product mediated inhibition. For example, the strains *S. stipitis* and *S. passalidarum* on xylose fermentation resulted in maximum ethanol titers of 29.9 g L^{-1} and 25 g L^{-1}, with a conversion yield of 0.47 and 0.41 g g^{-1}, and productivity of 1.5 and 1.04 g L^{-1} h^{-1}, respectively.[157–161]

The possibility of xylose as the feedstock to produce ethanol was explored in *S. cerevisiae* and to this end, XR and XDH genes from *S. stipitis* were overexpressed in *S. cerevisiae*. The heterologous expression resulted in a lower ethanol titer of 10.7 g L^{-1} with a conversion yield of 0.19 g g^{-1}, and xylitol titers and yield of 14.3 g L^{-1} and 0.26 g g^{-1}, respectively. In *Pichia* sp., there is a competition between ethanol and xylitol formation for the carbon flux. The carbon flux towards xylitol synthesis can be reduced by altering the cofactor specificity. Xiong *et al.* (2013) expressed a mutant form of XR (K270R) in *S. cerevisiae* with higher specificity of XR for NADH than NADPH which resulted in a higher ethanol (0.38 g g^{-1}) and reduced xylitol yield (0.08 g g^{-1}).[162] Along with ALE, polyploidy was also considered as an accelerative solution for adaptation of yeast. In the process, either the native or mutant haploid strains are subjected to mating to produce diploid or triploid strains. These strains were observed to have improved phenotypic and genotypic characteristics compared to the parent strains. Using this approach, *S. cerevisiae* XR-K270R mutant strain diploids and triploids were produced by Liu and associates. Furthermore, the comparative analysis between the haploid, diploid and triploid strains displayed better performance of the triploid on dilute acid and alkali pretreated corn cob and corn stover hydrolysates resulting in a maximum ethanol production yield of 87.3%, while the diploid strain yielded 76.2% ethanol.[163] The recent discovery of non-conventional yeast *S. passalidarum*, with xylose fermenting ability and possessing NADH dependent XR, could enable alternative research focusing on heterologous expressions rather than protein or cofactor engineering of the known XR from *S. stipitis*.[157] Further research towards expression of XR and XDH from *Spathaspora* sp. could result in increased ethanol titers and yields in commercial yeasts.

5.6 *n*-Butanol

n-Butanol is a four-carbon straight chain alcohol and is considered a better biofuel than ethanol due to its high octane number, higher heating value, lower volatility, ignition problems, low miscibility with water and higher viscosity.[80] In a chemical approach, aldol condensation (oxo process) can produce *n*-butanol by hydroformylation and hydrogenation of propylene. In the biological route, *n*-butanol is a part of acetone–butanol–ethanol (ABE) fermentation and *Clostridium* spp. are well known cell factories with ABE fermentation (Fig. 6E).[164,165] However, the bio-butanol production suffers from low titers, yield, and product mediated inhibition. *Clostridium* strains can naturally ferment xylose into *n*-butanol *via* ABE fermentation. *C. beijerinckii* could accumulate 26.3 g L^{-1} ABE with a yield of 0.44 g g^{-1} using $Ca(OH)_2$ detoxified xylose-rich corn stover hydrolysate.[166] Although the *n*-butanol yield is 20% lower than that of ethanol, the energy generated from *n*-butanol is 32% higher than that from ethanol.[167] Currently with the available titers and yield, the cost of biobutanol production is around $1.8 L^{-1}, but further optimization of the biocatalysts and process conditions could reduce the production cost to $0.6 L^{-1} which is comparable to that of gasoline and other fossil fuels.[167] Jiang and associates implemented the process of consolidated bioprocessing (CBP), where a xylan degrading and *n*-butanol producing strain, *Thermoanaerobacterium* sp. M5, was evaluated. The strain was able to grow at 55 °C, with efficient expression of xylanase, β-xylosidase and alcohol dehydrogenase for the conversion of xylose to *n*-butanol through ABE fermentation.[168] As the *Thermoanaerobacterium* sp. M5 strain has efficient xylan degradation efficiency, a co-cultivation strategy was investigated along with solventogenic strain *C. acetobutylicum* NJ4. The co-cultivation of these strains resulted in 13.3 g L^{-1} *n*-butanol with a yield of 0.19 g g^{-1}.[169] Supplementing a crude hemicellulosic hydrolysate may be toxic to the microbial cells in the initial lag phases, and hence in a study, after growing C. *saccharoperbutylacetonicum* DSM 14923 on sugarcane molasses for 24 hours, hemicellulosic hydrolysate was added into the media resulting in 10 g L^{-1} butanol, with a yield and productivity of 0.31 g g^{-1} and 0.14 g L^{-1} h^{-1}, respectively.[164]

5.7 Polyhydroxybutyrate (polyhydroxyalkanoates)

Polyhydroxyalkanoates (PHAs) are hydroxy alkanoic polyesters which are stored as intracellular granules in various prokaryotic microorganisms and are accumulated when the carbon source is in surplus along with limitation of a key nutrient.[170,171] Although the primary function of these polyesters is the storage of carbon and energy, they also play a role in protecting the microbial cell from stress. Poly-3-hydroxybutyrate (PHB) and its derivatives like PHB-co-3-hydroxyvalerate (PHB-co-HV),[171] polylactate-co-3-hydroxybutyrate (PL-co-HB),[172] and 4-hydroxyhexanoate are a type of PHA produced by prokaryotes (Fig. 6F). PHAs have ample applications in the field of nanotechnology, drug delivery, medical prosthetics, *etc.* Although PHB is well

known and characterized, its brittle and crystalline structure limits its industrial relevance, but its derivatives like PHB-co-HV have impressive biomedical applications. A halophilic *Bacillus* sp. isolated from mangrove soil was observed to utilize a wide range of carbon sources. The strains could accumulate PHB-co-HV up to 73% of biomass weight on xylose-rich acid hydrolysates of sugarcane trash, under optimal conditions.[171]

Burkholderia sacchari, an industrially viable strain for the production of xylitol, xylonic acid and PHB, was engineered by overexpressing the xylose transporters (*XylE*, and *XylFGH*), metabolic genes (*XylA*, and *XylB*), and the regulatory gene (*XylR*). The engineered *B. sacchari* strain showed 55, 77.3 and 71% improvements in the growth rate, polymer yield and cell dry weight, respectively.[170] As explained in Section 5.3, an *E. coli* strain was engineered to hydrolyse the xylan fraction of hemicellulose by heterologous overexpression of β-xylosidase and an endoxylanase, and further the saccharified xylose was converted to PLA-co-HB. The resulting strain on a xylan based production medium with additional pentose sugar as a co-substrate increased the polymer yield up to 37% in comparison to the strain cultivated on pure xylose as a sole carbon source.[173] In a lignocellulosic biorefinery, thermophiles are of utmost importance due to the benefit of simultaneous saccharification and fermentation as most of the enzymes utilized for hydrolysis of hemicellulosic and cellulosic residues are active at around 50 °C. The thermophilic bacterium *Schelegelella thermodepolymerans* DSM 15344 is a natural polymer degrading microorganism with optimal growth at 55 °C. The genome mapping revealed a conserved PHA biosynthesis pathway, with 70–76% similarity to the model PHA accumulating microorganism *Cupriavidus necator* N-1. The interesting feature identified in the *S. thermodepolymerans* strain is accumulation of more PHB on xylose (54%) in comparison to glucose (37%) as a carbon source.[174] The interesting and highly investigated strain for PHA production is *Ralstonia eutropha* which lacks the ability to metabolize xylose. The recombinant *R. eutropha* strain expressing the *E. coli XylAB* genes was able to accumulate 33.7 g L^{-1} PHB which is 79% of biomass weight, and the same strain when cultured on the hydrolysate solution of sunflower stalk consisting of 16.8 g L^{-1} glucose and 5.9 g L^{-1} xylose resulted in production of 7.86 g L^{-1} PHB corresponding to 72.5% CDW.[175] As PHB accumulation in the microorganism is growth dependent, the optimal conditions for the cell growth would favour PHB accumulation. A new isolate, *B. megaterium* J-65, was able to accumulate 35% CDW under optimal conditions with 2% xylose as the sole carbon source.[176] Supplementing pretreated corn husk hydrolysate along with nitrogen deficient production media to *B. megaterium* could accumulate 57.8% PHB which is almost 3-fold higher than on glucose as a sole carbon source.[177]

In earlier years, researchers were more focussed on valorisation of both the carbohydrate fractions of lignocellulosic biomass to ethanol. But lately, the trend has changed, and a diverse product portfolio is preferred as it has been found to be more profitable as compared to targeting a single product. Particularly, in the last five years researchers have attempted to integrate the developed process modules with techno-economics to understand the benefits associated with holistic utilization of all biomass components. For instance, Ou *et al.* (2021) showed that if 1500 tonnes of miscanthus were processed for sugar production per day, the minimum sugar selling price (MSSP) would be $446 per tonne.[178] However, when the xylose stream obtained after auto-hydrolysis was diverted for xylitol production, the MSSP was reduced to $347 per tonne. Similar observations were made by Giuliano *et al.* (2018), who found that if only cellulosic ethanol was targeted from steam exploded corn stover, the payback ethanol price was €1.62 per kg.[179] But when the hydrolysed xylose stream was bio-transformed to xylitol, it reduced the overall cost of ethanol by 50.9%. In yet another study, xylitol co-production could raise the profitability of cellulosic ethanol by 2.3-fold during sugarcane biorefining when the fed-batch fermentation strategy was adopted.[180] Recently, Ranganathan (2020) showed that when glucose derived from rice straw was used for ethanol production, but xylose was kept intact, the cost of ethanol was $0.627 L^{-1}. But when xylose was converted to furfural and lignin was upgraded to biochemical its cost reduced to merely $0.25 L.[181] Thus, all these recent studies give a fair indication on how xylan/xylose valorisation can augment the carbohydrate economy and increase the profitability of LCB-based biorefineries. Researchers are relentlessly working towards accelerating the biotechnological production of some bio-based and commercially important chemicals through genetic and protein engineering approaches as shown in Table 5.

6. Exploring the efficiency of multiple xylose assimilatory pathways for carbon flux towards SA and biomass production using the established genome scale models

Small scale metabolic networks were constructed by retrieving information from genome scale metabolic models. Xylose assimilation pathways were incorporated into the metabolic network of *C. glutamicum*, *E. coli*, *A. succinogenes* and *Y. lipolytica*. Elementary flux mode analysis was implemented to elucidate optimal pathways for producing biomass or succinic acid (SA) through different xylose assimilation pathways. Theoretical maximum yields are summarised in Table 6.

6.1 *Corynebacterium glutamicum*

C. glutamicum is a well-known industrially relevant bacterium that is widely engineered to produce value-added products from a wide range of carbon sources.[182] The xylose isomerase (XI) pathway was previously implemented in *C. glutamicum*,[183] which showed a 30% theoretical maximum yield of succinic acid from xylose. As seen from Table 6, XI and XR–XDH pathways have the potential to produce yields equivalent to those on glucose on a carbon basis. Theoretical maximum yields of up to 80% can be achieved when the Weimberg (WMB) pathway is used while the lowest possible maximum yield of 40% is observed with the Dahms pathway. Optimal routes using the different xylose assimilating pathways are shown in Fig. 7. As seen from Fig. 7,

Table 5 Performance of engineered strains for product formation from xylose *via* a microbial route

Product	Microorganism	Modification	Improvement	References
Xylitol	*Meyerozyma guilliermondii*	Cloning and overexpression of XR, and knockout of XDH	The engineered strain exhibited a 3-fold improvement in xylitol yield	243
	E. coli	Expression of XR and glucose dehydrogenase	The immobilized recombinant cells could maintain the enzyme activity up to 80% after 10 repeated batches	244
	K. marxianus	Expression of XR and transporter genes	The engineered strain efficiently utilized glucose and xylose from xylose-rich hydrolysate for production of xylitol > 100 g L^{-1}	245
	S. cerevisiae	Expression of the constitutive GPD promoter for the *ZWF1*(cytoplasmic G6P dehydrogenase) gene to increase the NADPH pool, a cofactor for XR	The heterologous expression of a constitutive promoter resulted in a 12% increase in xylitol yield (0.78 vs. 0.88)	246
Lactic acid	*S. cerevisiae*	Heterologous overexpression of the lactate dehydrogenase (*ldhA)* gene from *Rhizopus oryzae* under the control of the PGK1 promoter through chromosome integration	High lactate dehydrogenase activity and LA titers of 28.9 g L^{-1} with 0.69g g^{-1} yield	247
	Scheffersomyces stipitis	Heterologous overexpression of *ldh* from *L. helveticus* under the control of the native ADH1 promoter	Ethanol production decreased 15 to 30% and carbon flux is shifted towards LA from xylose resulting in 58 g L^{-1} LA with 0.58 g g^{-1} yield	248
	Pediococcus acidilactici	Heterologous expression of xylose assimilating genes *XylA* and *XylB*, substitution of endogenous phosphoketolase with heterologous transketolase and transaldolase	The metabolic carbon flux is concentrated towards LA biosynthesis resulting in 97.3 g L^{-1} LA with 0.93 g g^{-1} conversion yield	219
	Lactococcus lactis	Disruption of the phosphoketolase gene, introduction of the transketolase gene	High LA titers of 50.1 g L^{-1} with 1.58 mol mol^{-1} yield and 99.6% purity after the downstream processing was quantified	249
	Candida sonorensis	Integrating lactate dehydrogenasegene from *L. helveticus*	The engineered strains were able to accumulate 31 g L^{-1} LA with 0.62 g g^{-1} yield under microaerobic conditions	250
Succinic acid	*Yarrowia lipolytica* PSA02004	Overexpressing the pentose pathway cassette (XR, XDH and XK genes)	The engineered strain could grow on xylose as a sole energy and carbon source producing 22.3 g L^{-1} SA	144
	Corynebacterium glutamicum	Heterologous expression of XI, overexpression of XK, transaldolase, 6-phosphogluconate dehydrogenase and phosphoketolase	The recombinant strain enhanced the growth and xylose consumption rate resulting in 7.22 g L^{-1} SA with 0.18 g g^{-1} yield	251
	Escherichia coli KJ122	Deletion of *XylFGH* and *XylE* genes and ALE	Improved succinate titers of 85 g L^{-1} with 0.85 g g^{-1} yield, and 0.7 g L^{-1} h^{-1} productivity	142
	E. coli K12	Inactivation of pyruvate formate lyase (*pflB*) and lactate dehydrogenase (*ldhA*)	Significant increase in cell mass (2.5 g L^{-1}) and succinate (11.6 g L^{-1}) production	252
	Aspergillus niger	Overexpression of fumarate reductase, disruption of gluconic acid and oxalic acid production	The engineered strain was able to utilize xylose-rich hydrolysates derived from sugar beet and wheat straw to produce 23 and 9 g L^{-1} SA	253
2,3-Butanediol	*S. cerevisiae*	Heterologous expression of the BDO biosynthetic pathway, deletion of ethanol and glycerol assimilatory genes. Restoration of redox balance by overexpression of NADH oxidase	Highest yield (0.41 g g^{-1}) and productivity (1.43 g L^{-1} h^{-1}) using *S. cerevisiae* as the host	85
	Enterobacter cloacae	Expression of BDO dehydrogenase, inactivation of glucose transporter and overexpression of galactose permease	The engineered strain could overcome CCR and was able to utilize glucose and xylose simultaneously, producing 119.4 g L^{-1} BDO with 2.3 g L^{-1} h productivity	254

Table 5 (*Contd.*)

Product	Microorganism	Modification	Improvement	References
	Zymomonas mobilis	Heterologous expression of BDO biosynthetic pathway consisting of acetolactate synthase, acetolactate decarboxylase, and butanediol dehydrogenase	The engineered strain was able to produce BDO (13.3 g L^{-1}) utilizing both C5 and C6 sugars	255
	S. cerevisiae	Expression of *S. stipitis* transaldolase, xylose reductase, *L. lactis* NADH oxidase and overexpression of *pdc* from *C. tropicalis*	A 2.1-fold increase in xylose consumption and 1.8-fold increase in BDO productivity	256
	K. pneumoniae	Overexpression of transketolase, NADP transhydrogenase subunit alpha, and NADH dehydrogenase subunit F	The engineered strain increased the xylose consumption and BDO production resulting in 38.6 g L^{-1} BDO with 0.62 g L^{-1} h^{-1} productivity	149
Ethanol	*S. cerevisiae*	Overexpressing pentose pathway genes (XR and XDH)	Assimilation of xylose towards ethanol biosynthesis with a conversion yield of 0.19 g g^{-1}	162
	S. cerevisiae	Overexpression of mutant XR K270R	Increased specificity towards NADH rather than NADPH, resulting in increased ethanol yield (0.38 g g^{-1}) and reduced xylitol yield (0.08 g g^{-1})	162
n-Butanol	*E. coli*	Expression of a synthetic butanol pathway	In a defined medium 4.32 g L^{-1} *n*-butanol was produced	257
	Clostridium tyrobutyricum	Heterologous expression of *XylT*, *XylA*, and *XylB* from *C. acetobutylicum* and overexpression of native alcohol dehydrogenase	The engineered strain could accumulate 12 g L^{-1} *n*-butanol with 0.12 g g^{-1} yield	258
PHB	*E. coli*	Heterologous expression of XI, XK and pentose transport protein from *B. subtilis* in *E. coli* harbouring the PHB pathway from *Ralstonia eutropha*	Simultaneous utilization of glucose and xylose increased PHB titers 2-fold	259
	S. cerevisiae	Heterologous overexpression of the PHB biosynthesis pathway from *Cupriavidus necator*	The engineered strain could produce 1.99 mg PHB/g xylose	260
	S. cerevisiae	Heterologous overexpression of NADH dependent acetoacetyl-CoA from *Allochromatiumvinosum* replacing the gene from *C. necator*	PHB titers increased 5-fold under aerobic and 8.4-fold under oxygen limited conditions	261

Table 6 Theoretical maximum yields of biomass and succinic acids from xylose assimilation *via* different pathways

Yield	Glucose	Xylose-XR–XDH pathway (XR–XDH)	Xylose-isomerase pathway (XI)	Xylose-Weimburg pathway (XW)	Xylose-Dahms pathway (XD)
C. glutamicum					
Biomass yield (c-mol biomass c-mol substrate^{-1})	0.84	0.81	0.84	0.59	0.54
Succinic acid yield (c-mol succinate c-mol substrate^{-1})	0.67	0.67	0.67	0.80	0.40
E. coli					
Biomass yield (c-mol biomass c-mol substrate^{-1})	0.90	0.90	0.90	0.63	0.58
Succinic acid yield (c-mol succinate c-mol substrate^{-1})	0.67	0.67	0.67	0.80	0.40
A. succinogenes					
Biomass yield (c-mol biomass c-mol substrate^{-1})	0.34	0.34	0.34	NA	NA
Succinic acid yield (c-mol succinate c-mol substrate^{-1})	0.67	0.80	0.80	NA	NA
Y. lipolytica					
Biomass yield (c-mol biomass c-mol substrate^{-1})	0.73	0.70	0.72	0.49	0.46
Succinic acid yield (c-mol succinate c-mol substrate^{-1})	0.90	1.0	1.0	0.80	0.80

XR–XDH and XI show similar optimal routes for SA production and about 2 mol mol^{-1} of O_2 demand is observed for both the pathways. The WMB pathway seems to be the most efficient route that can reach a maximum yield of 1 mol SA per mol xylose. This is attributed to alpha-ketoglutarate that is generated in the upper xylose assimilation pathway which directly enters the TCA cycle. As seen, biomass yields are significantly lower compared to XI and XR–XDH pathways (~20%) in both the WMB and Dahms pathways. When the Dahms pathway is used only 40% of carbon can be theoretically converted to SA under non-biomass production conditions. Under non-biomass conditions which would be normally implemented for succinic acid production (*i.e.* dual fermentation mode), surplus ATP must be replenished which is seen as output of ATP for maintenance purposes. A futile cycle could be generated which can replenish this surplus ATP under non-biomass production

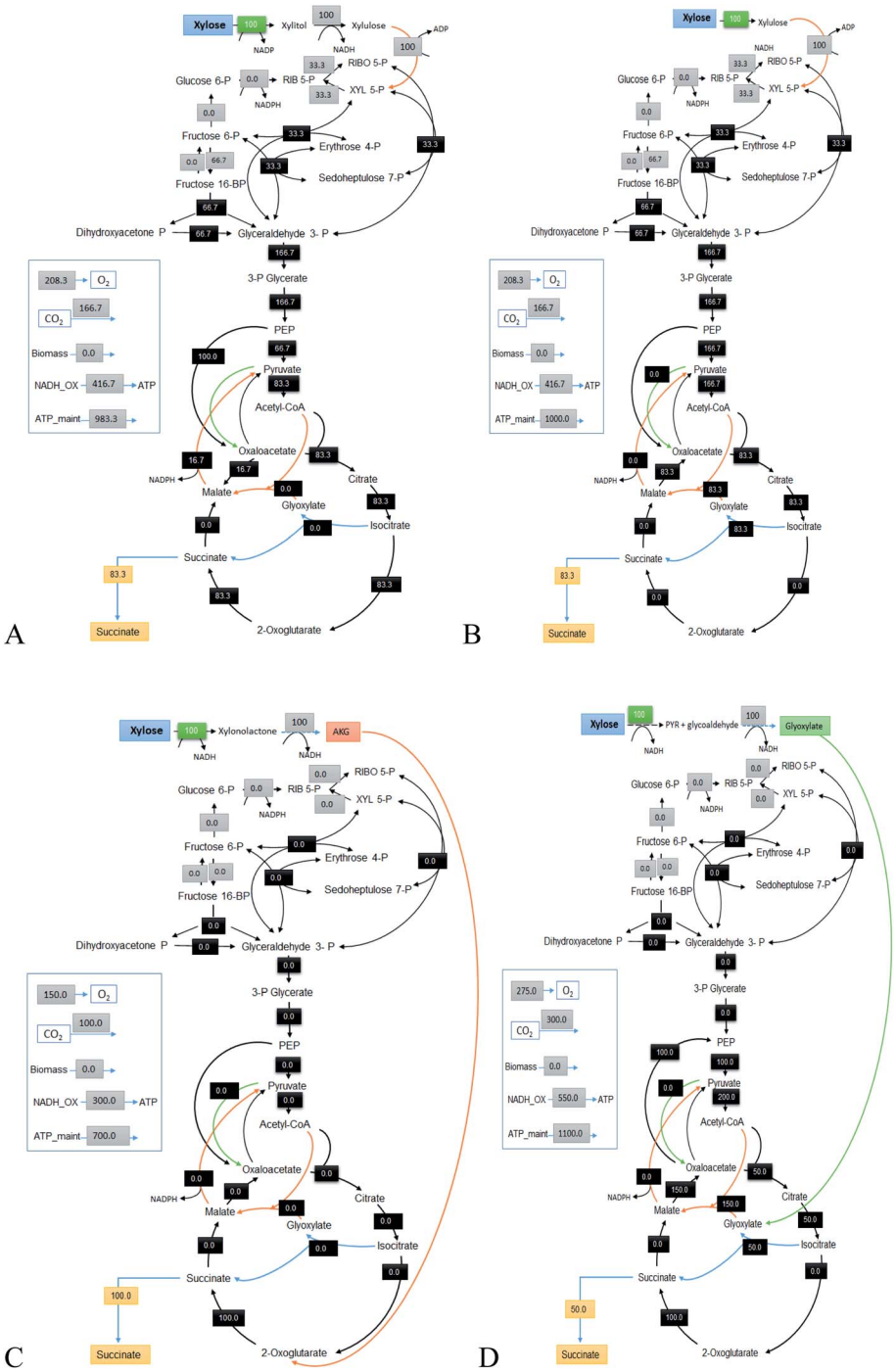

Fig. 7 Theoretical maximum (optimal) production of SA *via* (A) the XR–XDH pathway, (B) XI pathway, (C) XW pathway and (D) XD pathway in *C. glutamicum*. Values normalised to 100% xylose uptake rate (mmol g^{-1} h^{-1}).

conditions. The NADPH required for xylose assimilation *via* the XR–XDH pathway is mainly supplied by isocitrate dehydrogenase. Optimal succinate production modes were also observed (data not shown) where the glyoxylate cycle can be active and malic enzyme could be providing the required NADPH. The XW pathway was implemented previously in *C. glutamicum*,[184] which showed growth inhibition due to accumulation of xylose 5-phosphate. Since the advantage of using the XW pathway lies in preventing the loss of carbon *via* CO_2 production, there is about 40% less CO_2 being produced and 25% less O_2 demand in comparison to the XR–XDH and XI pathways. The XD pathway loses about 80% more carbon in the form of CO_2 and requires 30% more O_2 compared to the XR–XDH and XI pathways.

6.2 *Escherichia coli*

E. coli is more suitable for achieving higher biomass yields from xylose as seen in Table 6 due to its wider flexibility. The two transhydrogenases demonstrate their advantage in *E. coli's*

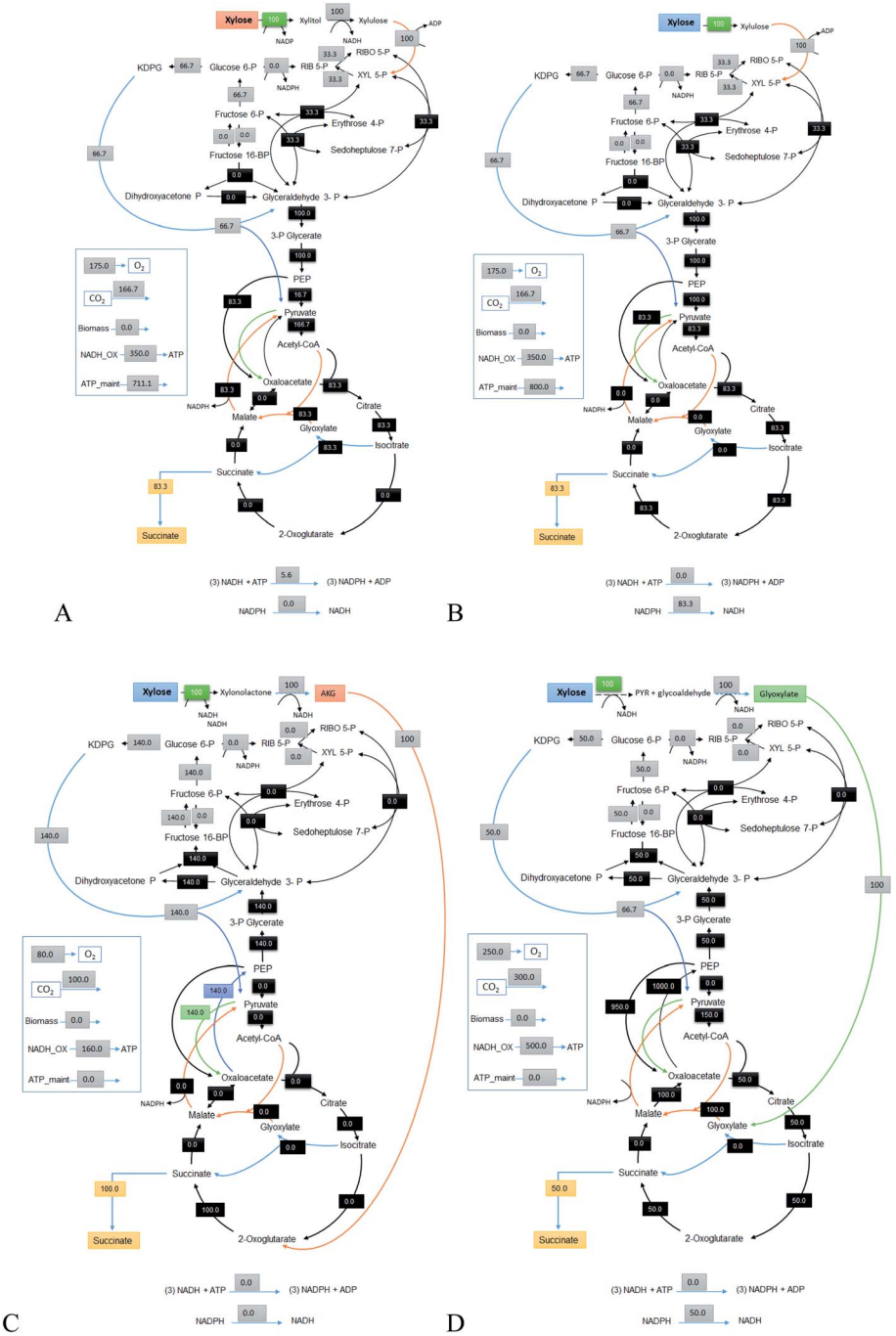

Fig. 8 Theoretical maximum (optimal) production of SA *via* (A) the XR–XDH pathway, (B) XI pathway, (C) XW pathway and (D) XD pathway in *E. coli*. Values normalised to 100% xylose uptake rate (mmol g^{-1} h^{-1}).

added metabolic flexibility. About 8% more biomass can be achieved for all the different pathways in *E. coli* compared to *C. glutamicum*. Similar theoretical maximum yields of succinate were observed in *E. coli* when compared to *C. glutamicum*. *E. coli* naturally harbours the XI pathway which enables it to assimilate xylose naturally.[185] Several anaerobic strategies and metabolic engineering routes have been reported for enhanced succinic acid production in *E. coli* on different carbon sources.[186] Only aerobic related succinic acid production strategies are depicted in Fig. 8. Under anaerobic conditions, pyruvate carboxylase or PEP carboxykinase overexpression together with succinate dehydrogenase deletion were proven to be efficient targets for enhanced succinic acid production implementing mainly the reductive TCA cycle. The shown optimal strategies using xylose are under aerobic conditions. As seen from the optimal strategies, owing to the flexibility of metabolism *i.e.* balancing reducing equivalents in *E. coli*, strategies were observed for both reductive as well as oxidative TCA cycle routes. As seen in Fig. 8, both the XR–XDH and XI pathways rely on the KDPG pathway and NADPH is mainly generated *via* malic enzyme for the XR–XDH pathway. Excess NADPH in converted back to NADH in the XI pathway *via* the soluble transhydrogenase. Similar to that observed in *C. glutamicum*, the XW pathway requires less O_2 per mol xylose assimilated and produces less CO_2 with a theoretical maximum yield of 1 mol succinate per mol xylose. To date, XW and XD pathways have not been implemented in *E. coli* to produce succinic acid. When the XD pathway is implemented a potential overexpression target would be the glyoxylate cycle, but as shown in Fig. 8, higher O_2 demand and carbon loss in the form of CO_2 will make this pathway inefficient for producing succinate from xylose.

6.3 *Actinobacillus succinogenes*

The acid tolerant strain *A. succinogenes* is known for its high production capacity of succinic acid. This facultative anaerobic bacterium can assimilate both C6 and C5 sugars. Certain studies also showed that higher biomass and succinic acid production was observed when CO_2 and/or H_2 are supplied additionally.[187] *A. succinogenes* does not harbour a complete TCA cycle and it is an auxotroph of glutamine, methionine and cysteine. A detailed flux analysis has been performed on *A. succinogenes* giving insights into its metabolism.[188] It is also identified that it does not comprise the glyoxylate cycle. As shown in Fig. 9, both the XR–XDH and XI pathway yields are 1 mol succinate per mol xylose. Interestingly, most of the optimal succinic acid production pathways produced ethanol as a by-product indicating that there was excess NADH to be replenished. NADPH is mainly supplied by the PP pathway for XR–XDH based xylose consumption. On xylose, the transhydrogenase present in *A. succinogenes* would be a very

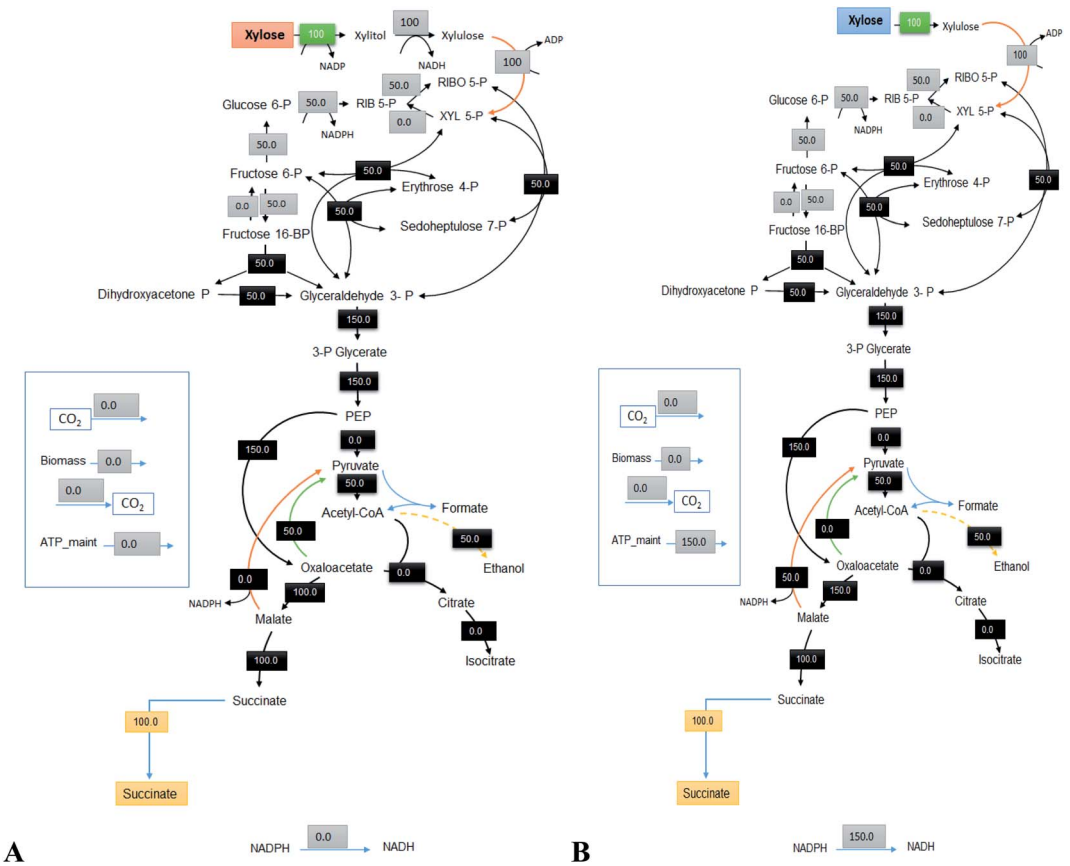

Fig. 9 Theoretical maximum (optimal) production pathways of SA *via* (A) the XR–XDH pathway and (B) XI pathway in *A. succinogenes*. Values normalised to 100% xylose uptake rate (mmol g^{-1} h^{-1}).

essential reaction in balancing NADH and NADPH. To incorporate the XW pathway into *A. succinogenes*, alpha-ketoglutarate dehydrogenase and a succinyl-CoA synthetase have to be expressed. This could also eliminate the glutamine auxotroph. For the XD pathway, the glyoxylate cycle genes, isocitrate lyase and malate synthase must be expressed which would enable the uptake of glyoxylate produced from the XD pathway.

6.4 *Yarrowia lipolytica*

Owing to its well-known potential in producing lipids, citric acid and other value-added products, *Y. lipolytica* has been demonstrated for its effectiveness in producing succinic acid from xylose.[144] Availability of genetic tools and engineering for a wider substrate spectrum, tolerance at reduced pH and flexible metabolism makes this yeast a potential cell factory for succinic acid production. As depicted in Fig. 10, the optimal

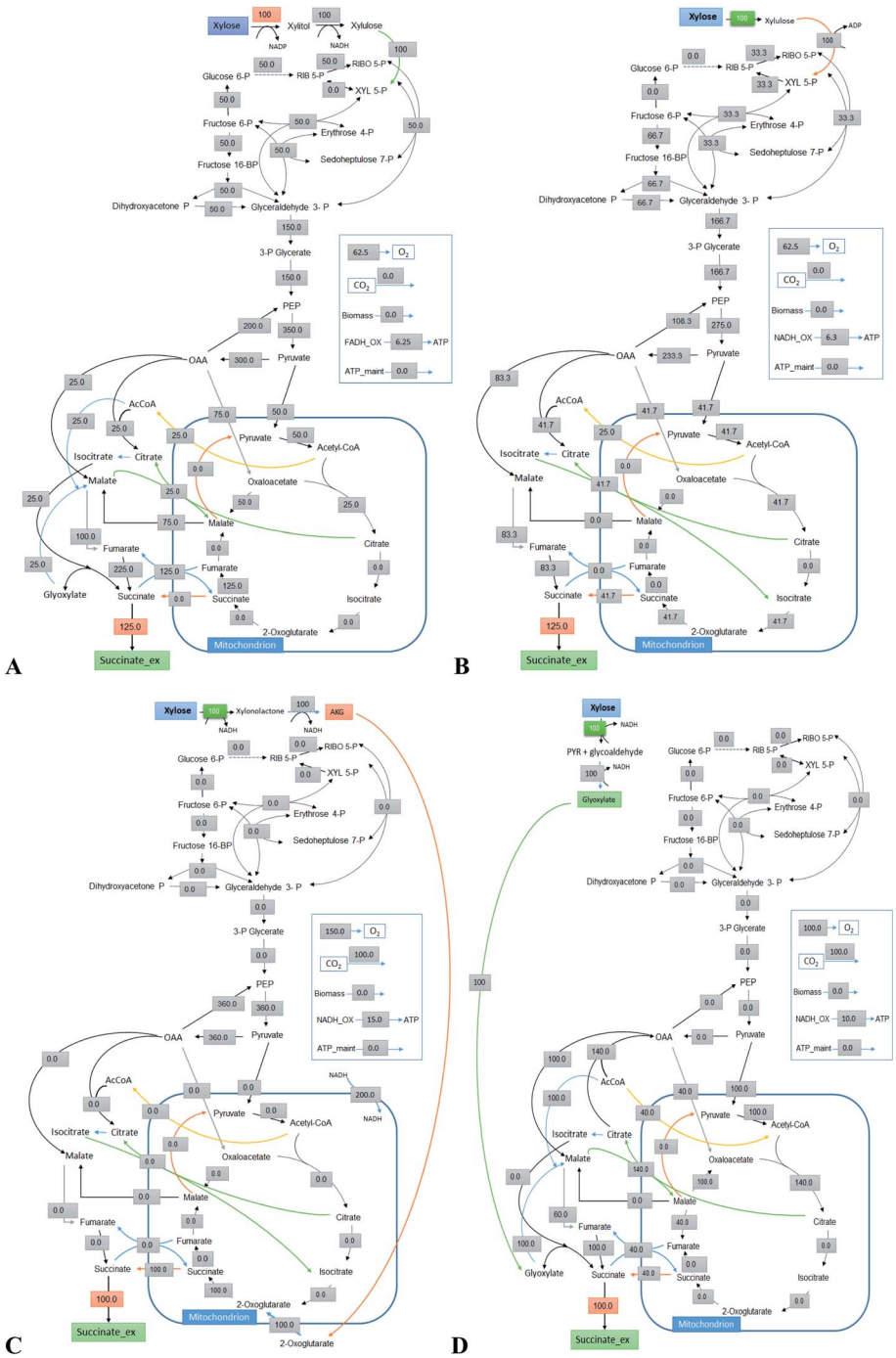

Fig. 10 Theoretical maximum (optimal) production of SA *via* (A) the XR–XDH pathway, (B) XI pathway, (C) XW pathway and (D) XD pathway in *Y. lipolytica*. Values normalised to 100% xylose uptake rate (mmol g^{-1} h^{-1}).

production of succinic acid can reach maximum yields of 1 c-mol succinic acid per c-mol xylose in XR–XDH and XI pathways. The PP pathway is shown to be the main NADPH supplying route for xylose uptake in the XR–XDH pathway which is also observed during lipid production.[189] O_2 demand is significantly lower per mol xylose when compared to the bacterial O_2 demand for succinic acid production. Interestingly, the XW pathway is not the optimal pathway for producing succinic acid in *Y. lipolytica* compared to what has been observed in *E. coli* and *C. glutamicum*. Carbon loss in the form of CO_2 is observed in the XW pathway in *Y. lipolytica*. As also observed, the bacterial XW and XD pathways require higher O_2 compared to the XR–XDH and XI pathways. Addition of external CO_2 to *A. succinogenes* and the consumption of this CO_2 by PEPC or PYC will reduce the overall succinic acid yield (0.56 c-mol c-mol^{-1}). The reductive TCA cycle is probably the best option, but optimal strategies can also be envisaged as observed in *E. coli* or *C. glutamicum* optimal pathways. As observed previously, an enhanced flux through the PP pathway especially for the XR–XDH pathway would be beneficial for enhanced xylose uptake and succinic acid production.

7. Challenges for xylose based bioproduction

Xylose is a renewable sugar with great potential but has been overlooked due to low metabolic capabilities and process limitations. Although various bacteria, yeast and fungi do assimilate xylose, they utilize it in a hierarchical fashion, and these are the bottlenecks that are limiting the commercial application.

7.1 Inefficient transport of pentose or absence of xylose specific transporters in the microbial cell

Xylose transport into bacterial, yeast or fungal cells through native or heterologous transporters was explained in Section 4.1. In all these microorganisms, the major limiting factor and a prerequisite objective to be addressed is the xylose uptake rate or transport efficiency of the individual cell. Most of the attempts to improve the xylose utilization efficiency of the native transporter or heterologous expression were made in *E. coli* and *S. cerevisiae*, but still the results are incomparable to glucose uptake rates. For example, the glucose uptake rate in an *S. cerevisiae* cell is 0.085 C-mol g_{CDW}^{-1} h^{-1}, while for xylose it is approximately three times slower (0.027 C-mol g_{CDW}^{-1} h^{-1}). In recent years, with the availability of advanced systems/synthetic biology tools and metabolic engineering techniques, there lies a scope of either engineering native promoters or investigating novel high efficiency xylose transporters through genome mining.

Relative modifications in genotype and phenotype can be achieved by subjecting the microbial consortia to selective pressure.[190] Radek *et al.* (2017) developed an automated and miniaturized ALE approach based on repetitive batch cultivations in microtiter plates. They subjected *Corynebacterium glutamicum pEKEx3-xylXABCDCc* bearing the Weimberg (WMB) pathway to ALE for improving xylose consumption. The evolved strain showed a 260% increase in xylose consumption efficiency.[191] Overexpression of the *S. stipitis Sut1* xylose transporter gene in *S. cerevisiae* improved the xylose uptake rate and ethanol yield by 25 and 17%, respectively, while xylose assimilation was enhanced by 25 and 40% with the introduction of *Arabidopsis thaliana* xylose transporter genes *At5g17010* and *At5g59250*, respectively.[192] A large improvement (75%) in xylose transport was achieved with *Gxf1*, a MFS transporter identified from *Candida intermedia*.[193] This traditional xylose transporter displayed improved xylose uptake efficiency at lower xylose concentrations ($\sim$10 g L^{-1}) while at higher levels, the efficiency was reduced drastically. Later, comparative genome analysis of *C. sojae* revealed the presence of two xylose specific transporters encoded by *Cs3894* and *Cs4130* genes, exhibiting a substantial xylose uptake rate at concentrations up to 50 g L^{-1}.[193] The quest for novel and efficient xylose specific transporters and expression of those xylose transporters could allow rapid transport of xylose, bypass the glucose mediated repression mechanisms and enable simultaneous fermentation of mixed sugars.[194]

7.2 Glucose imposed carbon catabolite repression

After xylose transport, the next challenge with xylose-based cell factories is the phenomenon of carbon catabolite repression or glucose mediated inhibition which impedes the simultaneous consumption of xylose and glucose. So, the first question that comes to mind is why we need to supplement both glucose and xylose together. LCB is the most abundant material, and the abundance is so high that it can replace all the carbon coming from fossil sources. The production and process economics of LCB-biorefineries can be improved if the host strain can simultaneously utilize both glucose and xylose saccharified from the LCB. The three basic mechanisms mediating CCR have been explained in Section 3.3 (Fig. 4). As per $EIIA^{Glc}$ mediated catabolite repression, high levels of cAMP activate the expression of genes responsible for the metabolism of non-glucose sugars. In a study by Ammar *et al.* (2018) when the culture medium was supplemented with 5–10 mM cAMP, CCR was not observed in glucose–galactose co-fermentation, but 10 mM cAMP concentration was not enough to overcome CCR for simultaneous utilization of glucose and xylose.[72]

7.3 Regulation of intracellular xylose metabolism

After passing the gateway and co-substrate mediated repression, the next obstacle to address would be the slow rate of biochemical reactions using xylose and its derivatives as substrates making the overall process sluggish. That is why cell growth and metabolite production rates on xylose are slower in comparison to glucose. *S. cerevisiae* has been in commercial use and is known to be the best hexose utilizer, the strain lacks an active xylose utilization pathway and most of the studies were concentrated on heterologous expression of the *S. stipitis* xylose assimilatory pathway in *S. cerevisiae*, but the results observed were not satisfactory.[195] *S. cerevisiae*, for example, has a specific growth rate of 0.25 h^{-1} on glucose *vs.* 0.05 h^{-1} on xylose, a nearly 5-fold difference that not only limits the biomass, but also influences cell physiology and metabolism. This indicates

insufficient understanding of the metabolic network and to decode this problem, it is very important to have deep understanding of the kinetics of xylose related reactions and underlying complex regulation as *in vivo* activity is burdened with several types of regulation. Hence, exploring the innate regulatory mechanisms of native and non-native xylose assimilatory microorganisms, and rational design and metabolic engineering leading to optimal metabolic flux and energy metabolism during the xylose assimilation is necessary.

7.4 Maintaining the redox homeostasis

It is challenging for most biological processes to maintain redox homeostasis. Any deficiency of redox cofactors leads to expression of alternative metabolic pathways leading to by-product synthesis. In the xylose oxidoreductive (XR–XDH) pathway, regeneration of NAD^+ is very important to direct the carbon flux into central carbon metabolism to allow smooth xylose assimilation. The imbalance between the enzymatic activities of XR and XDH results in NAD^+ limitation which leads to xylitol accumulation. Under aerobic conditions, the microbial cell has the ability to regenerate NAD^+, while oxygen limited or anaerobic conditions cause a shortage of NAD^+ supply. Thus, maintaining optimal oxygen levels or alternative routes to generate NAD^+ without interfering with the fermentation capability of the microbial strain is very important to facilitate xylose metabolism. Carlos Roseiro and associates observed the relationship between the volumetric oxygen transfer coefficient (K_{La}), a parameter which is a reflection of the ease of oxygen supply, and the xylitol production in a yeast, *Debaryomyces hansenii*. They found that increasing the K_{La} (h^{-1}) from 0.2 to 1.8 caused an improvement in the xylitol accumulation, and an increase beyond 1.8 boosted the ethanol production.[196] Bonan *et al.* (2020) attained highest ethanol titers of 28.6 g L^{-1} with 0.31 g g^{-1} yield and 1.12 g L^{-1} h^{-1} productivity with *Spathaspora passalidarum* at K_{La} (h^{-1}) of 45.[54] Hence, an ideal process engineering aspect would be to determine the optimal K_{La} value which maximizes the xylose flux towards the desired product with minimal or no secretion of xylitol, eventually benefiting the cell growth and product formation. Alternative approaches such as overexpression of NOX, modification of the cofactor specificity of XR, or expression of NADH specific XR over NADPH-dependent XR can alleviate the problem of redox imbalance and replenish the flux towards central carbon metabolism.[197] Most of them have been attempted and only limited success has been achieved so far.

8. Conclusion and future perspectives

Xylose is a readily available sugar with potential to serve as feedstock for biorefineries. For the economic viability of lignocellulose biorefineries, the efficient conversion of hemicellulosic sugars into value-added products is mandatory. Glucose-based commercially developed bioprocesses are prevalent while xylose-based ones are evolving at an industrial scale. Recent developments in biomass pretreatment technologies have led the way to extract xylose from the hemicellulosic fraction of plant cell walls with desired yields with a small amount of plant cell wall inhibitors. In nature, the xylose metabolising microorganisms are scanty compared to those metabolising glucose. Therefore, bioprospecting of novel microorganisms that could assimilate xylose separately or in combination with glucose with faster conversion rates will significantly promote efficiency of LCB-based biorefineries. However, the xylose uptake rates of the well-known xylose assimilating microorganisms are significantly lower than those assimilating glucose. Despite the exemplary developments in xylose bioconversion, there are still several challenges which need to be fixed for developing efficient microbial cell factories for high level manufacturing of biochemicals and biofuels. These challenges include efficient xylose transportation into microbial cells, faster uptake & metabolism of xylose similar to glucose, continuous availability of redox cofactors for maintaining homeostasis, glucose repression during co-fermentation, and feedback, substrate, and product mediated inhibition. Recent advancements in enzyme/metabolic/pathway engineering along with system/synthetic biology approaches have been employed to overcome these challenges but have been met with limited success. Though, xylose-based bioproduction has shown significant progress in the last few decades, many obstacles still need to be addressed to realize xylose as a feedstock at the industrial level.

List of abbreviations

ATP	Adenosine triphosphate
BDO	2,3-Butanediol
cAMP	3′,5′-Cyclic adenosine monophosphate
CBP	Consolidated bioprocessing
ccpA	Catabolite control protein A
CRE	Catabolite repressive element
CRP	cAMP receptor protein
DA	Dilute acid
DHA	Dihydroxyacetone
DHAP	Dihydroxyacetone phosphate
DXD	D-Xylose dehydrogenase
EMP pathway	Embden–Meyerhof–Parnas pathway
E4P	Erythrose-4-phosphate
F6P	Fructose-6-phosphate
GlpF	Glycerol facilitator protein
GlfZ	Glucose transporter
HT	Hydrothermal
K_{La}	Volumetric oxygen transfer coefficient
K_m	Michaelis–Menten constant
LA	Lactic acid
LAB	Lactic acid bacteria
LCB	Lignocellulosic biomass
LHW	Liquid hot water
NADH	Nicotinamide adenine dinucleotide
NADPH	Nicotinamide adenine dinucleotide phosphate
SE	Steam explosion
P_A/P_E	Promoters

PEP	Phosphoenol pyruvate
PHB	Polyhydroxybutyrate
PLA	Polylactic acid
PPP	Pentose phosphate pathway
SA	Succinic acid
TCA	Tricarboxylic acid
V_{max}	Maximum velocity of an enzyme mediated reaction
X1P	Xylulose-1-phosphate
X5P	Xylulose-5-phosphate
XDH	Xylitol dehydrogenase
XI	Xylose isomerase
XK	Xylulose kinase
XR	Xylose reductase
Xyl1	Xylose reductase gene
Xyl2	Xylitol dehydrogenase gene
XylA	Xylose isomerase gene
XylB/Xyl3	Xylulose kinase gene
XylC	Xylonolactonase
XylD	Xylonate dehydratase
XylX	2-Keto-3-deoxy-xylonate dehydratase

Data availability

Data sharing is not applicable to this Review article as no new data were created or analysed in this study.

Author contributions

NV: conceptualization, writing-original draft, reviewing & editing; RC, RB, DA, EA, KKP and AKC: writing-original draft, reviewing & editing; SKB, DK, PB and VG: reviewing & editing; VK: conceptualization, writing-original draft, reviewing & editing and project management.

Conflicts of interest

The authors declare that they have no competing interests.

Acknowledgements

This study was financially supported through the vWa Project (Grant BB/S011951/1) and we acknowledge BBSRC, Innovate UK and Department of Biotechnology, India for funding this project. The funders had no role in the study design, data collection and analysis, decision to publish, or preparation of the article.

References

1 V. Balan, *ISRN Biotechnol.*, 2014, **2014**, 1–31.
2 A. J. Ragauskas, G. T. Beckham, M. J. Biddy, R. Chandra, F. Chen, M. F. Davis, B. H. Davison, R. A. Dixon, P. Gilna, M. Keller, P. Langan, A. K. Naskar, J. N. Saddler, T. J. Tschaplinski, G. A. Tuskan and C. E. Wyman, *Sci. 80*, 2014, **344**, 1246843.
3 B. Satari, K. Karimi and R. Kumar, *Sustain. Energy Fuels*, 2019, **3**, 11–62.
4 S. H. Hazeena, R. Sindhu, A. Pandey and P. Binod, *Bioresour. Technol.*, 2020, **302**, 122873.
5 M. Dehghanzad, M. Shafiei and K. Karimi, *Renewable Energy*, 2020, **158**, 332–342.
6 V. Kumar, P. Binod, R. Sindhu, E. Gnansounou and V. Ahluwalia, *Bioresour. Technol.*, 2018, **269**, 443–451.
7 N. Vivek, M. Christopher, M. K. Kumar, E. Castro, P. Binod and A. Pandey, *Renewable Energy*, 2018, **129**, 794–799.
8 J. M. Gancedo, *Eur. J. Biochem.*, 1992, **206**, 297–313.
9 F. M. Gírio, F. Carvalheiro, L. C. Duarte and R. Bogel-ŁUkasik, in *D-xylitol: Fermentative Production, Application and Commercialization*, Springer-Verlag Berlin Heidelberg, 2012, pp. 3–37.
10 S. I. Mussatto and G. M. Dragone, in *Biomass Fractionation Technologies for a Lignocellulosic Feedstock Based Biorefinery*, Elsevier Inc., 2016, pp. 1–22.
11 L. R. Lynd, C. E. Wyman and T. U. Gerngross, *Biotechnol. Prog.*, 1999, **15**, 777–793.
12 M. E. Himmel, S. Y. Ding, D. K. Johnson, W. S. Adney, M. R. Nimlos, J. W. Brady and T. D. Foust, *Sci. 80*, 2007, **315**, 804–807.
13 R. Kumar, G. Mago, V. Balan and C. E. Wyman, *Bioresour. Technol.*, 2009, **100**, 3948–3962.
14 N. Uppugundla, L. Da Costa Sousa, S. P. S. Chundawat, X. Yu, B. Simmons, S. Singh, X. Gao, R. Kumar, C. E. Wyman, B. E. Dale and V. Balan, *Biotechnol. Biofuels*, 2014, **7**(1), 1–14.
15 K. Yao, Q. Wu, R. An, W. Meng, M. Ding, B. Li and Y. Yuan, *AIChE J.*, 2018, **64**, 1938–1953.
16 D. Steinbach, A. Kruse, J. Sauer and J. Storz, *Processes*, 2020, **8**, 1–12.
17 J. C. Solarte-Toro, Y. Chacón-Pérez, S. Piedrahita-Rodríguez, J. A. Poveda Giraldo, J. A. Teixeira, K. Moustakas and C. A. C. Alzate, *Energy*, 2020, **195**, 116986.
18 F. Rodríguez, A. Sanchez and L. Amaya-Delgado, *Ind. Crops Prod.*, 2019, **134**, 62–70.
19 J. S. Kim, Y. Y. Lee and T. H. Kim, *Bioresour. Technol.*, 2016, **199**, 42–48.
20 Y. Zhang, Y. Y. Liu, J. L. Xu, Z. H. Yuan, W. Qi, X. S. Zhuang and M. C. He, *Bioresources*, 2012, **7**, 345–353.
21 S. F. Fu, K. Q. Chen, R. Zhu, W. X. Sun, H. Zou and R. B. Guo, *Energy Convers. Manag.*, 2018, **159**, 121–128.
22 Z. Gong, X. Wang, W. Yuan, Y. Wang, W. Zhou, G. Wang and Y. Liu, *Biotechnol. Biofuels*, 2020, **13**, 1–15.
23 Q. Ibrahim and A. Kruse, *Bioresour. Technol. Rep.*, 2020, **11**, 100506.
24 A. Smit and W. Huijgen, *Green Chem.*, 2017, **19**, 5505–5514.
25 J. Xu, Y. Fu, G. Tian, Q. Li, N. Liu, M. Qin and Z. Wang, *Bioresour. Technol.*, 2018, **254**, 353–356.
26 Z. Chen, W. D. Reznicek and C. Wan, *ACS Sustainable Chem. Eng.*, 2018, **6**, 6910–6919.
27 G. Wang, S. Qi, Y. Xia, A. M. Parvez, C. Si and Y. Ni, *ACS Sustainable Chem. Eng.*, 2020, **8**, 2772–2782.

28 Q. Zhang, Y. Deng, X. Tan, W. Wang, Q. Yu, X. Chen, C. Miao, Y. Guo, Y. Zhang, X. Zhuang and Z. Yuan, *Ind. Crops Prod.*, 2020, **145**, 112091.
29 X. Zhang, W. Zhang, F. Lei, S. Yang and J. Jiang, *Bioresour. Technol.*, 2020, **309**, 123385.
30 C. Cai, K. Hirth, R. Gleisner, H. Lou, X. Qiu and J. Y. Zhu, *Green Chem.*, 2020, **22**, 1605–1617.
31 T. Y. Nguyen, C. M. Cai, O. Osman, R. Kumar and C. E. Wyman, *Green Chem.*, 2016, **18**, 1581–1589.
32 C. M. Cai, T. Zhang, R. Kumar and C. E. Wyman, *J. Chem. Technol. Biotechnol.*, 2014, **89**, 2–10.
33 J. Jae, G. A. Tompsett, Y.-C. Lin, T. R. Carlson, J. Shen, T. Zhang, B. Yang, C. E. Wyman, W. C. Conner and G. W. Huber, *Energy Environ. Sci.*, 2010, **3**, 358–365.
34 L. T. Mika, E. Cséfalvay and Á. Németh, *Chem. Rev.*, 2018, **118**, 505–613.
35 N. W. Dulie, B. Woldeyes, H. D. Demsash and A. S. Jabasingh, *Waste Biomass Valorization*, 2021, **12**, 531–552.
36 J. Cui, J. Tan, X. Cui, Y. Zhu, T. Deng, G. Ding and Y. Li, *ChemSusChem*, 2016, **9**, 1259–1262.
37 X. Hu, Y. Song, L. Wu, M. Gholizadeh and C. Z. Li, *ACS Sustainable Chem. Eng.*, 2013, **1**, 1593–1599.
38 D. Dasgupta, S. Bandhu, D. K. Adhikari and D. Ghosh, *Microbiol. Res.*, 2017, **197**, 9–21.
39 R. F. Perez, O. S. G. P. Soares, A. M. D. de Farias, M. F. R. Pereira and M. A. Fraga, *Appl. Catal., B*, 2018, **232**, 101–107.
40 J. Wisniak, M. Hershkowitz, R. Leibowitz and S. Stein, *Ind. Eng. Chem. Prod. Res. Dev.*, 1974, **13**, 75–79.
41 S. Kwak, J. H. Jo, E. J. Yun, Y. S. Jin and J. H. Seo, *Biotechnol. Adv.*, 2019, **37**, 271–283.
42 C. Zhao, Y. Zhang and Y. Li, *Biotechnol. Adv.*, 2019, **37**, 107402.
43 P. M. Bruinenberg, P. H. M. de Bot, J. P. van Dijken and W. A. Scheffers, *Eur. J. Appl. Microbiol. Biotechnol.*, 1983, **18**, 287–292.
44 C. De Macario, D. B. A. E. Miov and T. W. Jeffries, *Trends Biotechnol.*, 1985, **3**, 208–212.
45 Z. Zheng, X. Lin, T. Jiang, W. Ye and J. Ouyang, *Biotechnol. Lett.*, 2016, **38**, 1331–1339.
46 L. Fan, Y. Zhang, W. Qu, J. Wang and W. Shao, *Biotechnol. Lett.*, 2011, **33**, 593–598.
47 R. Y. Miyamoto, A. S. de Sousa, P. S. Vieira, R. R. de Melo, J. A. Scarpassa, C. H. I. Ramos, M. T. Murakami, R. Ruller and L. M. Zanphorlin, *Biochim. Biophys. Acta, Gen. Subj.*, 2020, **1864**, 129549.
48 D. Yang, S. Y. Park, Y. S. Park, H. Eun and S. Y. Lee, *Trends Biotechnol.*, 2020, 1–21.
49 K. Karhumaa, R. G. Sanchez and B. Hahn-hägerdal, *Microb. Cell Fact.*, 2007, **10**, 1–10.
50 P. M. Bruinenberg, P. H. M. de Bot, J. P. van Dijken and W. A. Scheffers, *Appl. Microbiol. Biotechnol.*, 1984, **19**, 256–260.
51 H. F. Son, S. Lee and K. Kim, *Sci. Rep.*, 2018, 1–11.
52 O. Bengtsson, B. Hahn-Hägerdal and M. F. Gorwa-Grauslund, *Biotechnol. Biofuels*, 2009, **2**, 1–10.
53 A. Mouro, A. A. Santos, D. D. Agnolo, G. F. Gubert, E. P. S. Bon, C. A. Rosa, C. Fonseca and B. U. Stambuk, *Fermentation*, 2020, **6**, 1–14.
54 C. I. D. G. Bonan, L. E. Biazi, S. R. Dionísio, L. B. Soares, R. Tramontina, A. S. Sousa, C. A. de Oliveira Filho, A. C. Costa and J. L. Ienczak, *Bioprocess Biosyst. Eng.*, 2020, **43**, 1509–1519.
55 A. A. Prabhu, E. Bosakornranut, Y. Amraoui, D. Agrawal, F. Coulon, V. Vivekanand, V. K. Thakur and V. Kumar, *Biotechnol. Biofuels*, 2020, **13**, 1–15.
56 D. K. Wilson, K. L. Kavanagh, M. Klimacek and B. Nidetzky, *Chem.–Biol. Interact.*, 2003, **144**, 515–521.
57 K. Correia, A. Khusnutdinova, P. Y. Li, J. C. Joo, G. Brown, A. F. Yakunin and R. Mahadevan, *bioRxiv*, 2018, **1–28**, 390401.
58 F. R. Rech, R. C. Fontana, C. A. Rosa, M. Camassola, M. A. Z. Ayub and A. J. P. Dillon, *Bioprocess Biosyst. Eng.*, 2019, **42**, 83–92.
59 P. Kijtter, R. Amore, C. P. Hollenberg, M. Ciriacy, I. Mikrobiologie, W. Dfisseldorf and F. Republic, *Curr. Genet.*, 1990, **1**, 493–500.
60 S. Watanabe, A. A. Saleh, S. P. Pack, N. Annaluru, T. Kodaki and K. Makino, *Microbiology*, 2007, **153**, 3044–3054.
61 R. Lunzer, Y. Mamnun, D. Haltrich, K. D. Kulbe and B. Nidetzky, *Biochem. J.*, 1998, **99**, 91–99.
62 L. B. Lockwood and G. E. N. Nelson, *J. Bacteriol.*, 1946, **52**(5), 581–586.
63 R. Weimberg, *J. Biol. Chem.*, 1961, **236**, 629–635.
64 H. Almqvist, S. J. Glaser, C. Tufvegren, L. Wasserstrom and G. Lidén, *Fermentation*, 2018, **4**, 1–11.
65 K. A. K. Köhler, L. M. Blank, O. Frick and A. Schmid, *Environ. Microbiol.*, 2015, **17**, 156–170.
66 L. Shen, M. Kohlhaas, J. Enoki, R. Meier, B. Schönenberger, R. Wohlgemuth, R. Kourist, F. Niemeyer, D. van Niekerk, C. Bräsen, J. Niemeyer, J. Snoep and B. Siebers, *Nat. Commun.*, 2020, **11**, 1–13.
67 K. N. G. Valdehuesa, K. R. M. Ramos, G. M. Nisola, A. B. Bañares, R. B. Cabulong, W. K. Lee, H. Liu and W. J. Chung, *Appl. Microbiol. Biotechnol.*, 2018, **102**, 7703–7716.
68 I. Bator, A. Wittgens, F. Rosenau, T. Tiso and L. M. Blank, *Front. Bioeng. Biotechnol.*, 2020, **7**, 1–18.
69 R. B. Cabulong, W. K. Lee, A. B. Bañares, K. R. M. Ramos, G. M. Nisola, K. N. G. Valdehuesa and W. J. Chung, *Appl. Microbiol. Biotechnol.*, 2018, **102**, 2179–2189.
70 W. Wei, P. Zhang, Y. Shang, Y. Zhou and B. C. Ye, *Bioresour. Technol.*, 2020, **314**, 123726.
71 T. W. Jeffries, *Curr. Opin. Biotechnol.*, 2006, **17**, 320–326.
72 E. M. Ammar, X. Wang and C. V. Rao, *Sci. Rep.*, 2018, **8**, 1–11.
73 Y. Gu, Y. Ding, C. Ren, Z. Sun, D. A. Rodionov, W. Zhang, S. Yang, C. Yang and W. Jiang, *BMC Genomics*, 2010, **11**, 1–14.
74 R. E. Hector and J. A. Mertens, *Mol. Biotechnol.*, 2017, **59**, 24–33.

75 C. Sievert, L. M. Nieves, L. A. Panyon, T. Loeffler, C. Morris, R. A. Cartwright, X. Wang and A. L. Demain, *Proc. Natl. Acad. Sci. U. S. A.*, 2017, **114**, 7349–7354.
76 J. G. Nijland, H. Y. Shin, R. M. De Jong, P. P. De Waal, P. Klaassen and A. J. M. Driessen, *Biotechnol. Biofuels*, 2014, **7**, 1–11.
77 K. A. Erlandson, J. H. Park, W. El Khal, H. H. Kao, P. Basaran, S. Brydges and C. A. Batt, *Appl. Environ. Microbiol.*, 2000, **66**, 3974–3980.
78 C. Sizemore, E. Buchner, T. Rygus, C. Witke, F. Götz and W. Hillen, *MGG, Mol. Gen. Genet.*, 1991, **227**, 377–384.
79 T. J. Verbeke, R. J. Giannone, D. M. Klingeman, N. L. Engle, T. Rydzak, A. M. Guss, T. J. Tschaplinski, S. D. Brown, R. L. Hettich and J. G. Elkins, *Sci. Rep.*, 2017, **7**, 1–11.
80 N. Vivek, L. M. Nair, B. Mohan, S. C. Nair, R. Sindhu, A. Pandey, N. Shurpali and P. Binod, *Bioresour. Technol. Rep.*, 2019, **7**, 100224.
81 B. Görke and J. Stülke, *Nat. Rev. Microbiol.*, 2008, **6**, 613–624.
82 G. Aidelberg, B. D. Towbin, D. Rothschild, E. Dekel, A. Bren and U. Alon, *BMC Syst. Biol.*, 2014, **8**(1), 1–12.
83 A. Ullmann and J. Monod, *FEBS Lett.*, 1968, **2**, 57–60.
84 J. E. Gonzalez and A. Peterkofsky, *Prog. Clin. Biol. Res.*, 1978, **22**, 325–332.
85 S. Kim and J. Hahn, *Metab. Eng.*, 2015, **1–7**, 94–101.
86 T. Rygus and W. Hillen, *J. Bacteriol.*, 1992, **174**, 3049–3055.
87 M. Bruder, M. Moo-Young, D. A. Chung and C. P. Chou, *Appl. Microbiol. Biotechnol.*, 2015, **99**, 7579–7588.
88 Y. Li, K. Jin, L. Zhang, Z. Ding, Z. Gu and G. Shi, *J. Agric. Food Chem.*, 2018, **66**, 9456–9464.
89 P. Chaillou, P. H. Pouwels and P. W. Postma, *J. Bacteriol.*, 1999, **181**, 4768–4773.
90 T. W. Jeffries, *Bioenergy*, 2014, 37–47.
91 K. L. Dunn and C. V. Rao, *Appl. Microbiol. Biotechnol.*, 2014, **98**, 6897–6905.
92 A. Farwick, S. Bruder, V. Schadeweg, M. Oreb and E. Boles, *Proc. Natl. Acad. Sci. U. S. A.*, 2014, **111**, 5159–5164.
93 M. Jeppsson, O. Bengtsson, K. Franke, H. Lee, B. Hahn-Hägerdal and M. F. Gorwa-Grauslund, *Biotechnol. Bioeng.*, 2006, **93**, 665–673.
94 S. G. Kilian and N. van Uden, *Appl. Microbiol. Biotechnol.*, 1988, **27**, 545–548.
95 C. Wang, X. Bao, Y. Li, C. Jiao, J. Hou, Q. Zhang, W. Zhang, W. Liu and Y. Shen, *Metab. Eng.*, 2015, **30**, 79–88.
96 E. M. Young, A. D. Comer, H. Huang and H. S. Alper, *Metab. Eng.*, 2012, **14**, 401–411.
97 E. M. Young, A. Tong, H. Bui, C. Spofford and H. S. Alper, *Proc. Natl. Acad. Sci. U. S. A.*, 2014, **111**, 131–136.
98 A. Singh, M. D. Lynch and R. T. Gill, *Metab. Eng.*, 2009, **11**, 347–354.
99 J. Hou, N. F. Lages, M. Oldiges and G. N. Vemuri, *Metab. Eng.*, 2009, **11**, 253–261.
100 J. Hou, G. N. Vemuri, X. Bao and L. Olsson, *Appl. Microbiol. Biotechnol.*, 2009, **82**, 909–919.
101 C. Zhao, Q. Zhao, Y. Li and Y. Zhang, *Microb. Cell Fact.*, 2017, **16**, 1–11.
102 B. Bergdahl, D. Heer, U. Sauer, B. Hahn-Hägerdal and E. W. Van Niel, *Biotechnol. Biofuels*, 2012, **5**, 1–19.
103 K. Shimizu and Y. Matsuoka, *Biotechnol. Adv.*, 2019, **37**, 107441.
104 G. C. Zhang, J. J. Liu and W. T. Ding, *Appl. Environ. Microbiol.*, 2012, **78**, 1081–1086.
105 G. C. Zhang, T. L. Turner and Y. S. Jin, *J. Ind. Microbiol. Biotechnol.*, 2017, **44**, 387–395.
106 B. Petschacher and B. Nidetzky, *Microb. Cell Fact.*, 2008, **7**, 1–12.
107 S. Watanabe, A. A. Saleh, S. P. Pack, N. Annaluru, T. Kodaki and K. Makino, *Microbiology*, 2007, **153**, 3044–3054.
108 J. K. Lee, B. S. Koo and S. Y. Kim, *Appl. Environ. Microbiol.*, 2003, **69**, 6179–6188.
109 H. Suga, F. Matsuda, T. Hasunuma, J. Ishii and A. Kondo, *Appl. Microbiol. Biotechnol.*, 2013, **97**, 1669–1678.
110 J. Hou, G. N. Vemuri, X. Bao and L. Olsson, *Appl. Microbiol. Biotechnol.*, 2009, **82**, 909–919.
111 C. Roca, J. Nielsen and L. Olsson, *Appl. Environ. Microbiol.*, 2003, **69**, 4732–4736.
112 J. Liu, Z. Wang, V. Kandasamy, S. Y. Lee, C. Solem and P. R. Jensen, *Metab. Eng.*, 2017, **44**, 22–29.
113 C. Zhu, Q. Li, L. Pu, Z. Tan, K. Guo, H. Ying and P. Ouyang, *ACS Catal.*, 2016, **6**, 4989–4994.
114 M. Celton, I. Sanchez, A. Goelzer, V. Fromion, C. Camarasa and S. Dequin, *BMC Genomics*, 2012, **13**(1), 1–14.
115 S. L. Baptista, J. T. Cunha, A. Romaní and L. Domingues, *Bioresour. Technol.*, 2018, **267**, 481–491.
116 J. Trivedi, A. K. Bhonsle and N. Atray, *Processing Food Waste for the Production of Platform Chemicals*, Elsevier Inc., 2019.
117 X. Yuan, J. Wang, J. Lin, L. Yang and M. Wu, *J. Ind. Microbiol. Biotechnol.*, 2019, **46**, 1061–1069.
118 Y. Lugani and B. S. Sooch, *Lwt*, 2020, **134**, 109988.
119 S. Tiwari and A. Baghela, *Challenges and Prospects of Xylitol Production by Conventional and Non-conventional Yeasts*, Elsevier B.V., 2020.
120 J. Jo, S. Oh, H. Lee, Y. Park and J. Seo, *Biotechnol. J.*, 2015, **10**, 1935–1943.
121 A. A. Prabhu, D. J. Thomas, R. Ledesma-Amaro, G. A. Leeke, A. Medina, C. Verheecke-Vaessen, F. Coulon, D. Agrawal and V. Kumar, *Microb. Cell Fact.*, 2020, **19**, 1–18.
122 J. H. Kim, K. C. Han, Y. H. Koh, Y. W. Ryu and J. H. Seo, *J. Ind. Microbiol. Biotechnol.*, 2002, **29**, 16–19.
123 C. Gao, C. Ma and P. Xu, *Biotechnol. Adv.*, 2011, **29**, 930–939.
124 Z. Qiu, Q. Gao and J. Bao, *Bioresour. Technol.*, 2018, **249**, 9–15.
125 D. Wischral, J. M. Arias, L. F. Modesto, D. de França Passos and N. Pereira, *Biotechnol. Prog.*, 2019, **35**(1), e2718.
126 D. Parra-Ramírez, A. Martinez and C. A. Cardona, *Bioresour. Technol.*, 2019, **273**, 86–92.
127 Z. Qiu, Q. Gao and J. Bao, *Bioresour. Technol.*, 2017, **245**, 1369–1376.
128 H. Lu, X. Zhao, Y. Wang, X. Ding, J. Wang, E. Garza, R. Manow, A. Iverson and S. Zhou, *BMC Biotechnol.*, 2016, **16**, 1–10.
129 V. Novy, B. Brunner and B. Nidetzky, *Microb. Cell Fact.*, 2018, **17**, 1–11.

130 T. L. Turner, G. C. Zhang, E. J. Oh, V. Subramaniam, A. Adiputra, V. Subramaniam, C. D. Skory, J. Y. Jang, B. J. Yu, I. Park and Y. S. Jin, *Biotechnol. Bioeng.*, 2016, **113**, 1075–1083.
131 Z. Dai, F. Guo, S. Zhang, W. Zhang, Q. Yang, W. Dong, M. Jiang, J. Ma and F. Xin, *Biofuels, Bioprod. Biorefin.*, 2020, **14**, 965–985.
132 Y. Chen and J. Nielsen, *Curr. Opin. Biotechnol.*, 2016, **37**, 165–172.
133 M. Jiang, J. Ma, M. Wu, R. Liu, L. Liang, F. Xin, W. Zhang, H. Jia and W. Dong, *Bioresour. Technol.*, 2017, **245**, 1710–1717.
134 J. J. Beauprez, M. De Mey and W. K. Soetaert, *Process Biochem.*, 2010, **45**, 1103–1114.
135 M. F. A. Bradfield, A. Mohagheghi, D. Salvachúa, H. Smith, B. A. Black, N. Dowe, G. T. Beckham and W. Nicol, *Biotechnol. Biofuels*, 2015, **8**, 1–17.
136 M. F. A. Bradfield and W. Nicol, *Bioprocess Biosyst. Eng.*, 2016, **39**, 233–244.
137 D. Salvachúa, A. Mohagheghi, H. Smith, M. F. A. Bradfield, W. Nicol, B. A. Black, M. J. Biddy, N. Dowe and G. T. Beckham, *Biotechnol. Biofuels*, 2016, **9**, 1–15.
138 C. Pateraki, H. Almqvist, D. Ladakis, G. Lidén, A. A. Koutinas and A. Vlysidis, *Biochem. Eng. J.*, 2016, **114**, 26–41.
139 J. Lu, Y. Lv, Y. Jiang, M. Wu, B. Xu, W. Zhang, J. Zhou, W. Dong, F. Xin and M. Jiang, *ACS Sustainable Chem. Eng.*, 2020, **8**, 9035–9045.
140 K. Jantama, X. Zhang, J. C. Moore, K. T. Shanmugam, S. A. Svoronos and L. O. Ingram, *Biotechnol. Bioeng.*, 2008, **101**, 881–893.
141 K. Jantama, M. J. Haupt, S. A. Svoronos, X. Zhang, J. C. Moore, K. T. Shanmugam and L. O. Ingram, *Biotechnol. Bioeng.*, 2008, **99**, 1140–1153.
142 P. Khunnonkwao, S. S. Jantama, S. Kanchanatawee and K. Jantama, *Appl. Microbiol. Biotechnol.*, 2018, **102**, 127–141.
143 F. Zhang, J. Li, H. Liu, Q. Liang and Q. Qi, *PLoS One*, 2016, **11**, 1–12.
144 A. A. Prabhu, R. Ledesma-Amaro, C. S. K. Lin, F. Coulon, V. K. Thakur and V. Kumar, *Biotechnol. Biofuels*, 2020, **13**, 1–15.
145 J. Wang, C. Li, Y. Zou and Y. Yan, *Proc. Natl. Acad. Sci. U. S. A.*, 2020, **117**, 19159–19167.
146 A. P. Zeng and W. Sabra, *Curr. Opin. Biotechnol.*, 2011, **22**, 749–757.
147 X. X. Wang, H. Y. Hu, D. H. Liu and Y. Q. Song, *Nat. Biotechnol.*, 2016, **33**, 16–22.
148 Y. Amraoui, V. Narisetty, F. Coulon, D. Agrawal, A. K. Chandel, S. Maina, A. Koutinas and V. Kumar, *ACS Sustainable Chem. Eng.*, 2021, **9**, 10381–10391.
149 X. W. Guo, Y. Zhang, L. L. Li, X. Y. Guan, J. Guo, D. G. Wu, Y. F. Chen and D. G. Xiao, *Biotechnol. Biofuels*, 2018, **11**, 1–18.
150 J. W. Kim, S. O. Seo, G. C. Zhang, Y. S. Jin and J. H. Seo, *Bioresour. Technol.*, 2015, **191**, 512–519.
151 S. J. Kim, H. J. Sim, J. W. Kim, Y. G. Lee, Y. C. Park and J. H. Seo, *Bioresour. Technol.*, 2017, **245**, 1551–1557.
152 B. Dey, B. Roy, S. Datta and K. G. Singh, *Comprehensive Overview and Proposal of Strategies for the Ethanol Sector in India*, Biomass Conversion and Biorefinery, 2021.
153 Sujata and P. Kaushal, *Biofuels*, 2020, **11**, 763–775.
154 NITI-Aayog, *Ethanol Blending in India 2020-25*, 2020.
155 V. Menon and M. Rao, *Prog. Energy Combust. Sci.*, 2012, **38**, 522–550.
156 S. H. Lee, T. Kodaki, Y. C. Park and J. H. Seo, *J. Biotechnol.*, 2012, **158**, 184–191.
157 X. Hou, *Appl. Microbiol. Biotechnol.*, 2012, **94**, 205–214.
158 S. C. Nakanishi, L. B. Soares, L. E. Biazi, V. M. Nascimento, A. C. Costa, G. J. M. Rocha and J. L. Ienczak, *Biotechnol. Bioeng.*, 2017, **114**, 2211–2221.
159 T. F. Pacheco, B. R. C. Machado, W. G. de Morais Júnior, J. R. M. Almeida and S. B. Gonçalves, *Appl. Biochem. Biotechnol.*, 2021, **193**, 2182–2197.
160 T. Watanabe, I. Watanabe, M. Yamamoto, A. Ando and T. Nakamura, *Bioresour. Technol.*, 2011, **102**, 1844–1848.
161 U. Klinner, S. Fluthgraf, S. Freese and V. Passoth, *Appl. Microbiol. Biotechnol.*, 2005, **67**, 247–253.
162 M. Xiong, A. Woodruff, X. Tang, X. Tian, J. Zhang and L. Cao, *J. Taiwan Inst. Chem. Eng.*, 2013, **44**, 605–610.
163 L. Liu, M. Jin, M. Huang, Y. Zhu, W. Yuan, Y. Kang, M. Kong, S. Ali, Z. Jia, Z. Xu, W. Xiao and L. Cao, *Front. Bioeng. Biotechnol.*, 2021, **9**, 1–11.
164 S. J. Chacón, G. Matias, C. F. dos S. Vieira, T. C. Ezeji, R. Maciel Filho and A. P. Mariano, *Ind. Crops Prod.*, 2020, **155**, 112837.
165 L. D. Gottumukkala, B. Parameswaran, S. K. Valappil, K. Mathiyazhakan, A. Pandey and R. K. Sukumaran, *Bioresour. Technol.*, 2013, **145**, 182–187.
166 N. Qureshi, B. C. Saha, R. E. Hector, B. Dien, S. Hughes, S. Liu, L. Iten, M. J. Bowman, G. Sarath and M. A. Cotta, *Biomass Bioenergy*, 2010, **34**, 566–571.
167 N. R. Baral and A. Shah, *Energy Fuels*, 2016, **30**, 5779–5790.
168 Y. Jiang, D. Guo, J. Lu, P. Dürre, W. Dong, W. Yan, W. Zhang, J. Ma, M. Jiang and F. Xin, *Biotechnol. Biofuels*, 2018, **11**, 1–14.
169 Y. Jiang, Y. Lv, R. Wu, J. Lu, W. Dong, J. Zhou, W. Zhang, F. Xin and M. Jiang, *Biotechnol. Bioeng.*, 2020, **117**, 2985–2995.
170 L. P. Guamán, C. Barba-Ostria, F. Zhang, E. R. Oliveira-Filho, J. G. C. Gomez and L. F. Silva, *Microb. Cell Fact.*, 2018, **17**, 1–11.
171 D. Moorkoth and K. M. Nampoothiri, *Bioresour. Technol.*, 2016, **201**, 253–260.
172 J. M. Nduko, K. Matsumoto, T. Ooi and S. Taguchi, *Metab. Eng.*, 2013, **15**, 159–166.
173 L. Salamanca-Cardona, C. S. Ashe, A. J. Stipanovic and C. T. Nomura, *Appl. Microbiol. Biotechnol.*, 2014, **98**, 831–842.
174 X. Kourilova, I. Pernicova, K. Sedlar, J. Musilova, P. Sedlacek, M. Kalina, M. Koller and S. Obruca, *Bioresour. Technol.*, 2020, **315**, 123885.
175 H. S. Kim, Y. H. Oh, Y. A. Jang, K. H. Kang, Y. David, J. H. Yu, B. K. Song, J. il Choi, Y. K. Chang, J. C. Joo and S. J. Park, *Microb. Cell Fact.*, 2016, **15**, 1–13.

176 H.-K. Jun, Y.-H. Jin, H.-N. Kim, Y.-T. Kim, S.-W. Kim and H.-S. Baik, *J. Life Sci.*, 2008, **18**, 1625–1630.
177 L. de Souza, Y. Manasa and S. Shivakumar, *Biocatal. Agric. Biotechnol.*, 2020, **28**, 101754.
178 L. Ou, C. Dou, J. H. Yu, H. Kim, Y. C. Park, S. Park, S. Kelley and E. Y. Lee, *Biofuels, Bioprod. Biorefin.*, 2021, **15**, 404–415.
179 A. Giuliano, D. Barletta, I. De Bari and M. Poletto, *Techno-economic Assessment of a Lignocellulosic Biorefinery Co-producing Ethanol and Xylitol or Furfural*, Elsevier Masson SAS, 2018, vol. 43.
180 P. Unrean and N. Ketsub, *Ind. Crops Prod.*, 2018, **123**, 238–246.
181 P. Ranganathan, *Biomass Convers. Biorefin.*, 2020, 1–4.
182 J. Becker, C. M. Rohles and C. Wittmann, *Metab. Eng.*, 2018, **50**, 122–141.
183 S. Jo, J. Yoon, S. M. Lee, Y. Um, S. O. Han and H. M. Woo, *J. Biotechnol.*, 2017, **258**, 69–78.
184 A. Radek, K. Krumbach, J. Gätgens, V. F. Wendisch, W. Wiechert, M. Bott, S. Noack and J. Marienhagen, *J. Biotechnol.*, 2014, **192**, 156–160.
185 T. Xia, E. Altman and M. A. Eiteman, *Eng. Life Sci.*, 2015, **15**, 65–72.
186 K. K. Cheng, G. Y. Wang, J. Zeng and J. A. Zhang, *BioMed Res. Int.*, 2013, **1**, 1–12.
187 J. B. McKinlay and C. Vieille, *Metab. Eng.*, 2008, **10**, 55–68.
188 J. B. McKinlay, Y. Shachar-Hill, J. G. Zeikus and C. Vieille, *Metab. Eng.*, 2007, **9**, 177–192.
189 W. Sabra, R. R. Bommareddy, G. Maheshwari, S. Papanikolaou and A. P. Zeng, *Microb. Cell Fact.*, 2017, **16**, 1–14.
190 G. L. Peabody, J. Winkler and K. C. Kao, *Curr. Opin. Chem. Eng.*, 2014, **6**, 9–17.
191 A. Radek, N. Tenhaef, M. F. Müller, C. Brüsseler, W. Wiechert, J. Marienhagen, T. Polen and S. Noack, *Bioresour. Technol.*, 2017, **245**, 1377–1385.
192 R. E. Hector, N. Qureshi, S. R. Hughes and M. A. Cotta, *Appl. Microbiol. Biotechnol.*, 2008, **80**, 675–684.
193 J. G. R. Bueno, G. Borelli, T. L. R. Corrêa, M. B. Fiamenghi, J. José, M. De Carvalho, L. C. De Oliveira, G. A. G. Pereira and L. V. Dos Santos, *Biotechnol. Biofuels*, 2020, **13**, 1–20.
194 S. R. Kim, S. J. Ha, N. Wei, E. J. Oh and Y. S. Jin, *Trends Biotechnol.*, 2012, **30**, 274–282.
195 J. H. Van Vleet and T. W. Jeffries, *Curr. Opin. Biotechnol.*, 2009, **20**, 300–306.
196 J. C. Roseiro, M. A. Peito, F. M. Gírio and M. T. Amaral-Collaço, *Arch. Microbiol.*, 1991, **156**, 484–490.
197 K. O. Osiro, D. P. Brink, C. Borgström, L. Wasserstrom, M. Carlquist and M. F. Gorwa-Grauslund, *FEMS Yeast Res.*, 2018, **18**, 1–15.
198 S. Cao, Y. Pu, M. Studer, C. Wyman and A. J. Ragauskas, *RSC Adv.*, 2012, **2**, 10925–10936.
199 T. H. Kim, H. J. Ryu and K. K. Oh, *Bioresour. Technol.*, 2016, **218**, 367–372.
200 P. N. Ciesielski, W. Wang, X. Chen, T. B. Vinzant, M. P. Tucker, S. R. Decker, M. E. Himmel, D. K. Johnson and B. S. Donohoe, *Biotechnol. Biofuels*, 2014, **7**(1), 1–12.
201 S. M. de Vasconcelos, A. M. P. Santos, G. J. M. Rocha and A. M. Souto-Maior, *Bioresour. Technol.*, 2013, **135**, 46–52.
202 E. Liu, L. Das, B. Zhao, M. Crocker and J. Shi, *BioEnergy Res.*, 2017, **10**, 1079–1093.
203 X. Ji, H. Ma, Z. Tian, G. Lyu, G. Fang, J. Chen and H. A. M. Saeed, *Bioresources*, 2017, **12**, 7084–7095.
204 J. T. Cunha, A. Romaní, K. Inokuma, B. Johansson, T. Hasunuma, A. Kondo and L. Domingues, *Biotechnol. Biofuels*, 2020, **13**, 1–15.
205 G. Batista, R. B. A. Souza, B. Pratto, M. S. R. dos Santos-Rocha and A. J. G. Cruz, *Bioresour. Technol.*, 2019, **275**, 321–327.
206 D. H. Fockink, J. H. Sánchez and L. P. Ramos, *Ind. Crops Prod.*, 2018, **123**, 563–572.
207 H. J. Zhang, X. G. Fan, X. L. Qiu, Q. X. Zhang, W. Y. Wang, S. X. Li, L. H. Deng, M. A. G. Koffas, D. S. Wei and Q. P. Yuan, *Bioprocess Biosyst. Eng.*, 2014, **37**, 2425–2436.
208 G. J. M. Rocha, A. R. Gonçalves, S. C. Nakanishi, V. M. Nascimento and V. F. N. Silva, *Ind. Crops Prod.*, 2015, **74**, 810–816.
209 R. Agrawal, A. Satlewal, R. Gaur, A. Mathur, R. Kumar, R. P. Gupta and D. K. Tuli, *Biochem. Eng. J.*, 2015, **102**, 54–61.
210 S. McIntosh, Z. Zhang, J. Palmer, H.-H. Wong, W. O. S. Doherty and T. Vancov, *Biofuels, Bioprod. Biorefin.*, 2016, **10**, 346–358.
211 M. Kapoor, S. Soam, R. Agrawal, R. P. Gupta, D. K. Tuli and R. Kumar, *Bioresour. Technol.*, 2017, **224**, 688–693.
212 D. J. Walker, J. Gallagher, A. Winters, A. Somani, S. R. Ravella and D. N. Bryant, *Front. Energy Res.*, 2018, **6**, 1–13.
213 V. Kumar, P. P. Sandhu, V. Ahluwalia, B. B. Mishra and S. K. Yadav, *Bioresour. Technol.*, 2019, **291**, 121931.
214 S. S. Dalli, M. Patel and S. K. Rakshit, *Biomass Bioenergy*, 2017, **105**, 402–410.
215 F. Bonfiglio, M. Cagno, C. K. Yamakawa and S. I. Mussatto, *Ind. Crops Prod.*, 2021, **170**, 113800.
216 K. S. Dhar, V. F. Wendisch and K. M. Nampoothiri, *J. Biotechnol.*, 2016, **230**, 63–71.
217 X. Yuan, Y. Mao, S. Tu, J. Lin, H. Shen, L. Yang and M. Wu, *J. Agric. Food Chem.*, 2021, **69**, 9625–9631.
218 R. Alves de Oliveira, R. Schneider, C. E. Vaz Rossell, R. Maciel Filho and J. Venus, *Bioresour. Technol. Rep.*, 2019, **6**, 26–31.
219 Z. Qiu, Q. Gao and J. Bao, *Bioresour. Technol.*, 2017, **245**, 1369–1376.
220 Z. Zhang, Y. Li, J. Zhang, N. Peng, Y. Liang and S. Zhao, *Microorganisms*, 2020, **8**, 1–9.
221 X. Kong, B. Zhang, Y. Hua, Y. Zhu, W. Li, D. Wang and J. Hong, *Bioresour. Technol.*, 2019, **273**, 220–230.
222 R. Glaser and J. Venus, *Biotechnol. Rep.*, 2018, **18**, e00245.
223 K. L. Ong, C. Li, X. Li, Y. Zhang, J. Xu and C. S. K. Lin, *Biochem. Eng. J.*, 2019, **148**, 108–115.
224 H. Bao, R. Liu, L. Liang, Y. Jiang, M. Jiang, J. Ma, K. Chen, H. Jia, P. Wei and P. Ouyang, *Enzyme Microb. Technol.*, 2014, **66**, 10–15.

225 A. M. Olajuyin, M. Yang, T. Mu, J. Tian, A. Thygesen, O. A. Adesanoye, O. A. Adaramoye, A. Song and J. Xing, *Bioprocess Biosyst. Eng.*, 2018, **41**, 1497–1508.
226 D. Ladakis, K. Michailidi, A. Vlysidis, A. Koutinas and I. K. Kookos, *Biochem. Eng. J.*, 2018, **137**, 262–272.
227 Y. Mao, G. Li, Z. Chang, R. Tao, Z. Cui, Z. Wang, Y. J. Tang, T. Chen and X. Zhao, *Biotechnol. Biofuels*, 2018, **11**, 1–17.
228 C. Wang, H. Zhang, H. Cai, Z. Zhou, Y. Chen, Y. Chen and P. Ouyang, *Appl. Biochem. Biotechnol.*, 2014, **172**, 340–350.
229 R. Liu, L. Liang, F. Li, M. Wu, K. Chen, J. Ma, M. Jiang, P. Wei and P. Ouyang, *Bioresour. Technol.*, 2013, **149**, 84–91.
230 A. Sharma, V. Nain, R. Tiwari, S. Singh and L. Nain, *Chem. Eng. Commun.*, 2018, **205**, 402–410.
231 P. R. D. Cortivo, J. Machado, L. R. Hickert, D. M. Rossi and M. A. Z. Ayub, *Biotechnol. Prog.*, 2019, **35**, 1–8.
232 D. Yang, S. Y. Park, Y. S. Park, H. Eun and S. Y. Lee, *Trends Biotechnol.*, 2020, 1–21.
233 C. C. Okonkwo, V. Ujor and T. C. Ezeji, *Ind. Crops Prod.*, 2021, **159**, 113047.
234 S. Rehman, M. Khairul Islam, N. Khalid Khanzada, A. Kyoungjin An, S. Chaiprapat and S. Y. Leu, *Bioresour. Technol.*, 2021, **333**, 125206.
235 J. Wu, Y. J. Zhou, W. Zhang, K. K. Cheng, H. J. Liu and J. A. Zhang, *AMB Express*, 2019, **9**, 1–9.
236 A. Kuenz, M. Jäger, H. Niemi, M. Kallioinen, M. Mänttäri and U. Prüße, *Fermentation*, 2020, **6**, 86.
237 E. Tomás-Pejó, J. M. Oliva, M. Ballesteros and L. Olsson, *Biotechnol. Bioeng.*, 2008, **100**, 1122–1131.
238 T. F. Pacheco, B. R. C. Machado, W. G. de Morais Júnior, J. R. M. Almeida and S. B. Gonçalves, *Appl. Biochem. Biotechnol.*, 2021, **193**, 2182–2197.
239 A. M. Zetty-Arenas, R. F. Alves, C. A. F. Portela, A. P. Mariano, T. O. Basso, L. P. Tovar, R. Maciel Filho and S. Freitas, *Biomass Bioenergy*, 2019, **126**, 190–198.
240 W. Guan, G. Xu, J. Duan and S. Shi, *Ind. Eng. Chem. Res.*, 2018, **57**, 775–783.
241 Y. Jiang, Y. Lv, R. Wu, J. Lu, W. Dong, J. Zhou, W. Zhang, F. Xin and M. Jiang, *Biotechnol. Bioeng.*, 2020, **117**, 2985–2995.
242 R. Allard-Massicotte, H. Chadjaa and M. Marinova, *Fermentation*, 2017, **3**, 31–41.
243 D. Atzmüller, N. Ullmann and A. Zwirzitz, *AMB Express*, 2020, **10**, 1–11.
244 N. H. Abd Rahman, J. Md. Jahim, M. S. Abdul Munaim, R. A. Rahman, S. F. Z. Fuzi and R. Md. Illias, *Enzyme Microb. Technol.*, 2020, **135**, 109495.
245 Y. Hua, J. Wang, Y. Zhu, B. Zhang, X. Kong, W. Li, D. Wang and J. Hong, *Microb. Cell Fact.*, 2019, **18**, 1–18.
246 S. M. S. Reshamwala and A. M. Lali, *Biotechnol. Prog.*, 2020, **36**, e2972.
247 T. L. Turner, G. C. Zhang, S. R. Kim, V. Subramaniam, D. Steffen, C. D. Skory, J. Y. Jang, B. J. Yu and Y. S. Jin, *Appl. Microbiol. Biotechnol.*, 2015, **99**, 8023–8033.
248 M. Ilmén, K. Koivuranta, L. Ruohonen, P. Suominen and M. Penttilä, *Appl. Environ. Microbiol.*, 2007, **73**, 117–123.
249 S. Shinkawa, K. Okano, S. Yoshida, T. Tanaka, C. Ogino, H. Fukuda and A. Kondo, *Appl. Microbiol. Biotechnol.*, 2011, **91**, 1537–1544.
250 K. T. Koivuranta, M. Ilmén, M. G. Wiebe, L. Ruohonen, P. Suominen and M. Penttilä, *Microb. Cell Fact.*, 2014, **13**, 1–14.
251 S. Jo, J. Yoon, S. M. Lee, Y. Um, S. O. Han and H. M. Woo, *J. Biotechnol.*, 2017, **258**, 69–78.
252 R. Liu, L. Liang, K. Chen, J. Ma, M. Jiang, P. Wei and P. Ouyang, *Appl. Microbiol. Biotechnol.*, 2012, **94**, 959–968.
253 L. Yang, M. M. Henriksen, R. S. Hansen, M. Lübeck, J. Vang, J. E. Andersen, S. Bille and P. S. Lübeck, *Biotechnol. Biofuels*, 2020, **13**, 1–12.
254 L. Li, K. Li, Y. Wang, C. Chen, Y. Xu, L. Zhang, B. Han, C. Gao, F. Tao, C. Ma and P. Xu, *Metab. Eng.*, 2015, **28**, 19–27.
255 S. Yang, A. Mohagheghi, M. A. Franden, Y. C. Chou, X. Chen, N. Dowe, M. E. Himmel and M. Zhang, *Biotechnol. Biofuels*, 2016, 1–15.
256 S. J. Kim, J. W. Kim, Y. G. Lee, Y. C. Park and J. H. Seo, *Appl. Microbiol. Biotechnol.*, 2017, **101**, 2241–2250.
257 A. S. Abdelaal, K. Jawed and S. S. Yazdani, *J. Ind. Microbiol. Biotechnol.*, 2019, **46**, 965–975.
258 L. Yu, J. Zhao, M. Xu, J. Dong, S. Varghese and M. Yu, *Appl. Microbiol. Biotechnol.*, 2015, **99**, 4917–4930.
259 G. Huo, Y. Zhu, Q. Liu, R. Tao, N. Diao and T. Chen, *J. Chem. Technol. Biotechnol.*, 2017, **92**, 2739–2745.
260 A. G. Sandström, A. Muñoz, D. Heras, D. Portugal-nunes and M. F. Gorwa-grauslund, *AMB Express*, 2015, **5**, 1–14.
261 A. Muñoz, D. Heras, N. Rizza, A. G. Sandström and M. F. G. Grauslund, *Microb. Cell Fact.*, 2016, **7**, 1–12.